11-21-1977

Texture, Fabric and Composition of Fine-Grained Terrigenous Sediments from the Graneros Member of the Mancos Shale, San Juan Basin, New Mexico

Anthony J. Skeryanc

THE UNIVERSITY OF NEW MEXICO
ALBUQUERQUE, NEW MEXICO 87131

Policy on Use of Theses and Dissertations

Unpublished theses and dissertations accepted for master's and doctor's degrees and deposited in the University of New Mexico Library are open to the public for inspection and reference work. *They are to be used only with due regard to the rights of the authors.* The work of other authors should always be given full credit. Avoid quoting in amounts, over and beyond scholarly needs, such as might impair or destroy the property rights and financial benefits of another author.

To afford reasonable safeguards to authors, and consistent with the above principles, anyone quoting from theses and dissertations must observe the following conditions:

1. Direct quotations during the first two years after completion may be made only with the written permission of the author.

2. After a lapse of two years, theses and dissertations may be quoted without specific prior permission in works of original scholarship provided appropriate credit is given in the case of each quotation.

3. Quotations that are complete units in themselves (e.g., complete chapters or sections) in whatever form they may be reproduced and quotations of whatever length presented as primary material for their own sake (as in anthologies or books of readings) ALWAYS require consent of the authors.

4. The quoting author is responsible for determining "fair use" of material he uses.

This thesis/dissertation by Anthony J. Skeryanc has been used by the following persons whose signatures attest their acceptance of the above conditions. (A library which borrows this thesis/dissertation for use by its patrons is expected to secure the signature of each user.)

NAME AND ADDRESS	DATE
[signature] Amoco Prod Co. Denver	7-20-84

7/76-500

Anthony J. Skeryanc
Candidate

Geology
Department

This thesis is approved, and it is acceptable in quality and form for publication on microfilm:

Approved by the Thesis Committee:

Rodney C. Ewing, Chairperson

Raymond V. Ingersoll

Stephen G. Wells

Barry S. Kues

Accepted: Bernard Spolsky

Dean, Graduate School

November 21, 1977

Date

TEXTURE, FABRIC AND COMPOSITION OF FINE-GRAINED TERRIGENOUS SEDIMENTS FROM THE GRANEROS MEMBER OF THE MANCOS SHALE, SAN JUAN BASIN, NEW MEXICO

BY

ANTHONY J. SKERYANC

B.S., University of Texas at Arlington, 1973

THESIS

Submitted in Partial Fulfillment of the
Requirements for the Degree of
Master of Science in Geology

in the Graduate School of
The University of New Mexico
Albuquerque, New Mexico
December, 1977

ACKNOWLEDGEMENTS

I would like to express my gratitude to:

El Paso Natural Gas Company, particularly R. A. Ullrich, T. L. Malone and Dan Machalek, for permitting access to core materials and well log files that were used in this study;

Geochemical Laboratories, Inc., Houston, Texas, for their consideration in performing the organic analyses;

John Husler, University of New Mexico Staff Chemist, and Gina Glugla for performing the whole rock analyses;

Gerry Gomez for thin section preparation;

Dr. Robert Waterman, University of New Mexico - Department of Anatomy and Physiology, and his staff, for access to the scanning electron microscope. Dr. Waterman's open cooperation and attitude are a model for interdisciplinary progress in the sciences;

The entire Geology faculty at the University of New Mexico, who contribute immeasurably to any student's progress. Particular thanks to Dr. R. C. Ewing, my committee chairman and advisor, whose encouragement sustained me through ebbs in spirit, while his scientific discipline reserved me from unrestrained enthusiasm;

A special thanks to Don Powers, University of New Mexico Staff. No student can pass through the Geology Department and not be touched by Don's kindness and infinite capacity for helping others;

My wife, Bertha, not only for her professional secretarial

abilities, but also for her continuing support, patience and understanding.

TEXTURE, FABRIC AND COMPOSITION OF FINE-GRAINED TERRIGENOUS SEDIMENTS FROM THE GRANEROS MEMBER OF THE MANCOS SHALE, SAN JUAN BASIN, NEW MEXICO

BY

Anthony J. Skeryanc

ABSTRACT OF THESIS

Submitted in Partial Fulfillment of the
Requirements for the Degree of
Master of Science in ~~Biology~~ Geology
in the Graduate School of
The University of New Mexico
Albuquerque, New Mexico
December, 1977

TEXTURE, FABRIC AND COMPOSITION OF
FINE-GRAINED TERRIGENOUS SEDIMENTS FROM
THE GRANEROS MEMBER OF THE MANCOS SHALE,
SAN JUAN BASIN, NEW MEXICO

Anthony J. Skeryanc, M.S.
Department of Geology
The University of New Mexico, 1977

Petrography, scanning electron microscopy (SEM), porosity and permeability, radiography, x-ray diffraction (clay mineralogy), whole rock wet chemistry and organic analysis are used to examine the texture, fabric and composition of fine-grained terrigenous sediments from the Graneros Member of the Mancos Shale, San Juan Basin, New Mexico. Grain content is highly variable and determines the configuration of the fabric during compaction. A scale of the degree of parallel orientation is compared to grain content and reveals a decrease in parallelism with an increase in grain content. Grain content also affects permeability, thus controlling the degree of authigenic mineralization.

Although clay composition is consistent throughout the Graneros, clay morphologies vary considerably. Authigenic clays occur as primary void (interstitial) fillings, secondary void fillings (pits on grain surfaces, basal cleavage partings), pore-lining, fracture filling and alteration surfaces. SEM analyses reveals the following paragenesis of authigenic components: (1) pyrite,

(2) overgrowths on quartz and anatase, (3) calcite and dolomite, (4) illite-montmorillonite and illite, (5) cabbage-head type structures and other authigenic clays except kaolinite and (6) kaolinite. Matrix-supported fabrics contain contorted pore-fluid channels. Contorted pore-fluid channels and authigenic mineralization occur during initial thermal dehydration.

The maturation and transformation of organic material into petroleum and subsequent migration of petroleum from source beds to reservoir rock occurs during initial thermal migration. Level of organic metamorphism (LOM) calculations reveal that the portion of the Mancos Shale below the Carlisle-San Juan Basin generated the oil that occurs in the basin. Organic analyses and LOM studies of probable source beds are excellent exploration tools for oil and gas. Authigenic mineralization may result in petroleum accumulations in unlikely structural positions. Thick accumulations of montmorillonite-rich fine-grained terrigenous sediments that have undergone initial thermal dehydration might be excellent nuclear waste disposal sites.

TABLE OF CONTENTS

LIST OF FIGURES

LIST OF TABLES

LIST OF PLATES

INTRODUCTION

Statement of Problem

Fine-grained terrigenous sedimentary rocks are the most abundant rocks on the earth's surface. Despite this, they are the least studied of sedimentary rocks. Only 16% of the papers published in the Journal of Sedimentary Petrology concern fine-grained clastic rocks or sediment and although the number of papers doubled from 1960 to 1969, the percentage devoted to each rock and sediment class remained remarkably constant (Picard, 1971).

In recent years interest in the texture (size and shape of the particles), fabric (internal arrangement of the particles) and composition (mineralogy and chemistry) of fine-grained terrigenous sediments has significantly increased. This is due in part to the availability of new technologies that allow detailed examination of sediments. More important is the increased interest in fine-grained sediments as source beds for hydrocarbons.

Many petroleum exploration targets are sequences of sediments dominated by fine-grained terrigenous material. For several years "shales and mudstones" were regarded as negative factors in the reservoir sequence and these portions of cores were described as "10 ft. of black shale", for example, then discarded. The petroleum and natural gas industry is now aware of the importance of fine-grained terrigenous sediments as source beds and under certain

circumstances even reservoirs. Little is known about the detailed relationships of texture, fabric and composition of fine-grained sediments to reservoir properties.

Recent studies (Webb, 1974; Dickey, 1975) indicate that the migration of hydrocarbons through fine-grained source beds and clay-bearing sandstone reservoirs is controlled by their texture, fabric and composition and that clay-organic reactions may indicate the direction of hydrocarbon migration.

A growing concern in the energy industry and elsewhere is the safe storage of nuclear waste products. Fine-grained terrigenous sediments may be a favorable alternative to bedded salt deposits. A thorough understanding of texture, fabric and composition of fine-grained sediments is essential to the consideration of such sediments as nuclear waste storage sites.

Purpose of Study

This study analyzes in detail the texture, fabric and composition of fine-grained terrigenous sediments from the Graneros, in order to more precisely define their relationships to important reservoir properties (porosity, permeability and organic content), to the environment of deposition and general geologic history.

This study focuses on fine-grained sedimentary rocks in the San Juan Basin of northwestern New Mexico (Fig. 1) which contain significant accumulations of oil and gas.

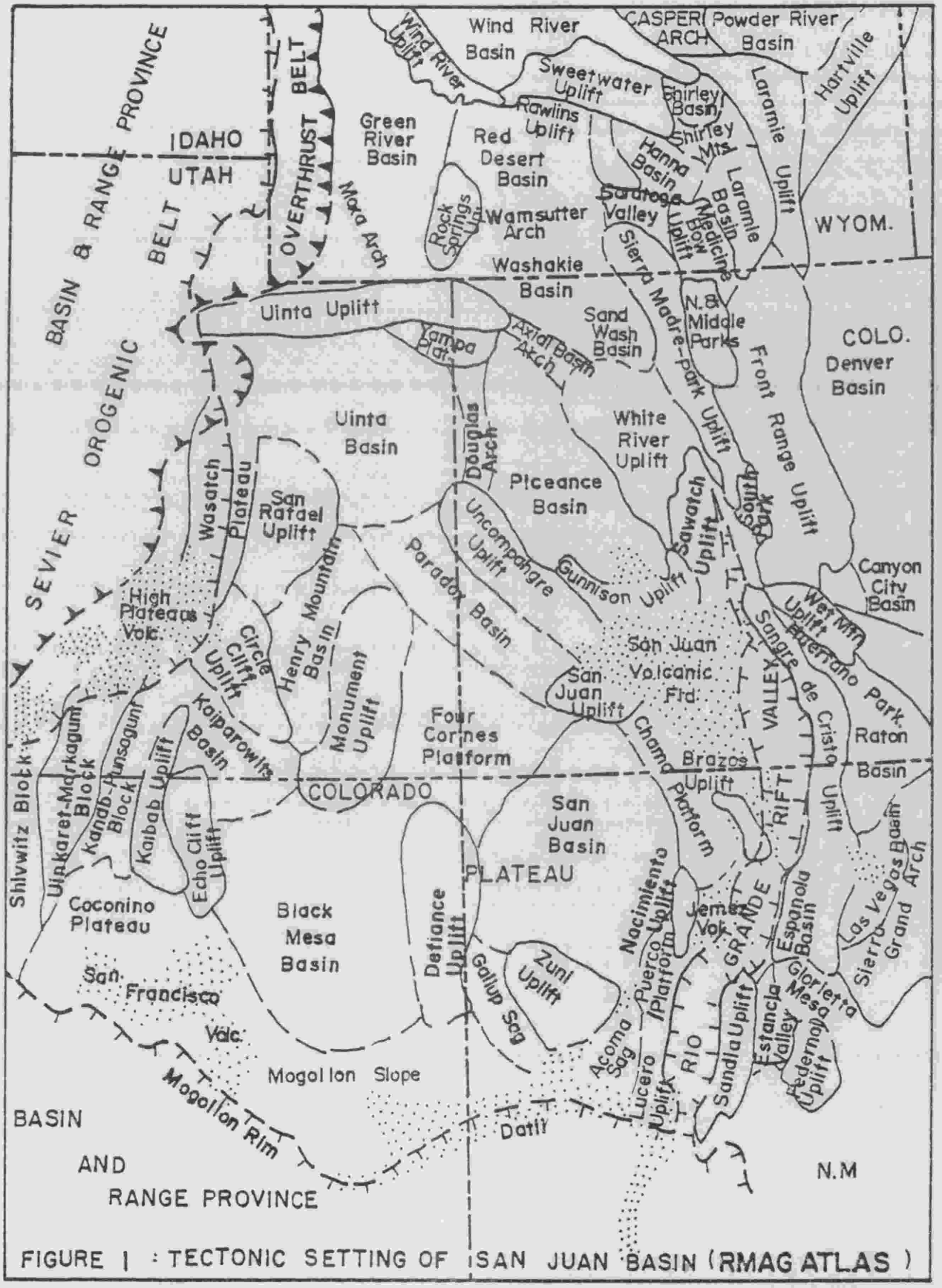

FIGURE 1 : TECTONIC SETTING OF SAN JUAN BASIN (RMAG ATLAS)

Rocks of Cretaceous age were chosen, as numerous producing intervals occur in Cretaceous strata (i.e. Dakota Sandstone, Point Lookout Sandstone and sand lenses in the Graneros Member of the Mancos Shale).

The unit selected for detailed analysis, the Graneros Member of the Mancos Shale (Fig. 2), is well suited to the study because:

1. it is well delineated on subsurface well logs;
2. it is a major source bed for hydrocarbons;
3. adequate core chip samples and well logs are available;
4. the core samples are not affected by weathering and surface alteration;
5. core samples are well indurated, enhancing sample preparation for thin section and SEM (scanning electron microscope) study;
6. the environment of deposition is not so variable as to preclude the delineation of meaningful horizontal and vertical trends in texture, fabric and composition.

Methods of Investigation

Textural properties of the samples were determined with the petrographic microscope and SEM; fabric was examined by radiography, petrographic microscope and SEM; and composition was determined by whole rock wet chemical analysis, organic analysis, petrographic microscope, SEM and x-ray

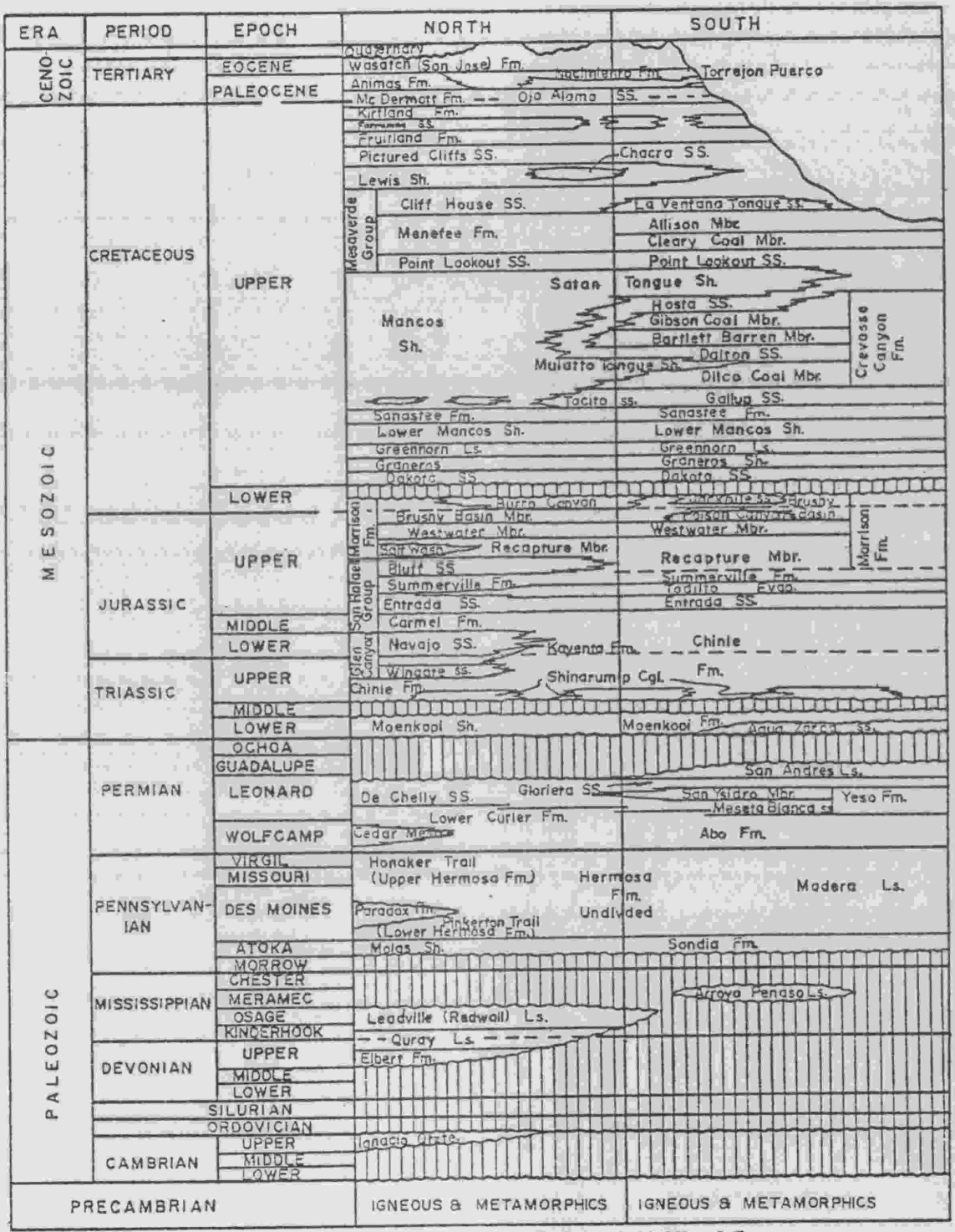

FIGURE 2 : STRATIGRAPHIC CORRELATION CHART OF SAN JUAN BASIN (After Peterson and others, (1965).

diffraction. Porosity and permeability were obtained by actual measurement and by petrophysical well log calculation. Each of these techniques will be discussed in more detail in later sections.

A brief basin analysis of the San Juan Basin is included as a framework in which to discuss variations in texture, fabric and composition of the Graneros. The implications for petroleum exploration and development and nuclear waste disposal are then discussed.

Geologic Setting

Tectonic Setting

The San Juan Basin occupies the southeastern portion of the Colorado Plateau. Uplifts bound the basin on the northern, eastern, southern and western margins, and broad platforms are located on the northwestern, northeastern, southwestern and southeastern edges. These local uplifts and platforms are located within a broad regional zone of basins and uplifts that are considered to be the stable foreland area of the Cordilleran geosyncline which lay west of this area during Paleozoic and much of Mesozoic time (Fig. 1).

The foreland belt is bounded on the west by the overthrust belt and on the east by the Rocky Mountains and the Rio Grande Rift Valley. The Basin and Range Province, characterized by tilted fault blocks and intervening intermontaine basins, wraps around the entire region on the south and west (Fig. 1).

Stratigraphy and Depositional Environments

The stratigraphic nomenclature used in this thesis was taken from a summary and discussion of the San Juan Basin by Peterson and others (1965). Three Figures (Fig. 2, Fig. 3 and Fig. 4) illustrate the basic geometry and thickness of the units discussed.

Cambrian transgression deposited the thin widespread Ignacio Sandstone along the broad and gentle northwestern flank of the Transcontinental Arch. This was followed by Ordivician-Silurian-Early Devonian regression as no rocks of these ages have been recognized in the Four Corners area. Late Devonian-Early Mississippian transgression deposited marine clastics and carbonates in the basin area. Late Mississippian-Early Pennsylvanian regression occurred, and karst topography developed on Mississippian carbonate surfaces as a result of regional uplift. Pennsylvanian-Permian Ancestral Rockies tectonism resulted in strong uplift and associated downwarping of a northwest-southeast lineament. Marine carbonates and clastics were deposited in this trough resulting in the earliest development of the San Juan Basin.

Late Permian and Triassic strata are dominated by red to red-brown shale, siltstone and sandstone with some conglomerates. The basal units represent near-shore marine and non-marine environments and the upper units dominantly continental environments. Jurassic rocks consist of interbedded sandstone, siltstone and shale with minor amounts

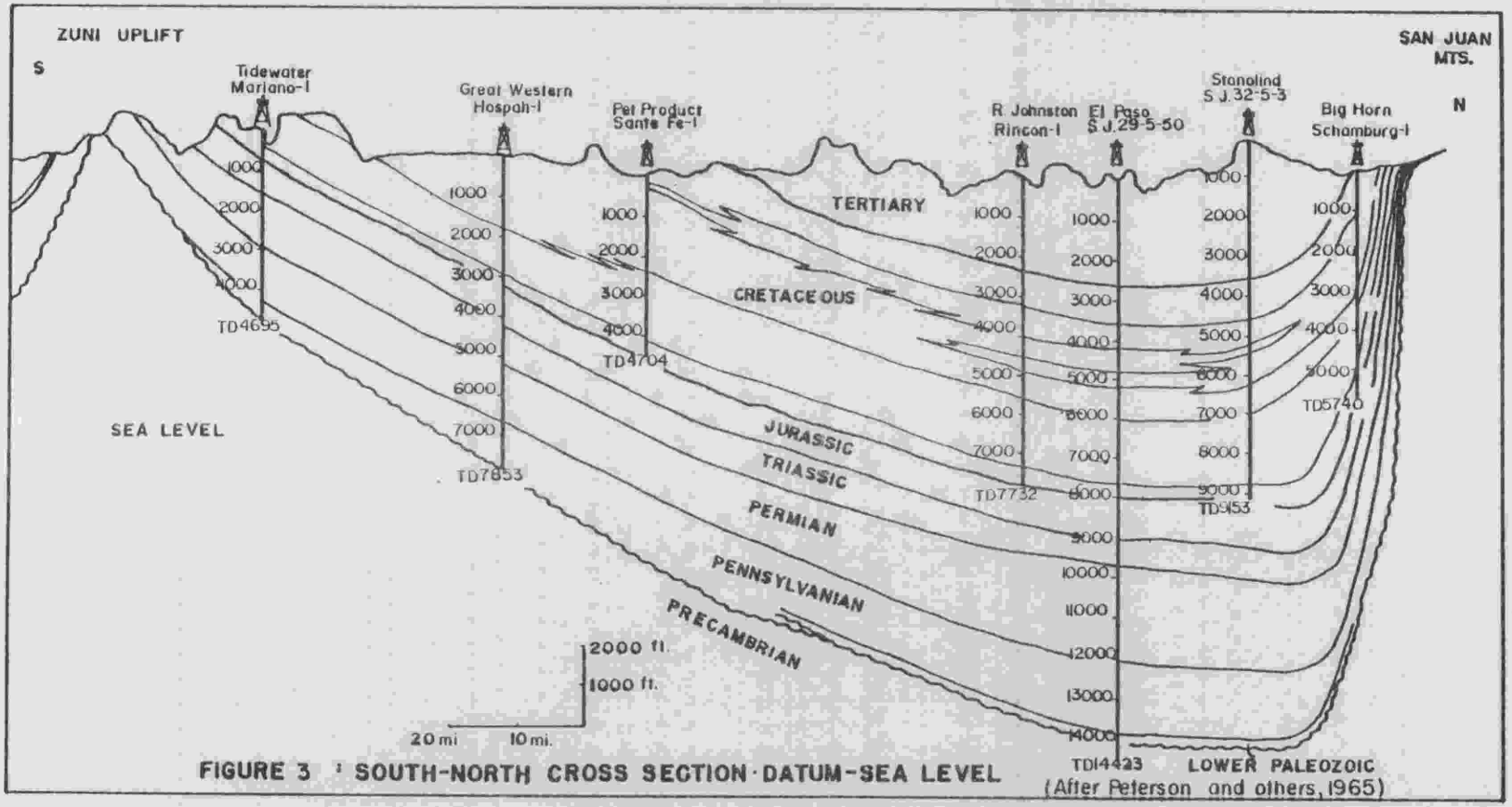

FIGURE 3 : SOUTH-NORTH CROSS SECTION · DATUM-SEA LEVEL
(After Peterson and others, 1965)

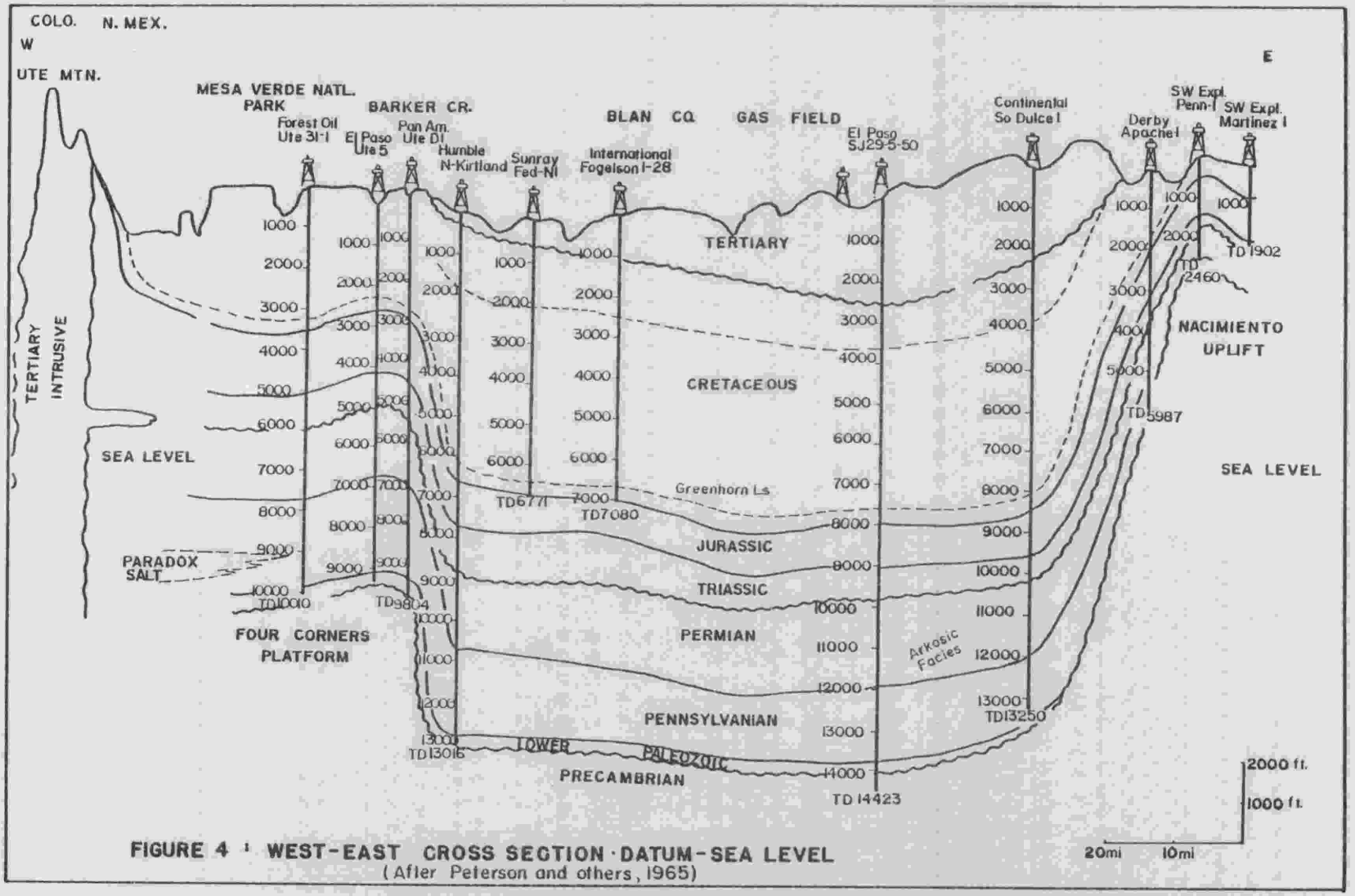

FIGURE 4 : WEST-EAST CROSS SECTION · DATUM-SEA LEVEL
(After Peterson and others, 1965)

of carbonate and anhydrite or gypsum. The sequence represents a progression from aeolian deposits near the base to fluviatile and lacustrine deposits through the upper units.

A diagrammatic stratigraphic cross section of Cretaceous and Tertiary rocks of the San Juan Basin (Fig. 5) illustrates the complex interrelationship of those units. Sears and others (1941) attributed this complexity to several transgressions and regressions which occurred along the margin of a broad, shallow trough in the San Juan Basin. These events are recorded in the alternating marine and continental deposits around the margins of the trough.

The Dakota Sandstone is a sequence progressing from fluvial, flood plain and paludal deposits in the lower part to strandline and offshore marine deposits that intertongue with the overlying Graneros in the upper part. On the northwestern side of the basin, the basal portion of the Graneros is carbonaceous and contains no fossils (Lamb, 1968) indicating non-marine deposition. In the northeastern portion of the basin, the Graneros is marine, containing microfauna indicative of open ocean conditions (Lamb, 1968). The shoreline was oriented north-south and the sea transgressed from east to west. In the southeastern portion of the basin, only the upper few feet of the Graneros contains fossils. The remainder is more arenaceous than calcareous indicating a clastic source near the southeastern portion of the basin (Lamb, 1968). Abrupt thinning of the Graneros near the western margin and an abundance of Gryphaea

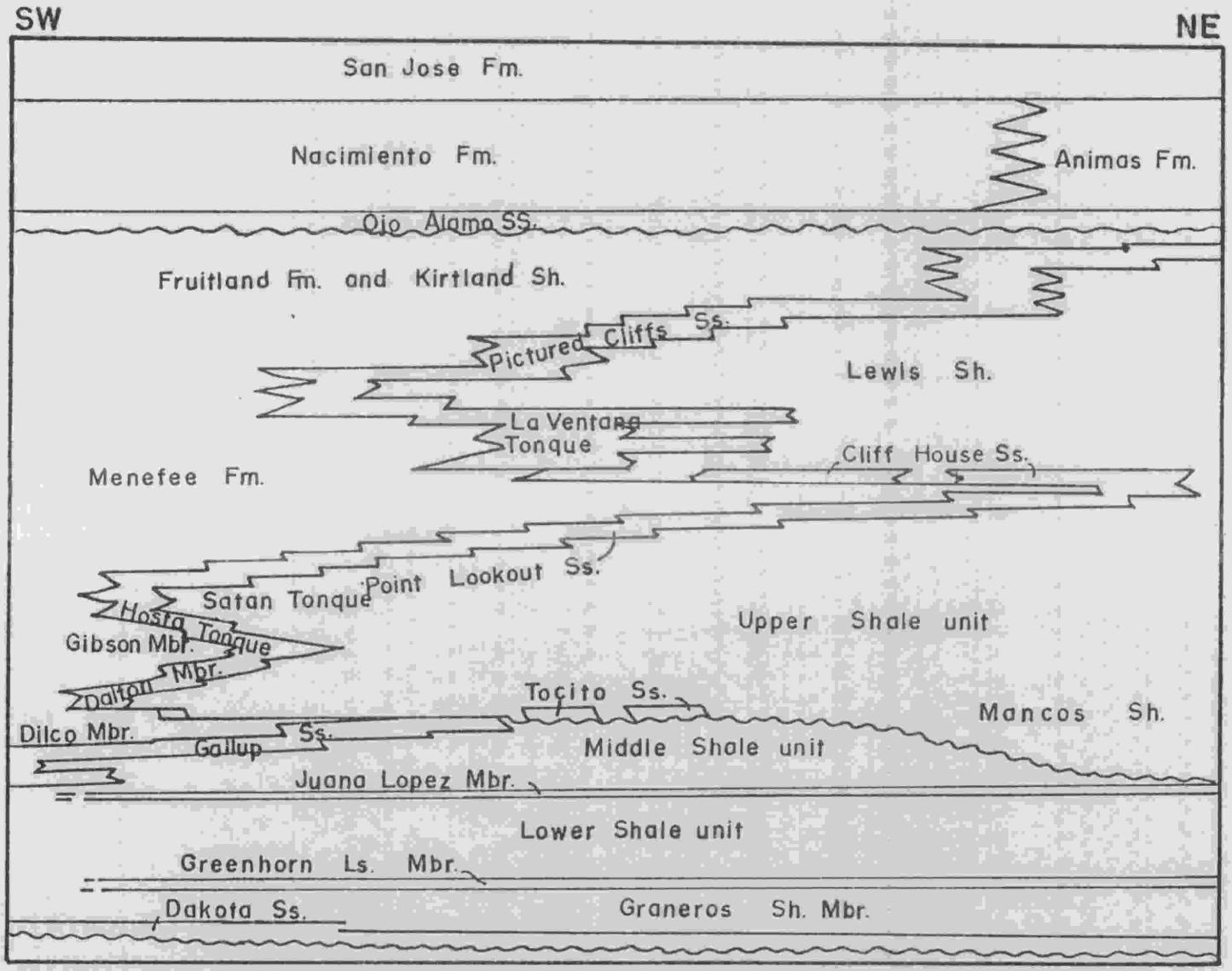

FIGURE 5: Diagrammatic Stratigraphic Cross Section of Cretaceous and Tertiary Rocks of the San Juan Basin (After Fassett, 1974)

newberryi on the northwestern margin of the basin indicate a shelf edge over which the seas transgressed to the west and south (Lamb, 1968). According to Lamb (1968), the "abundance of pelagic forms indicates a direct open ocean connection, while the relative abundance of Lagenidae and Rotaliidae among the benthonic forms indicates an epineritic environment". A slowing of the rate of basin subsidence and an increase in clastic influx are indicated by a faunal change between the Rotalipora zone and the overlying Bigenerina zone and sandy zones in the middle and upper Graneros. The Greenhorn Limestone, which overlies the Graneros, consists of argillaceous foraminiferal biomicrites, containing some pyrite and organic material (Lamb, 1968). According to Rubey (1930), conditions most favorable for formation of this lithologic assemblage are shallow water, rapid rate of accumulation and burial of organic matter. The Lower Mancos Shale overlies the Greenhorn and is similar to the Graneros. The overlying Sanastee Formation consists of calcarenites and calcareous shale. The Middle Shale overlies the Sanastee and is similar to the Lower Shale. The Middle Shale contains a major unconformity (Carlisle-Niobrara unconformity). The units described above constitute the Dakota-Mancos Transgressive Stage of Sears and others (1941). During this transgression, when subsidence continued and the seas encroached upon the land to the southwest, zones of swamp and beach deposition moved landward over the old land surface. The other zones were buried under offshore

muds that became the first beds of the transgressive Mancos Shale (Sears and others, 1941).

The coastal swamps and beach deposits are represented respectively by the Dilco Coal and Gallup Sandstone. These units represent the Mancos-to-Dilco Regressive Stage (Sears and others, 1941). The overlying sequence (Fig. 2), consisting of the Mulatto Tongue, Dalton Sandstone, Bartlett Barren Member and Gibson Coal Member, contains similar lithologies to the units representing the Dakota-Mancos Transgressive and Mancos-to-Dilco Regressive Stages and represents the Dilco-Mulatto Transgressive and Mulatto-to-Lower Gibson Regressive Stages (Sears and others, 1941).

The Lower Gibson-to-Satan Transgressive Stage and Satan-to-Allison Regressive Stage are represented by the Lower Gibson Member, the Hosta Sandstone, the Satan Tongue Shale, the Point Lookout Sandstone, the Cleary Coal Member and the Allison Member. Between the marine strandline sandstones, the Point Lookout and Cliff House, the continental coal-bearing Menefee Formation was deposited. The Lewis Shale was deposited in deeper offshore water and represents the last transgression of Cretaceous seas. The Pictured Cliffs Sandstone consists dominantly of sandstone, but contains siltstone with concretionary zones and thin, shaley, carbonaceous zones. According to Fassett and Hinds (1971), it is a "regressive strandline sandstone deposited during the last retreat of the Cretaceous sea from the San Juan Basin area".

The Fruitland Formation represents swamp, river, lake and flood plain deposits laid down further inland from and over the Pictured Cliffs Sandstone (Fassett, 1974). The conglomerates and sandstones of the Ojo Alamo Sandstone interfinger northward with the McDermott Shale and the overlying Animas Formation. The Animas grades into the Nacimiento Formation to the south and contains variegated shale and arkosic sandstone with some conglomerate and rare coal beds. The overlying shales, sandstones and conglomerates of the San Jose Formation contain fossils of Eocene age.

Previous Work

The earliest significant discussion of clay fabric was presented by Karl Terzaghi (1925), who postulated that cohesion in soils was the result of adhesion between adjacent minerals. He felt that fine and coarse grained muds were composed of aggregates of grains resembling honeycomb structures. Casagrande (1940) supported the concept of honeycomb structures in soils. Lambe (1953) and Tan (1958), through idealized drawings, suggested respectively "card-house" and "edge-face" arrangements of flakes.

Ingram (1953) examined fissility in "mudrocks" and concluded that fissility is usually associated with a parallel arrangement of the micaceous clay particles and non-fissility with a random arrangement. He suggested two mechanisms by which clay minerals attain a parallel arrangement:

(1) gravity settling, or (2) flocculation and compaction. Any cement, with the exception of organic matter, was associated with a decrease in fissility. There was no correlation between fissility and clay mineralogy.

Actual photographs of clay flakes in undisturbed sediments were first taken by Rosenqvist (1959, 1963). Those photographs support the postulated "cardhouse" arrangement. Using oil immersion photographs in conjunction with the electron microscope (EM), Gipson (1965) studied particle orientation and fissility in shale and concluded that fissile planes occur in (1) zones of preferentially-oriented particles, (2) at interfaces between zones of preferentially-oriented particles and organic material and (3) at interfaces between zones of randomly-oriented particles and organic material.

Gipson (1966) observed that porosity decreased slightly with increasing depth of burial and with increasing preferred orientation of clay minerals in Pennsylvanian shales. No apparent correlation existed between depth and preferred orientation of clay minerals; presumably the physical and chemical conditions of the environment of deposition and diagenesis were more important factors than compaction pressures. Increasing silt content was accompanied by a decrease in preferred clay mineral orientation.

Quigley and Thompson (1966) used x-ray diffraction to measure the effect of compaction on clay mineral orientation. When "undisturbed" clays were subjected to increasingly

higher consolidation pressures, a corresponding increase in the intensity of the 10 Å clay peaks was observed, resulting from reorientation of clay minerals into the plane perpendicular to the direction of consolidation pressure. This verified Gipson's (1966) conclusion that increase in parallelism was accompanied by a pronounced reduction in porosity.

Meade (1966) studied various factors that influence compaction of clays and sands at pressures between 0 and 100 kg/cm^2. His results differed from Gipson's (1966); Meade placed greater emphasis on compaction pressure as a mechanism for preferred clay mineral orientation. Greater initial water content, carbonaceous organic matter and lesser concentrations of interstitial electrolytes enhance preferred orientation of clay minerals.

Odom (1967) observed that an increase in preferred orientation of clay minerals from "very poor" to "very good" was accompanied by a progression of shale fabric from massive to flakey to fissile. Increasing organic content was accompanied by an increase in fissility. Large amounts of carbonates, silt, iron oxides and sulfides were detrimental to clay mineral orientation. Odom (1967) found no correlation between clay fabric and clay mineralogy, with the possible exception of montmorillonite, which, when present in appreciable amounts, appears to be associated with massive fabrics. Odom reached the same conclusion as Gipson (1966), "the amount of particle rearrangement during early compaction might be

aided by geochemical variations in pore solutions".

O'Brien (1968) observed a good correlation between organic material and parallel orientation of clay minerals. The organic material was finely disseminated and could not be resolved with the EM; consequently, the organic material was possibly present as adsorbed organic molecules. He noted that the addition of a very small amount of particular organic anions promotes dispersion of clay suspensions by neutralizing surface charges. Organic-rich clays could be deposited in a dispersed state, accounting for the parallelism.

Gillot (1969) was one of the first investigators to use scanning electron microscopy to examine the fabric of fine-grained sediments. He examined silt, clay, dolomite and soils, and concluded that the SEM had considerable potential as a tool in the petrographic investigation of fine-grained rocks.

Bowles and others (1969) used the EM to demonstrate a correlation in preferred orientation of marine sediments and confining pressure. They observed a major reduction in void ratio at low pressures. Up to pressures of 0.5 kg/cm^2, sediment structure retained an open, random arrangement of particles. At 4.0 kg/cm^2, the structure was dense with clumps and packets of particles with little orientation. At 32 and 64 kg/cm^2, a high degree of parallel orientation developed with some "local" areas of random orientation.

O'Brien (1970a) used an EM to study shale fabric. He established a good correlation between preferred orientation

of clay minerals and fissility and suggested that fissile fabrics in shales may result from either the deposition of dispersed clay or the collapse of clay floccules after deposition.

O'Brien (1970b) also studied the fabric of kaolinite and illite floccules which had been produced in the laboratory and noted little difference in either kaolinite or illite floccules formed in saline or salt-free water. Saline solutions did, however, promote flocculation. The fabrics produced were edge-face and face-face aggregates. He preferred the idealized "honeycomb" structure proposed by Terzaghi (1925) over the "cardhouse" model proposed by Casagrande (1940).

Heling (1970) determined that clay-mineral fabric reacts to compaction pressure by increasing its parallel orientation until depth of burial reaches 1000m. He interpreted an increase in illite at that depth as the result of the alteration of mixed-layer smectite minerals to illite. Once the mineral transformation process begins, the fabrics lose their original grain-size distribution and porosities are no longer controlled by mechanical effects.

Bucke and Mankin (1970) determined that permeability was the basic control of the degree of diagenesis in shales and sandstones. Factors contributing to the growth of authigenic kaolinite were organic material, which helps maintain a low pH, an aluminum and silicon source in potassium feldspars, potassium acceptors in the form of degraded illite

and water-filled pores as a medium and space for kaolinite growth. They concluded that all the constituents for authigenic kaolinite were present in situ.

Sarkisyan (1971) recognized the potential of the SEM in determining how the quality and quantity of clay cement affect reservoir properties of sedimentary rocks. In sediments of the Volgograd region, allogenic kaolinite occurs mainly in zones of early epigenesis at depths of 300 to 2000m in random arrangements. Porosities could be as great as 20% and permeability of 8.85mD. Authigenic kaolinite occurred at depths of 2000 to 3000m and was characterized by compact, regularly packed pseudohexagonal crystals. Porosities (10.75% porosity) and permeabilities (.18mD permeability) were low. Authigenic chlorite occurred in the same zone as authigenic kaolinite. The individual crystals were thinner but larger particles, often exhibiting the same pseudohexagonal form as kaolinite. The presence of authigenic chlorite resulted in poor reservoir properties: 9.06% porosity and permeabilities less than 0.01mD.

Webb (1974) observed the presence of authigenic clay minerals in sandstones lacking hydrocarbons and a lack of such minerals in sandstones containing hydrocarbons, and deduced that hydrocarbon migration displaced formation waters before or shortly after kaolinite precipitation began. Precipitation of clay minerals continued where hydrocarbons had not penetrated. These areas could serve as seals preventing further hydrocarbon migration and with subsequent

tectonic activity could preserve hydrocarbon traps in unlikely structural settings.

Dickey (1975) considered the problem of primary oil migration from source rock in oil phase and concluded that there simply has not been enough work to date to understand the mechanisms of primary migration in oil. He did speculate on the nature of water in shales as they become compacted. Water tends to take on the structural characteristics of the clay minerals immediately adjacent to it. It therefore behaves, somewhat, as part of the solid matrix (Langmuir, 1917; Hardy, 1926; Bauer, 1936; Winterkorn, 1943; Grim, 1945; Low, 1961). Such behavior of water effectively leaves the oil to occupy a large fraction of the pore volume and, according to Dickey, permits free movement. Grim (1968) referred to such structured water as "nonordinary" or "nonliquid" water and noted that because of the thinness of such layers the water in pores would be substantially liquid water, with nonliquid water forming only a thin film on the surface of the pores and where adjacent clay-mineral particles come together. Grim (1968) pointed out that these interstitial structured waters are driven off at temperatures of 100 to 150°C, corresponding very closely to Burst's (1969) second stage dehydration temperature (105°C). Burst, however, found second stage dehydration to correlate to the depth of maximum petroleum occurrence in Gulf Coast sediments and cited the removal of such water as a mechanism for the migration of petroleum from source bed to reservoir rock rather than the

structuring of the water itself.

Wijeyesekera and Freitas (1976) subjected kaolinitic clays to pressures ranging from 2000psi (140 kg/sq cm) to 6500psi (455 kg/sq cm) to observe changes in the fabric of the clays and the chemistry of the expelled pore fluid. It should be noted that the descriptive term "kaolinitic" refers to a preponderance of kaolinite in the samples (58%). Other minerals present were quartz (17%), illite (12%), chlorite (3%), mixed-layer minerals (5%), and others (5%). They used two samples having different initial pore-fluid chemistry: distilled water and artificial sea water. The changes in pore-fluid chemistry were more marked in the distilled water sample with the possible exception of K^+ ions which showed a sharp decrease in concentration with an increase in pressure in both samples. SO_4^{--} and Cl^- ions showed an initial slight decrease, then a slight increase up to maximum pressure. Na^+ ions were depleted in both samples, but in the distilled water sample the decrease was uniform, whereas in the sea water sample the decrease was initially very sharp, then fairly constant to maximum pressure. The behavior of Ca^{++} and Mg^{++} ions differed in the two samples in a similar fashion. In the distilled water sample, both showed an initial slight decrease in concentration, then a gradual increase to maximum pressure. In the artificial sea water sample, both declined more sharply initially, then increased quite rapidly to maximum pressure. The lowest final concentration was shown in K^+ ion concentration regardless of

initial pore-water chemistry. Maximum increase at final concentration was shown by Mg^{++} ions. Wijeyesekera and Freitas observed that the peak in the pore-water pressure variation seemed to indicate the commencement of a marked change in the state of the pore fluid, perhaps the mobilization of water layers adsorbed on the clay minerals. In relation to fabric, they noted that the development of preferred orientation of the clay particles is prevented by the presence of high pore pressures at the undrained end of samples, and that localized concentration of pore-fluid pressure will induce the fabric of the specimen at that point to attain a configuration conducive to its dissipation. This could lead to contorted pore-fluid channels and, perhaps, fissures.

Hower and others (1976) investigated the burial metamorphism of argillaceous sediment. Their study was based upon mineralogical and chemical analyses of shale cuttings from a Gulf Coast well. The major zone of mineralogical change occurred between 2000 to 3700m. They observed that illite/smectite undergoes a conversion to dominantly illite; calcite decreases to zero, potassium feldspar decreases to zero and chlorite increases. The $<0.1m$ fraction showed a large increase in K_2O and Al_2O_3 and a decrease in SiO_2. The proportions closely approximated the reaction:

$$\text{smectite} + Al^{+3} + K^{+} \quad \text{illite} + Si^{+4}$$

They attributed the source of potassium and aluminum to potassium feldspar (possibly mica) and concluded that the

shale acted as a closed system for all components except H_2O, CaO, Na_2O and CO_2.

Wilson and Pittman (1977) distinguished authigenic and allogenic clays in sandstones. They observed that authigenic clays occur as pore linings, pore fillings, pseudomorphic replacements and fracture fillings. Factors that aid in the recognition of authigenic clays are delicacy of morphology, occurrence as pore linings and composition radically different than associated allogenic clays. With the SEM they associated unique morphologies with major clay groups. Smectite occurred as "highly wrinkled or honeycomb-like pore linings, the individual flakes of which are not resolvable". Illite was observed to form "pore-lining overlapping flakes whose edges tend to curl away from the grain surface and from which highly elongate lath-like projections may extend". Mixed-layer smectite/illite minerals displayed the characteristics of both of the minerals when occurring individually. Chorite occurred as "pore-lining pseudohexagonal flakes with a cardhouse, honeycomb or rosette arrangement". Kaolinite and dickite usually occurred as pore-filling books of stacked pseudohexagonal flakes, but occasionally formed pore-lining sheets of overlapping pseudohexagonal flakes. Wilson and Pittman indicated that permeability and water saturation are particularly sensitive to the relative abundance of clays; hence, clays are important factors to be considered in petroleum exploration and development.

In summarizing previous work, it appears that clay

mineral fabrics are controlled by numerous factors which may be chemical, mechanical or physical. Preferred orientation is enhanced by gravity settling of the clay particles in a dispersed state at the time of deposition. Lower salinities may aid in that process. Other factors that aid in achieving preferred orientation are high initial water content, lesser concentrations of interstitial electrolytes, low silt content and high compaction pressures. Parallel arrangement of clay minerals and the presence of organic matter enhance fissility in shales. Detriments to fissility are nonorganic cement, high carbonate content, high silt content, iron oxides and iron sulfides.

Random fabrics have been described as honeycomb, card-house and bookhouse arrangements. Within these fabrics, grain-to-grain relationships have been described as face-to-face, edge-to-face and edge-to-edge contacts. Ordered fabrics have been attributed to parallelism of clay minerals that occur in parallel packets. High pore pressures may disrupt parallel fabrics and result in contorted pore-fluid channels and, perhaps, fissures.

In coarser sediments, authigenic clays occur as pore-linings, pore-fillings, pseudomorphic replacements and fracture fillings and may be distinguished from associated allogenic clays by their delicacy of morphology, occurrence as pore-linings, and radically different composition.

There seems to be a relationship between clay mineralogy and depth of occurrence. Allogenic kaolinite has been cited

as dominant at depths of 300 to 2000m, while authigenic kaolinite occurs at depths of 2000 to 3000m. From 2000 to 3700m mixed-layer illite/smectite converts to illite, calcite decreases markedly as do potassium feldspars, and chlorite content increases. The chemistry of pore fluids expelled by pressure substantiates such a trend. With increasing pressures, the Mg and Ca content of the expelled pore fluids increases while the Na and K content decreases.

ANALYTICAL RESULTS

Introduction

Analytical procedures include: petrographic, x-ray, scanning electron microscopy (SEM), whole rock wet chemical analysis, radiography and organic analysis. The analytical data from each procedure is discussed independently. Some procedures (whole rock analysis, organic analysis, porosity-permeability) require reference to data acquired from other procedures.

The sample locations are numbered 1 through 15, from south to north (Fig. 6). The core chips available were of insufficient size to supply enough material for all analyses; consequently, sample intervals varying from 3 to 15 ft. were selected. More than one interval was selected in some wells in order to detect vertical variations. The well names and respective sample numbers are shown in Table 1.

FIGURE 6: San Juan Basin as delineated by the Lewis Shale, with sample locations.

STUDY NUMBER	WELL NAME	GRANEROS INTERVAL	THICKNESS OF GRANEROS (ft.)	SAMPLE INTERVAL
1	#4 Chacon-Jicarilla "D"	7300-7422	122	A 7321-7330
				B 7364-7367
				C 7376-7381
2	Canyon Largo #256	6889-7007	118	6889.5-6890
3	Jicarilla-Apache 92-2	8151-8294	143	8259-8274
4	Rincon #127	7339-7460	121	7410-7421
5	Rincon #159	7417-7534	117	7450-7460
6	Rincon #136	7336-7503	167	7365-7380
7	San Juan 28-7 #109	7185-7353	168	7315-7329
8	San Juan 28-6 #98	7256-7410	154	7326-7331
9	San Juan 28-4 #24-26	8395-8518	123	8467-8474
10	San Juan 28-5 #35	7550-7700	150	7608-7616
11	San Juan 28-6 #122	7653-7800	147	A 7675-7676
				B 7790.5-7791
12	San Juan 29-4 #18-33	8514-8670	156	A 8656-8670
				B 8640-8655
13	San Juan 29-6 #35	7550-7686	136	7669-7684
14	San Juan 32-8 #35	7810-7943	133	7936-7943
15	Brookhaven #9	7135-7273	138	7149-7164

TABLE 1 : Sample key.Number corresponds to sample number in Fig. 6.

Petrography

Objectives

Petrographic analyses have provided valuable information on sandstones and, although most of the samples are fine-grained, such an analysis provides meaningful information about texture, fabric and mineralogy. These data provide a framework in which to view the results of the other analytical procedures (SEM, x-ray diffraction, organic and whole rock wet chemical analysis).

Techniques

Evaluation of the thin sections requires the distinction between "grains" and "matrix-cement" (interstitial material). "Grains" are defined here as those particles equal to or greater than 0.031mm in size. This is a natural division on the Wentworth (1922) clastic grain size scale between coarse silt and finer material. It is also the lower limit of grain sizes which can be mineralogically identified with reasonable accuracy with the petrographic microscope.

In most of the samples, the cement is disseminated throughout the matrix and determination of the relative percentages is difficult. In order to prevent errors due to arbitrary estimates, the matrix and cement are included together. "Matrix" is defined as the finer material between grains; "cement" as the binding material. Matrix-cement is essentially the interstitial material.

The distribution of constituents of the samples (grains,

interstitial material) was determined by point counting (Glagolev, 1933; Chayes, 1959). One hundred points were counted. The probable statistical error at 50% and 95.4% confidence levels is shown in Table 2 (Galehouse, 1969). Mineralogy and grain size were noted during the point count procedure. The degree of roundness of the grains was described using Taylor's (1950) terminology. Packing proximity was based on Kahn's (1956) method. A verbal description was used to evaluate sorting (i.e. very poorly sorted, poorly sorted, moderately sorted). These descriptions were observational and were not calculated from size distribution data.

The thin sections were ranked on a scale from 1 to 5 based upon the degree of parallel orientation of the thin sections. The degree of parallel orientation was based on the relationship between the orientation of matrix and grains and bedding direction. Maximum parallelism (5) corresponds to the alignment of matrix (platy minerals, lenticles of opaques and organic material, and elongate medium and fine silt) and elongate grains parallel to bedding. Moderate parallelism (3) corresponds to the alignment of matrix and grains subparallel to bedding. Minimum parallelism (1) corresponds to a random orientation of matrix and grains. An idealized sketch (Fig. 7) illustrates various degrees of parallel orientation.

Results

Table 3 is a compilation of the results of the

Total Number of Grains Counted	Estimated Percent of a Particular Species Present										
	5	10	20	30	40	50	60	70	80	90	95
100	±1.5	±2.0	±2.7	±3.1	±3.3	±3.4	±3.3	±3.1	±2.7	±2.0	±1.5
	Percent Error at 50 Confidence Level										
100	±4.4	±6.0	±8.0	±9.2	±9.8	±10	±9.8	±9.2	±8.0	±6.0	±4.4
	Percent Error at 95.4 Confidence Level										

TABLE 2 : Number of grains counted of a particular mineral species and the probable error of the number at 50 and 95.4 confidence levels (adapted from Galehouse,1969).

RANK

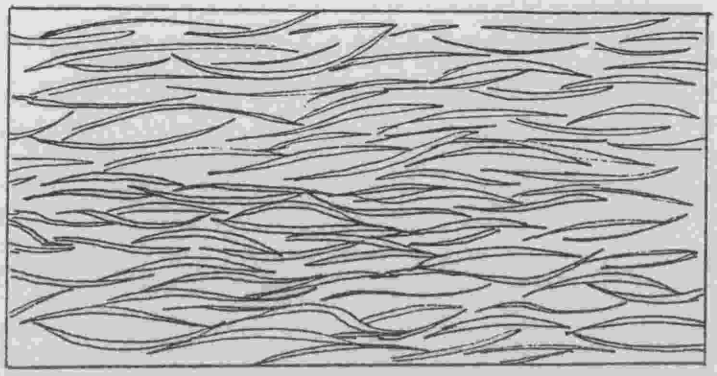

5

A. Matrix parallel to bedding, maximum degree of parallel orientation.

3

B. Matrix subparallel to grain boundaries and bedding.

1

C. Matrix and grains randomly oriented.

FIGURE 7: Idealized sketch of samples with degrees of parallel orientation of 1, 3, and 5.

Sample Number	Thin Section Interval	Texture GR.	M-C.	MGS	Ch	Qm	F	C	Mi	ULF	HM	M-C	Opq	Fabric Sort.	GR.SHP.	CONT.	Pk. Prox. %	o// ORI
IA	7329-7330	93	7	0.19	01	75	16	Tr	Tr	Tr	Tr	7	Tr	M-W	SA-R	L	100	1
					01	82	17											
1B	7365-7367	53	47	0.11	03	37	12	Tr	Tr	01	Tr	42	05	M-P	SA-SR	L, T	60	3
					06	70	23			02								
1C	7380-7381	46	54	0.20	01	27	11	03	01	02	01	54	03	M-P	SA-A	T, L	50	3
					02	59	24	07	02	03	02							
2	6829.5-6830	43	57	0.	00	03	00	40	00	00	00	57	03	P			<10	3
3	8262-8263	32	68	0.05	01	22	03	05	01	Tr	Tr	65	03	VPS	A-SA	T	20	4
					03	69	00	16	03									
	8268-8269	68	32	0.06	01	54	07	05	01	Tr	Tr	24	07	P-M	SA-R	L, T	40	2.5
					02	00	10	07	01									
	8272-8273	65	35	0.12	10	37	12	05	Tr	01	Tr	32	03	VPS	A-R	L, T	40	2.5
					15	57	19	03		01								
	8251-8252	34	66	0.08	02	25	04	02	Tr	01	Tr	61	05	VPS	A-SR	L, T	30	3
					06	74	12	05		01								
4	7420-7421	63	37	0.07	02	35	10	11	04	01	Tr	30	07	VPS	A-SR	L	60	2.5
					03	55	16	17	06	02								
	7415-7416	As Above																
	7410-7411	As Above																
5	7450-7451	47	53	0.15	02	35	07	01	01	01	Tr	46	07	VPS	SA-SR	T	20	4
					04	75	15	02	02	02								
	7457-7458	76	24	0.17	03	52	16	01	01	03	Tr	23	01	PS	SA-R	L	80	1
					04	63	21	01	01	04								
6	7366-7367	58	42	0.08	05	43	05	02	Tr	02	Tr	37	05	VPS	A-SR	L	50	1.5
					09	74	10	03		03								
	7370-7371	As Above																
	7373-7374	As Above																
7	7324-7325	65	35	0.07	01	33	15	10	01	Tr	Tr	34	01	P-M	A-SA	L	60	1.5
					02	59	23	15	01									
	7318-7319	80	20	0.12	05	45	26	02	Tr	01	Tr	20	Tr	P	A-SR	L	80	1
					06	58	33	02		01								
8	7327-7328	60	40	0.08	Tr	38	11	10	Tr	01	Tr	36	04	M	A-R	L	70	1.5
						63	18	17		02								
	7329-7330	68	32	0.09	02	43	15	07	Tr	01	Tr	31	01	P	SA-R	L	70	1.5
					03	63	22	10		01								
9	8467-8468	66	34	0.25	06	35	16	Tr	Tr	06	Tr	33	01	P-M	SA-SR	L	80	2.5
10	7615-7616	65	34	0.15	02	51	10	01	01	01	Tr	32	02	VPS	SA-SR	L	60	1.5
					03	77	15	02	01	02								
	7610-7611	66	34	0.15	03	37	16	01	Tr	01	Tr	33	01	VPS	SA-SR	L	60	1.5
					05	64	28	02		01								
11A	7675-7676	32	68	0.05	01	14	03	12	02	Tr	Tr	59	09	VPS	A	L, T	30	4.5
					03	44	09	38	06									
11B	7790.5-7791	25	75	0.05	Tr	11	02	09	03	Tr	Tr	67	08	PS	A	T	10	4.5
						44	08	36	12									
12A	8658-8659	45	55	0.07	03	20	09	10	01	02	Tr	43	12	P-M	SA-SR	T	30	3.5
					07	44	20	22	02	02								
	8660-8661	As Above (slightly higher, ULF & F slightly lower)												As Above				
	8661-8662	As Above												As Above				
	8659-8660	51	49	0.08	05	32	06	04	02	02	Tr	37	12	MS	A-SA	L, T	40	3
					9	53	12	08	04	04								
12B	8643-8649	22	78	0.085	01	15	04	02	--	Tr	Tr	78	05	VPS	A-SR	T	10	3.5
					05	63	18	09	--									
	8642-8643	43	57	0.06	04	27	01	06	04	01	Tr	53	04	VPS	A-SA	L, T	40	3.5
					09	63	02	18	06	02								
	8653-8654	42	58	0.07	01	29	04	05	01	02	Tr	53	05	VPS	A-SR	T*	20	3
					02	69	10	12	02	05								
13	7669-7670	54	46	0.15	05	37	10	02	Tr	Tr	Tr	44	02	VPS	SA-A	L, T	20	3
					09	69	19	03										
	7683-7684	13	87	0.06	--	09	01	01	Tr	02	Tr	80	07	PS	A-SR	T	10	5
					--	69	03	08		15								
14	7935-7937	47	53	0.10	--	33	05	04	Tr	01	Tr	51	02	PS	A-SR	T*	20	3
					--	70	13	09		08								
15	7149-7150	6	94	0.045	--	--	--	06	--	--	--	91	03	--	--	--	--	5
	7152-7153	As Above																
	7155-7156	As Above																
	7157-7158	13	87	0.04	--	06	01	04	02	Tr	Tr	84	03	VPS	A-SA	T*	10	4
						45	03	31	15									
Oak.	7196-7197	89	11	0.15	05	50	24	06	01	03	Tr	11	Tr	MS-WS	A-SR	L	100	1
					05	55	27	07	01	03								

LEGEND

Texture

GR ----------Grains
M-C----------Matrix-Cement
MGS----------Median Grain Size (mm)

Composition

Ch----------Chert
Qm----------Monocrystalline quartz
F----------Feldspars
C----------Calcite
Mi----------Micas
ULF------Unidentified lithic fragments
HM----------Heavy minerals
Opq----------Opaques
Tr----------Trace

Fabric

SORT----------Sorting
VP----------Very poor
P----------poor
M----------Moderate
GR.SHP.----------Grain shape
A----------Angular
SA----------Sub-angular
SR----------Sub-rounded
R----------Rounded
WR----------Well rounded
PK. PROX.(%)------Packing proximity
o//ORI------Degree of parallel orientation

Degree of parallel Orientation

5: Matrix and elongate grains or structures parallel bedding direction.
4: As above; subparallel.
3: Matrix subparallel to grain boundaries and bedding direction.
2: Matrix parallel to grain boundaries.
1: Matrix and grains randomly oriented.

TABLE 3 : Summary of petrographic analysis.

petrographic analysis and summarizes the texture, fabric and composition of each sample. Angular to subangular grains comprise 6 to 93 percent of the samples and are very poorly to moderately sorted. Grain contacts are generally long and tangential, with a few concave-convex contacts and rare sutured contacts (Taylor, 1950). Most grains appear to be coated with clay minerals, but it is not possible to discern the details of the relationship between grains and clay minerals. Grains often occur in scattered aggregates that resemble cut and fill structures. These structures are the most common bedform and are usually accentuated by a slightly higher cement content that contrasts with the surrounding matrix-cement. The matrix-cement contains more disseminated organic material and opaques than areas of high grain content and small fractures filled with opaques often bend around grain aggregates. Occasionally aggregates have slumped into the underlying material. Opaques occur as spherical or lenticular, framboidal clusters and when lenticular, tend to parallel the bedding direction.

The mineralogy of the samples varies considerably in the overall abundance of each constituent, but partial percentages (the percentage of the grains that a mineral constituent comprises) reveal consistency within the grain population throughout the sample suite. By partial percentage, quartz is the dominant constituent, comprising as much as 82 percent of the grains. Plagioclase feldspars are present in some of the samples, but comprise less than 1 percent of

of the total feldspars. Potassium feldspars comprise up to 33 percent of the grains. Minor constituents (calcite, chert, micas and lithic fragments) comprise less than 10 percent of the grains. Heavy minerals and opaques are present in most of the samples.

Discussion

Characteristics prevalent throughout the sample suite that should be conducive to a high degree of parallel orientation are: (1) a low percentage of cement (Ingram, 1953); (2) a high percentage of clay minerals (Ingram, 1953; Gipson, 1966); (3) a high organic content (Odom, 1967; Gipson, 1965; O'Brien, 1968); (4) high compaction pressures (Meade, 1966; Bowles and others, 1969; Heling, 1970). Petrographic evaluation corroborates the findings of Ingram (1953) because areas that contain greater percentages of cement exhibit lower degrees of parallel orientation. Gipson's (1966) observation that increasing silt content is accompanied by a decrease in parallel orientation is substantiated. Figure 8 demonstrates the degree of parallel orientation is inversely proportional to the abundance of grains. (See SEM discussion.)

As grain content increases, the sediment undergoes a transition from matrix-supported to grain-supported. This affects the distribution of stress generated by compaction pressure. With high percentages of platy minerals, increasing stress is accommodated by increasing alignment of platy

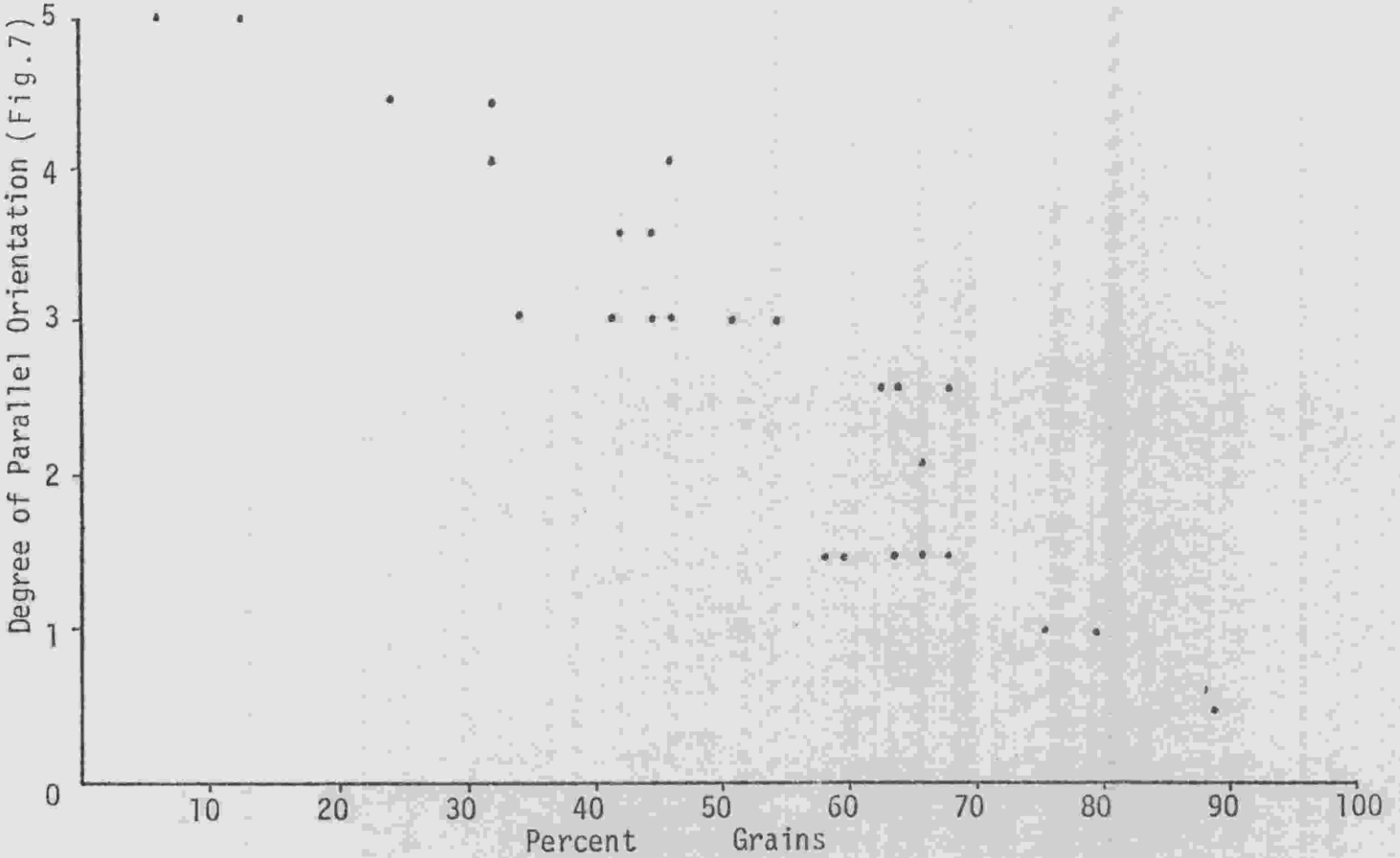

FIGURE 8 : Plot of grain percentage and degree of parallel orientation (see Fig.7).

minerals. As materials of higher sphericity (grains) increase in abundance, orientation planes for platy minerals are disrupted and platy minerals begin to bend around grain boundaries. This forms a closest packing arrangement of materials. When the sediment contains sufficient grains to be grain-supported, the stress is distributed along grain contacts with minimal effect on interstitial platy minerals.

Scanning Electron Microscopy

Introduction and Technique

Sample preparation required breaking small fragments from the core chips perpendicular to bedding. The fragments were mounted on metal stubs and coated with gold-palladium in a vacuum evaporator. An Etec Autoscan SEM provided good resolution at magnifications up to 20000X.

Specimens were examined at progressively increasing orders of magnification. At 200 to 500X the general texture and fabric were apparent. Small areas which exemplified various characteristics of the fabric were selected for more detailed examination (500 to 20000X). A few EDS (energy dispersive system) analyses aided in identifying constituents. The primary method of identification of clay minerals was by morphology (Wilson and Pittman, 1977; Gard, 1971). Authigenic components were measured to determine if they significantly affect the cumulative curves of size analyses, thus yielding erroneous data on the size distribution of the original sediment.

Authigenic Morphologies

Authigenic clay minerals occur in numerous morphologies. Several characteristics of authigenic clays aid in distinguishing them from allogenic clays. These include delicate morphology, distinct crystalline form, lack of compaction effects and occurrence as alteration products on grain surfaces. These criteria were used successfully by Ross and Kerr (1931) and Wilson and Pittman (1977).

Kaolinite occurs in the form of pseudohexagonal plates (Plate 1A). The plates more frequently occur in "face-to-face" arrangements resembling stacked books (Plate 1B). The kaolinite is authigenic and occurs only in primary (interstitial) and secondary voids (indentations on grains, basal clevage partings) (Plate 2A). Occasionally, the kaolinite bookstacks are distorted and tightly packed against allogenic clays (Plate 2B). This suggests that kaolinite formed as void fillings prior to the cessation of compaction. This characteristic morphology of kaolinite was recognized by Ross and Kerr (1930), Grim (1968) and Wilson and Pittman (1977). The individual kaolinite plates ranged from 2 to 10$_{\mu}$ in size with bookstacks being 3 to 10 in length.

A distinctive morphology of pore lining or grain coating clays resembles authigenic mixed-layer illite-montmorillonite as described by Wilson and Pittman (1977). A detailed examination of these clay minerals (Plate 3) reveals a "cardhouse" stacking of plates. The plates are characterized by lobate edges. Wilson and Pittman (1977) pointed out that

A. Individual kaolinite plates in pore (upper center); illite laths(?) on the surface and in basal clevage parting on mica grain (right) (1100X).

B. Pseudohexagonal interstitial kaolinite arranged in extended bookstacks (3100X).

PLATE 1

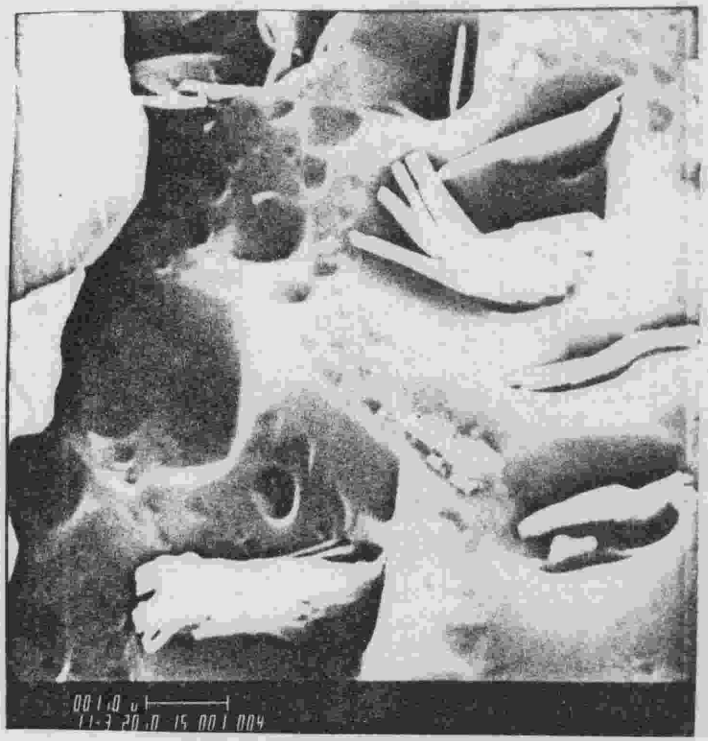

A. Kaolinite bookstack in pits on quartz grain (upper right); tube-like authigenic clay in pit (lower left) (11000X).

B. Distended kaolinite bookstack (upper center) (6000X).

PLATE 2

A. Mixed-layer illite-montmorillonite(?) in cardhouse arrangement; note lobate plate edges (5000X).

B. Mixed-layer illite-montmorillonite as in 3A (16000X).

PLATE 3

this morphology may be confused with a similar morphological occurrence of illite. The mixed-layer illite-montmorillonite(?) occurs in the fabric as pore linings (Plate 4A), grain coatings (Plate 4B), or fracture fillings (Plate 5A, B). The size of the individual plates ranged from 1 to 4μ in length, the majority being 3 to 4μ in length. Authigenic kaolinite bookstacks and mixed-layer illite-montmorillonite are the dominant authigenic clay mineral components, the latter being the most abundant.

Authigenic illite(?) occurs as alteration products on mica plates where it forms pillars connecting small voids between basal clevage partings (Plate 6A, B). The only other occurrence of illite(?) is in small (12μ) aggregates which appear to be composed of illite and kaolinite (Plate 7A, B). In both occurrences, illite appears as elongate blades or laths. The identification is uncertain since similar morphologies have been described for halloysites (Bates, 1971) and palygorskite (Vivaldi and Robertson, 1971). The illite(?) laths, however, did closely resemble illite laths depicted by Wilson and Pittman (1977). The laths varied from 1 to 7μ in length.

Numerous authigenic morphologies were not identifiable. Among these were tulip-bud (Plate 8A) and cabbage-head (Plate 8B) types. Only one occurrence of the previously undescribed tulip-bud morphology was observed. It was 8μ in length and 5.5μ in diameter. Cabbage-head morphologies composed of chlorite have been described by Wilson and Pittman

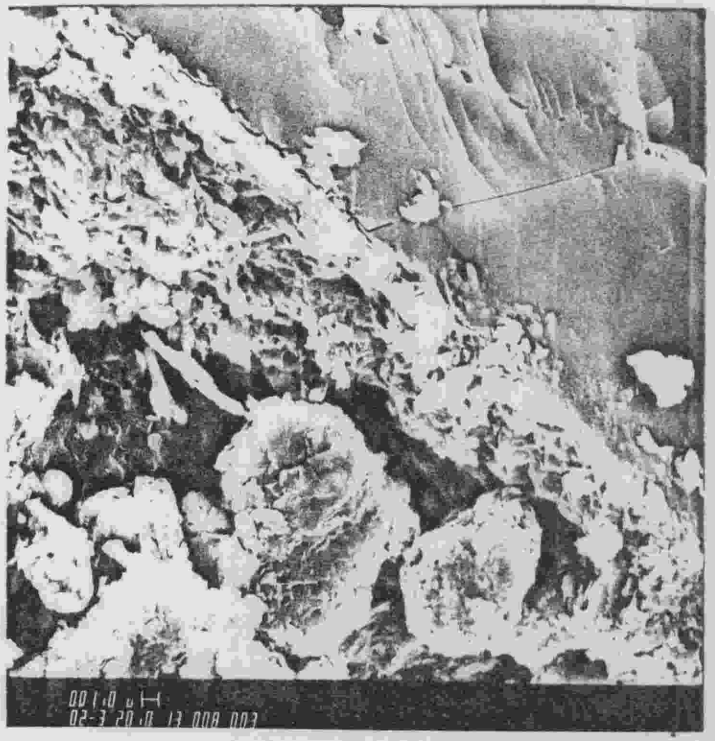

A. Pore-lining mixed-layer illite-montmorillonite (2000X).

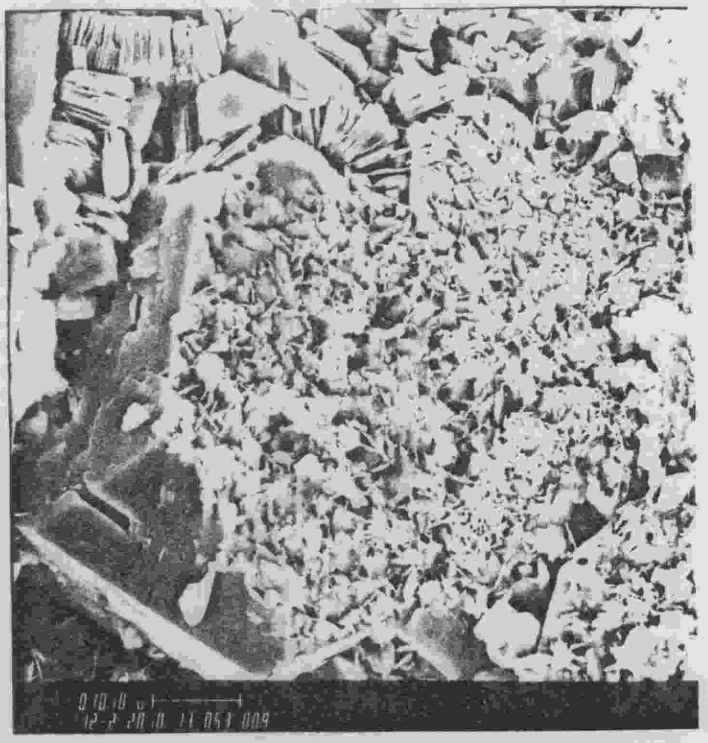

B. Kaolinite books in pore (upper left); grain coating illite-montmorillonite on anatase(?) grain (1200X).

PLATE 4

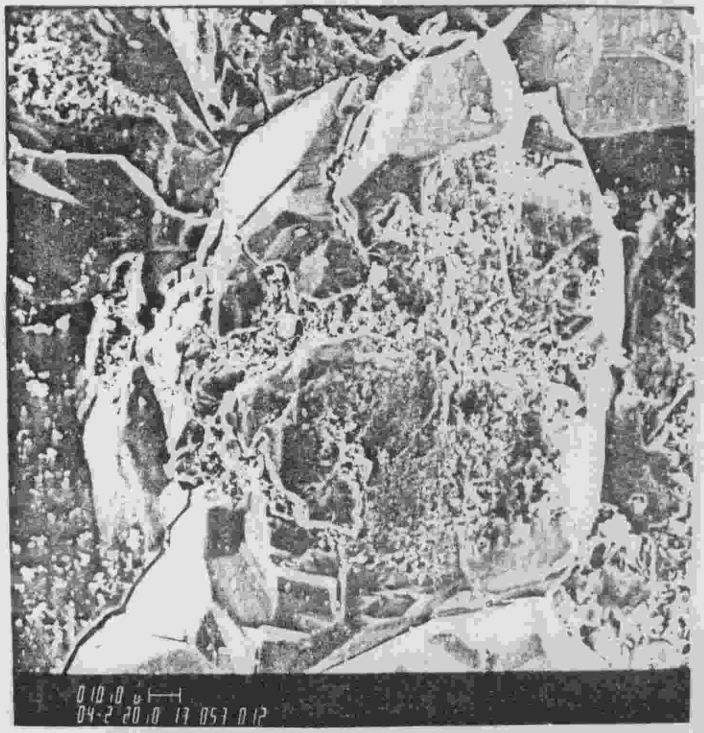

A. Quartz grain with distinct overgrowths; fracture in center filled with illite-montmorillonite (400X).

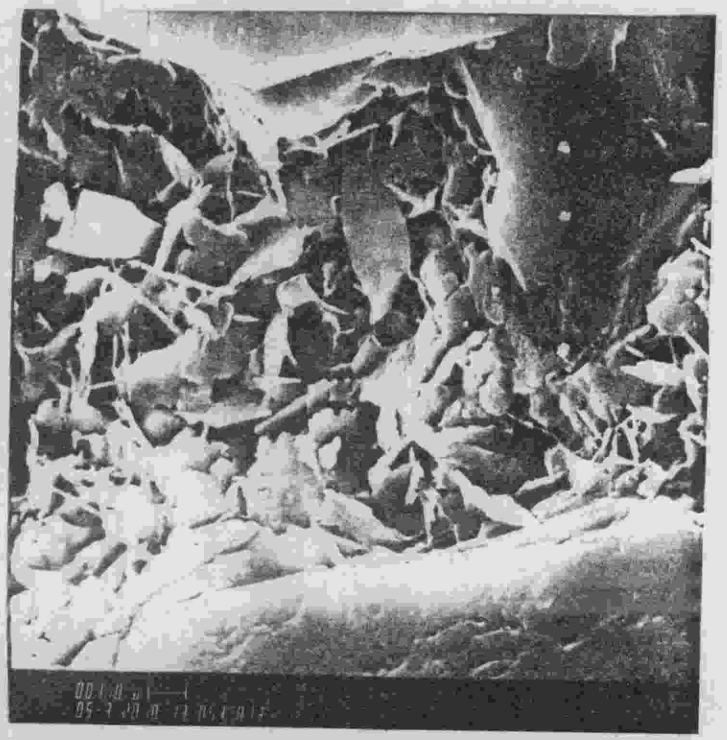

B. Illite-montmorillonite in fracture on grain shown in 5A (5000X).

PLATE 5

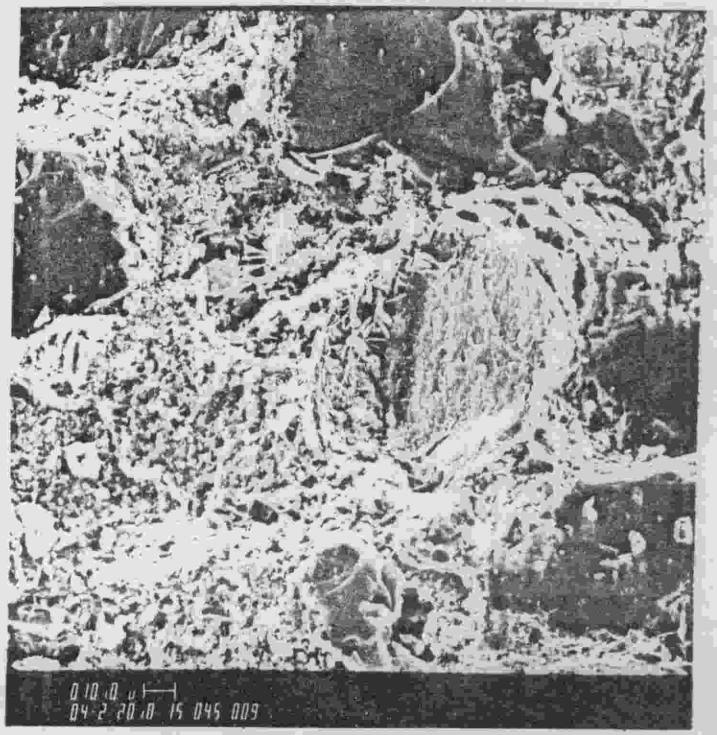

A. Mica grain (right center) with illite(?) laths projecting from surface. Kaolinite plates fill the void space to the left of the grain. Note the general lack of orientation due to high grain content (400X).

B. Highly magnified view of illite(?) laths on the surface of a mica grain. The laths form pillars in a basal clevage parting. Note the delicate morphology of the individual laths (8000X).

PLATE 6

A. Aggregate of illite(?) laths and rounded pseudohexagonal plates amidst sharply defined pseudo-hexagonal kaolinite which forms extended bookstacks (5000X).

B. Closer view of aggregate shown in 7A (15000X).

PLATE 7

A. Tulip-bud authigenic clay (12000X).

B. Cabbage-head type morphology composed of plates which curve outward and upward from the central portion of the structure. A more appropriate description for this new morphology would be rose-blossom structure (11000X).

PLATE 8

(1977). Two morphologies occur that superficially resemble cabbage-head chlorite but differ in detail. The cabbage-head type morphology illustrated in Plate 8B is constructed of plates that curve outward and upward from the central portion of the structure, much as the petals of a rose blossom. Cabbage-head chlorite depicted by Wilson and Pittman was a more dense, compact structure with a somewhat fibrous texture.

Another cabbage-head type structure (Plate 9A) superficially resembles the cabbage-head chlorite and chlorite rosettes depicted by Wilson and Pittman (1977); however, a closer examination (Plate 9B) reveals a structure consisting of numerous small plates ($<1\mu$) in an aggregate that exhibits no definite pattern or arrangement. Both forms of cabbage-head type structures differ from similar morphologies reported in other studies. Detailed EDS data will be required to identify the clay minerals in such structures.

Other authigenic clays resemble extended aggregates of plates (Plate 10A). In detail (Plate 10B), the structure is composed of face-to-face pseudohexagonal plates with somewhat rounded edges. The plates vary considerably in size (0.25 to 3.00μ) and are not symmetrically stacked (edges aligned) as kaolinite bookstacks tend to be. The plates resemble kaolinite, but identification is not conclusive. An annular structure of face-to-face, overlapping pseudohexagonal plates (Plate 11A) may be a unique morphology, but is more likely a distended kaolinite bookstack, the growth pattern having been determined by restricted pore space. A few tube structures

A. Cabbage-head type structures which have grown on pore-lining illite-montmorillonite (2300X).

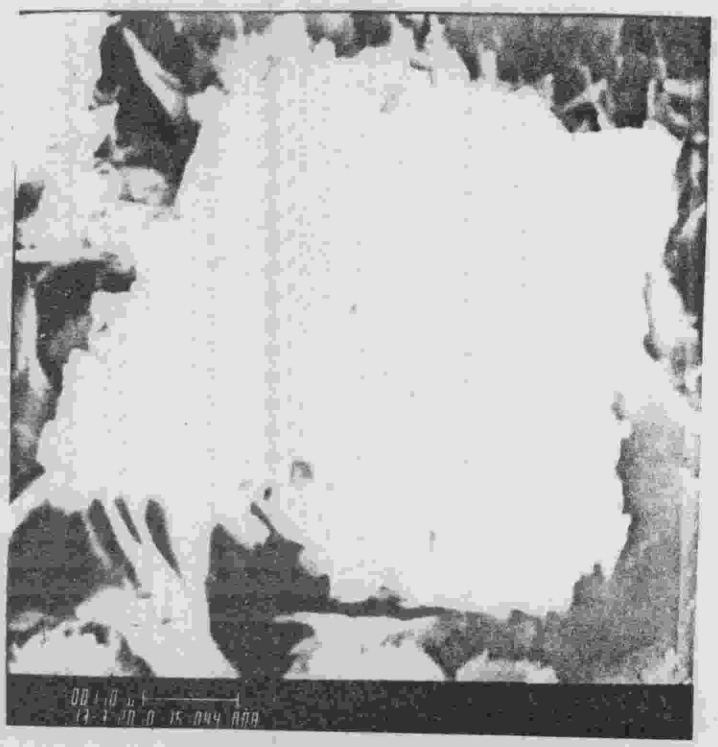

B. Detailed view of the cabbage-head type structures shown in 9A; the individual plates show no definite pattern or arrangement (13000X).

PLATE 9

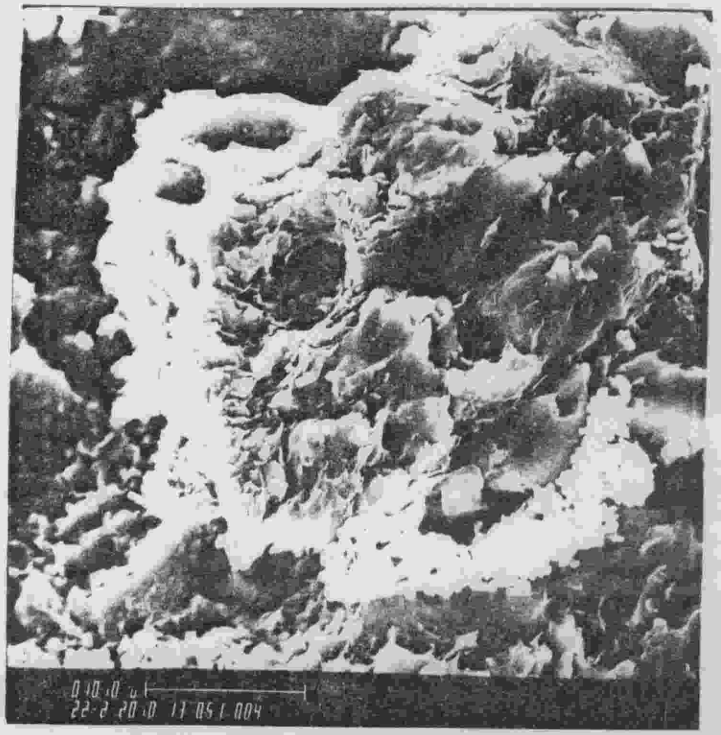

A. Clustered authigenic clays (lower right) on allogenic clays (2200X).

B. Higher magnification of structure shown in 10A. Individual plates are pseudohexagonal with rounded edges. Note the extensive variation in individual plate size (5000X).

PLATE 10

A. Annular arrangement of face-to-face overlapping, rounded pseudo-hexagonal plates; this may be a distended kaolinite bookstack (2000X).

B. Large tube-like structure (polygorskite? or hallyosites?); illite(?) laths and isolated authigenic clay plates also occur in the void (7000X).

PLATE 11

(Plate 11B) are present, but identification is difficult since several clay minerals are reported as having similar morphologies (i.e. halloysites, Bates, 1971; polygorskite, Vivaldi and Robertson, 1971).

The dominant non-clay mineral authigenic component is pyrite, which occurs as either lenticular (Plate 12A), or spherical (Plate 12B), framboidal clusters of euhedral crystals. High orders of magnification reveal mixed-layer illite-montmorillonite coatings (Plate 13A) or encasements (Plate 13B) around the pyrite grains. The pyrite was probably already present when the mixed-layer illite-montmorillonite began forming. Allogenic clays are distinctly foliated around pyrite clusters (Plate 14A, B). This indicates that the pyrite forms early in the diagenetic process, prior to significant compaction. Compaction causes the foliation of allogenic clays around the previously formed pyrite. Individual pyrite crystals range from 0.25 to 1.5μ.

Calcite cement (Plate 15A) is common in most of the samples, but anatase(?) occurs in only one sample (Plate 15B). The identification of anatase(?) is based on similar morphologies depicted by Flesch and Wilson (1974). Mixed-layer illite-montmorillonite coatings occur on both calcite cement and anatase(?), indicating that they form prior to the formation of mixed-layer illite-montmorillonite. Quartz overgrowths are also present (Plate 5A).

Sizes previously mentioned for authigenic components range from 1 to 10μ. The most abundant authigenic components

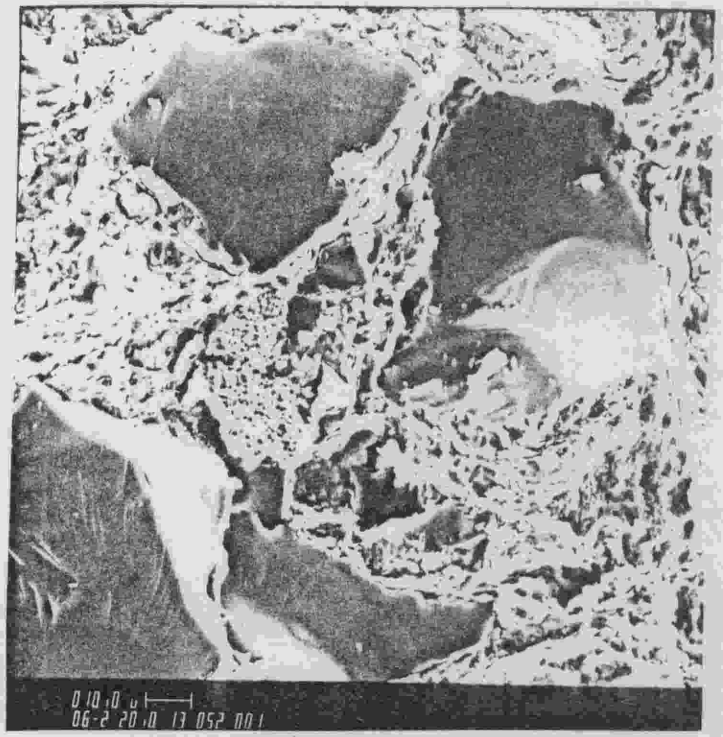

A. Lenticular framboidal cluster of authigenic pyrite in foliated allogenic clays amidst very fine sand (quartz) and silt grains; note the distinctive conchoidal fracture on the quartz grains (600X).

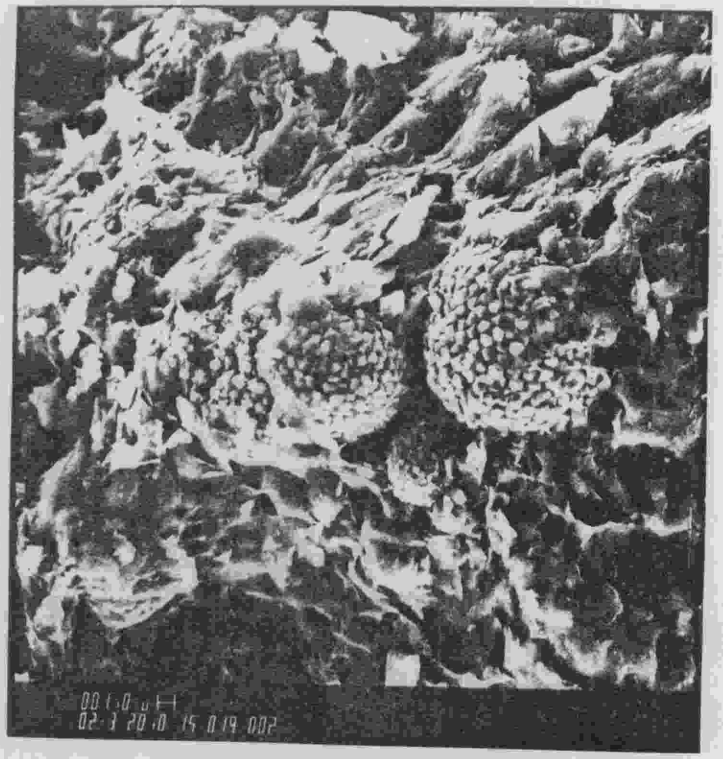

B. Spherical framboidal clusters of authigenic pyrite in allogenic clays (2000X).

PLATE 12

A. Cluster of euhedral pyrite crystals in allogenic clay fabric; note the small amounts of authigenic clay growing on and amidst the crystals (4000X).

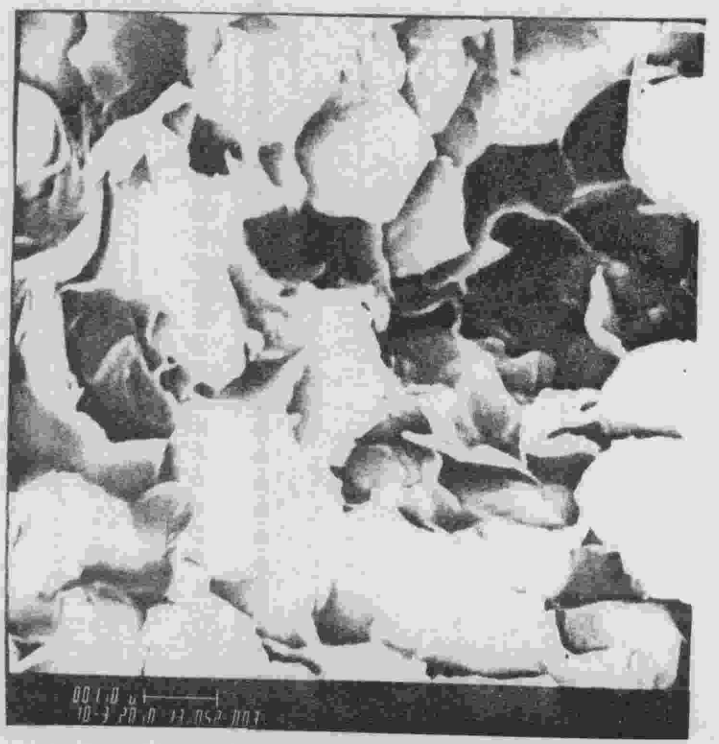

B. Encasements of authigenic clay (illite-montmorillonite?) which have formed around pyrite crystals (10000X).

PLATE 13

A. Distinct foliation of allogenic clays around pyrite clusters; this is indicative of pyrite formation prior to significant compaction (3000X).

B. Individual crystals of pyrite amidst foliated allogenic clays; note the foliation of allogenic clays parallel to the pyrite crystal which was removed during sample preparation (lower left) (3000X).

PLATE 14

A. Authigenic calcite cement (1100X).

B. Grain-supported fabric reveals extensive authigenic crystal development; kaolinite bookstacks (upper center); grain-coating illite-montmorillonite on anatase(?) grain (center) (400X).

PLATE 15

(kaolinite and illite-montmorillonite) range in size from 1 to 15μ, the majority being 3 to 10μ. This size range (0.001 to 0.015mm) involves a substantial portion of the sediment sizes measured by pipette analyses. A significant error is introduced into such analyses by the presence of authigenic material. Since authigenic components are more abundant in siltstones or very fine-grained sandstones, the pipette analysis of the pan fraction of such sediments may contain considerable error. The 0.001 to 0.015mm fraction, usually considered to be entirely allogenic, may be entirely authigenic. Siltstones or sandstones that appear to contain a significant quantity of fine material may have actually been very well sorted at the time of deposition.

Allogenic Components and Fabric

Allogenic components (mainly clay minerals and detrital silt and sand) are readily recognized by their fragmented or abraded textures. Silt and sand grains are angular and disrupt parallel orientation. Some parallelism between clay minerals is evident throughout the sample suite; however, the planes of parallelism are not necessarily parallel to bedding planes because of local disruptions in the fabric. Disruptions are dependent upon the grain (coarse silt and sand) content. A sample with a low percentage of silt (Plate 16A) exhibits a high degree of parallel orientation. Even at very high magnification (Plate 16B), the high degree of parallel orientation is evident. The shape of the grain is also a factor in the

A. A clay fabric with low silt content exhibits a high degree of parallel orientation (2100X).

B. Even at high magnification the fabric shown in 16A still exhibits strong parallel orientation (7000X).

PLATE 16

degree of disruption of the fabric. Flat, slab-like grains (Plate 17A) disrupt parallel orientation to a lesser degree than particles approximating a spherical configuration (Plate 17B) because the plane of greatest dimension of the slab-like grain tends to align parallel to the plane of greatest dimension of the clay minerals. As compaction pressures increase, realignment of clay minerals occurs; the clay minerals are contorted or flow around grains (Plate 18A); consequently, the higher the grain content, the greater the distortion of the fabric (Plate 18B). In such fabrics (Plate 18A, B), small fractures are often present between grain surfaces and adjacent allogenic clays. The fractures may be due to unloading effects as the core chips were taken from depths up to 7800 ft. Since the samples are well indurated, it is more likely that the fractures or channels are present at depth. The channels probably serve as permeable conduits for fluids. This indicates that during compaction migrating fluids are channeled along grain surfaces or laminae adjacent to grain surfaces.

Some samples (Plate 19) have unusually high grain contents and the disruptive effect of the grains on the fabric is evident (Plate 19A). In such cases, the individual clay minerals tend to parallel one another, but the overall parallelism of the sediment diminishes. When a sediment is very nearly grain-supported (Plate 19B), the configuration of the clay minerals spatially assumes the near intergrain configuration. In grain-supported fabrics (Plate 20A),

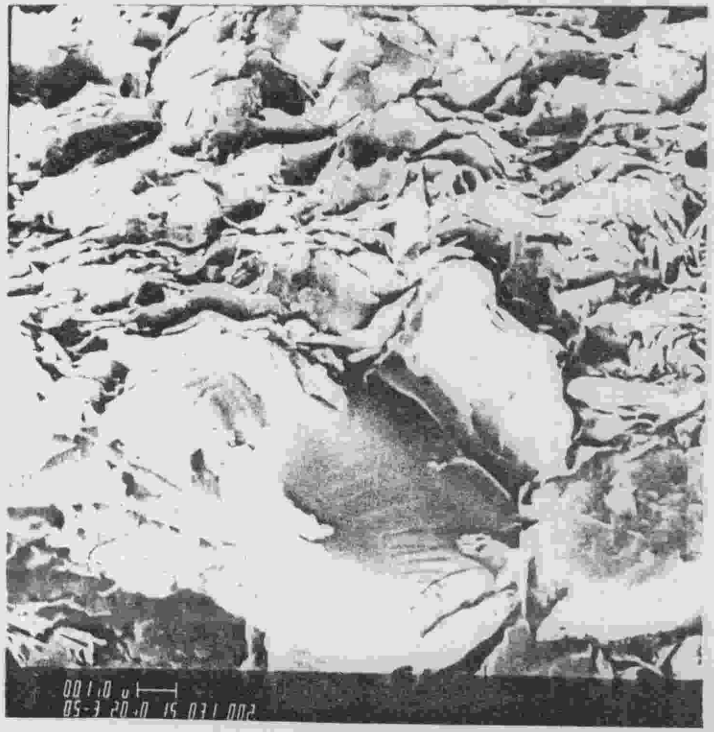

A. Slab-shaped detrital grains may have less disruptive effects on allogenic clay fabrics than spherical grains (5000X).

B. Spherical grains tend to disrupt allogenic clay fabrics more than platy detrital grains (7000X).

PLATE 17

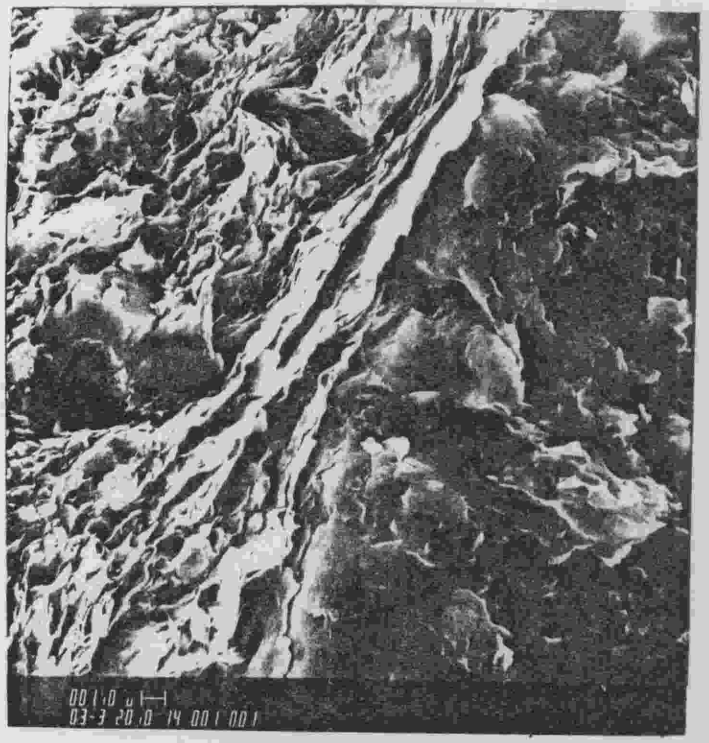

A. Flowage of allogenic clays parallel to grain surface; the partings in the clay laminae adjacent to the grain boundary may be pore-fluid channels (3000X).

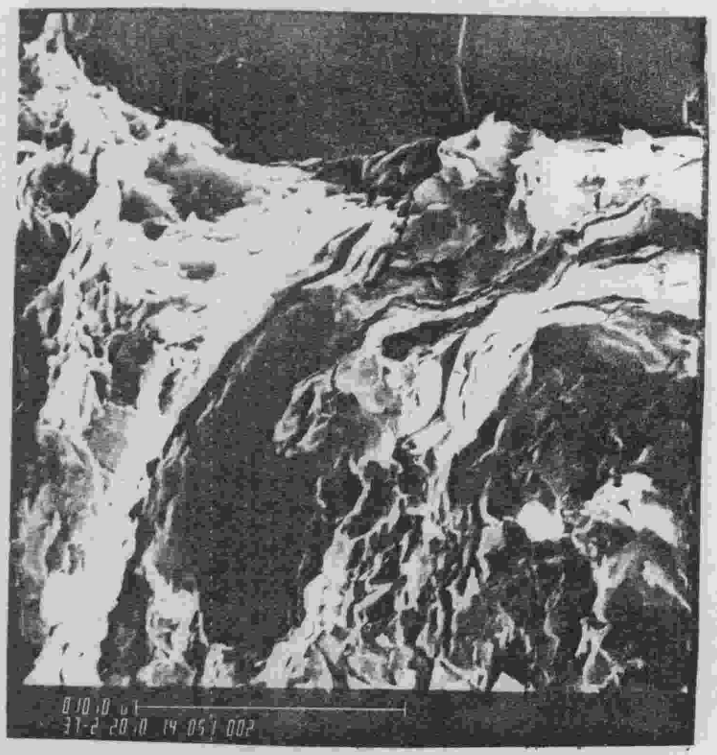

B. Foliation trends which intersect and have disruptive effects on the overall preferred orientation of the sediment (3700X).

PLATE 18

A. This area of high grain content exhibits the general disruption of fabric caused by increasing grain content (2000X).

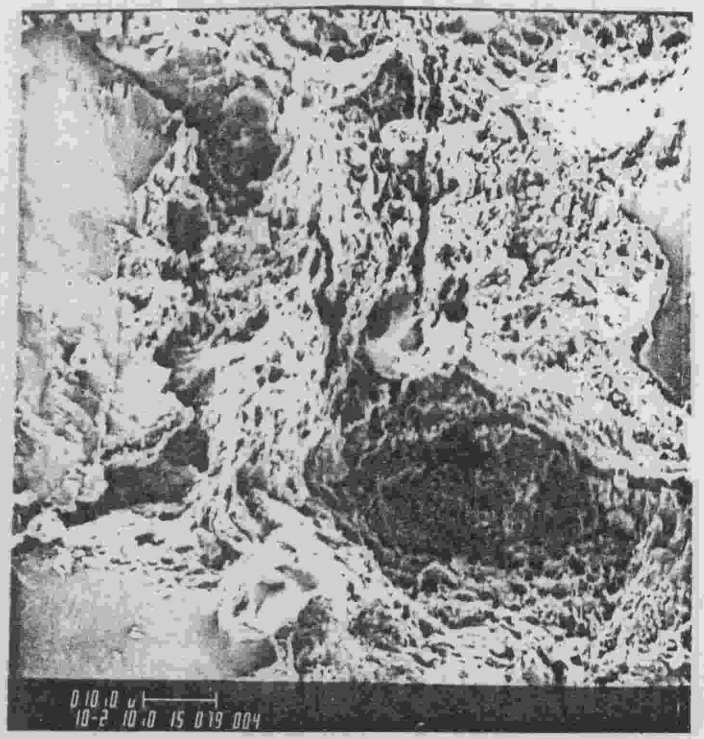

B. The area above illustrates the configuration of the clay fabric when the sediment is approaching a grain-supported fabric. The allogenic clays are forced into the near interstitial configuration (1000X).

PLATE 19

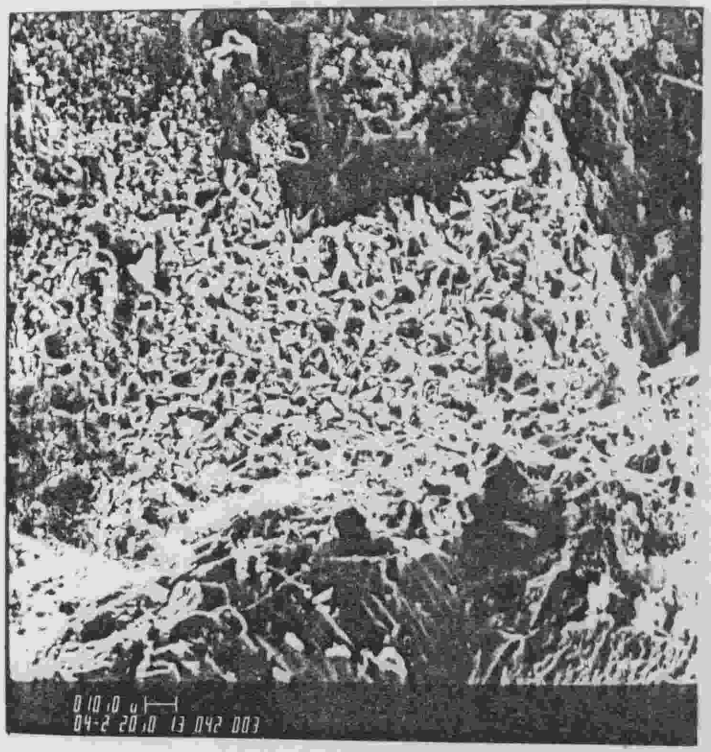

A. The clays in the interstitial area of this grain-supported fabric show no foliation (400X).

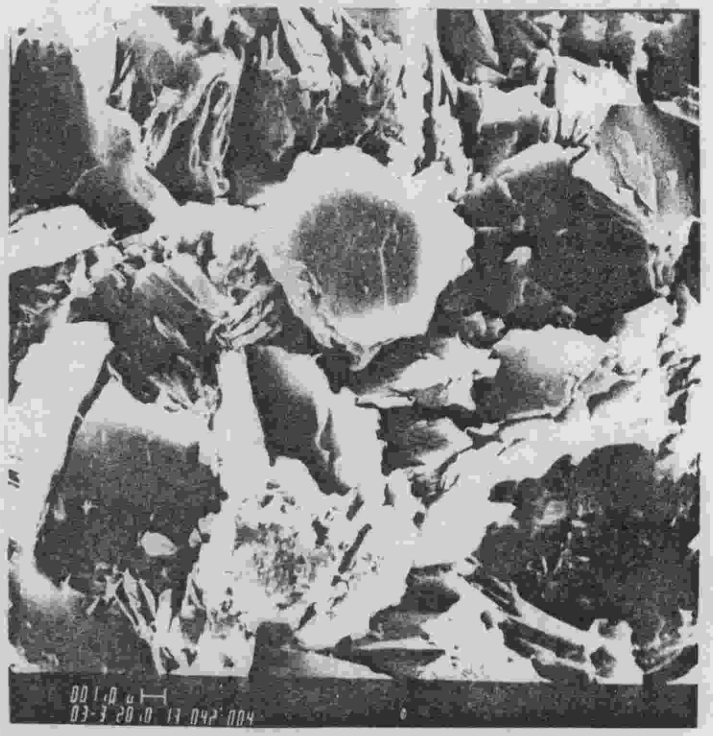

B. A closer examination of the interstitial clays shown in 20A reveal abraded plates indicating that they are allogenic, yet no foliation is evident (3000X).

PLATE 20

compaction pressures are apparently dispersed through the grain framework. Even at high magnification (Plate 20B), there is little evidence of compaction effects on the interstitial allogenic clays; their arrangement is essentially random.

High magnification of allogenic clay mineral fabrics (Plate 21A, B) reveal the nature of the pore configuration. Pore spaces are lenticular or tabular in shape with width to height ratios generally exceeding 10:1 and often reaching 30:1 (Fig. 9A).

A. Typical pore space in allogenic clay fabric.

B. Possible contorted pore space in allogenic clay fabric.

FIGURE 9: Pore configurations in allogenic clay fabrics.

Wijeyesekera and Freitas (1976) suggested that dissipation of high pore-fluid pressures could lead to contorted pore-fluid channels and, perhaps, fissures. Such channels were occasionally observed (Fig. 9B). Fractures or channels adjacent to grains (Plate 18A, B) likely result from high pore-fluid pressures.

Despite the small dimension of the pore spaces (0.2μ height, 30.0μ width), they appear somewhat permeable. Since porosity and permeability measurements indicate very low permeabilities, the third dimension of the pores (length) must

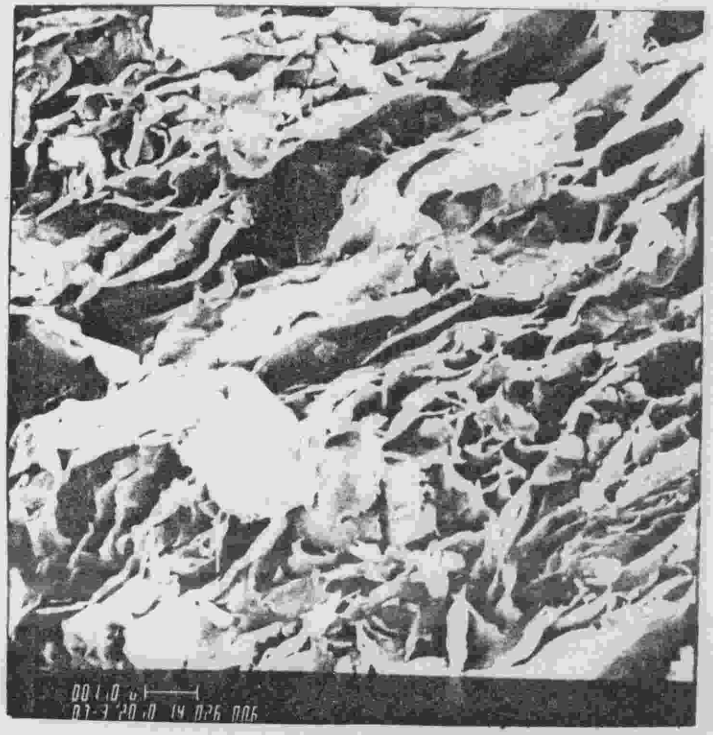

A. A detailed examination of an allogenic clay-supported fabric reveals pore configuration; note the lack of authigenic components (7000X).

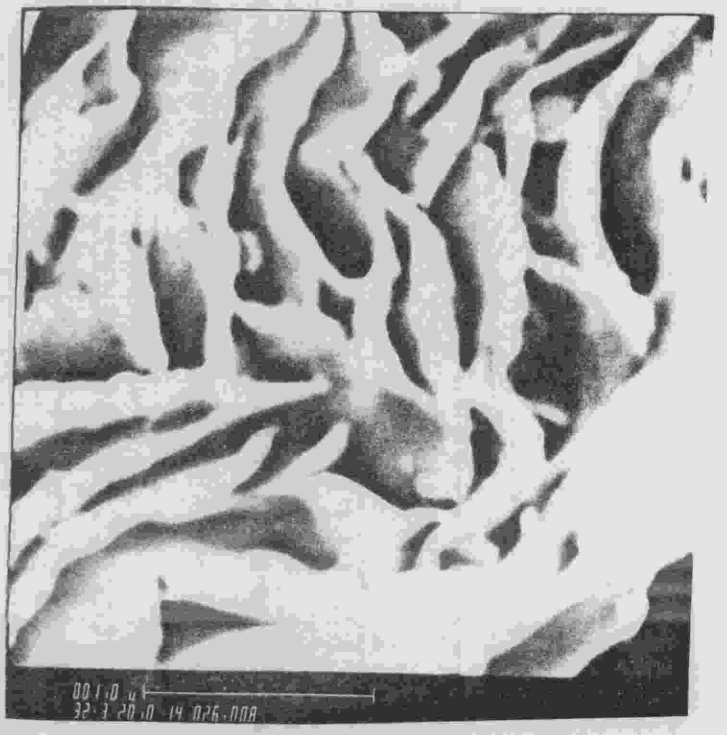

B. Increased magnification (32000X) of the fabric exhibited in 21A shows normal lenticular pores and a possible distorted pore-fluid channel (lower left).

PLATE 21

be relatively limited.

In progressing from grain-supported to matrix-supported fabrics, a marked decrease in the abundance of authigenic components occurs. The only authigenic mineral observed in matrix-supported fabrics is pyrite. High magnification of matrix-supported fabrics (Plate 21A, B) reveal no authigenic clays. Bucke and Mankin (1970) felt that permeability is the basic control of the degree of diagenesis. Apparently, pyrite forms while the sediment fabric is still open, perhaps within meters or a few tens of meters of the sediment-water interface. Samples containing dominantly grain-supported fabrics (Plate 4B, 6A) reveal abundant authigenic minerals. Almost no authigenic minerals occur in matrix-supported fabrics. Permeability in sediments composed dominantly of clay minerals must be significantly reduced prior to the initiation of significant authigenic mineral development.

Discussion of Fluid Migration

Burst (1969) described three stages of dehydration in Gulf Coast clay-rich sediments. Water in clay-rich sediments occurs in four forms: (1) water in pores, on the surfaces and around the edges of the discrete particles of the minerals composing the clay material; (2) interlayer water between the unit-cell layers; (3) water that occurs in tubular openings between elongate structural units; and (4) OH lattice water (Grim, 1968). In Burst's study, the original sediment

contained about 23% solids and 77% water. Pore water comprised 70% of the sediment; interlayer water 7%. Water in tubular openings in certain clays requires essentially the same energy for removal as interlayer water; consequently, it will be considered as interlayer water. Burst's first dehydration stage could be referred to as compaction dehydration, since overburden pressure is the primary mechanism. During compaction dehydration, pore water is reduced from 70% of the sediment (by volume) to 10%; interlayer water is not removed, therefore, it comprises about 20% of the sediment after compaction dehydration. Compaction dehydration is usually completed in the first thousand feet of burial. Because the overall sediment density is low and resistance to flow is minimal, it is not likely that distorted pore-fluid channels develop during compaction dehydration.

Burst's second stage dehydration is the initial thermal dehydration. The sediment water density has become sufficiently high to resist the effects of compaction. With increased depth of burial, more heat is absorbed by the sediment until heat accumulation is sufficient to mobilize pore water and one of the two remaining interlayer waters. During initial thermal dehydration, about 50% of the remaining water is removed. Pore water is reduced from 10% to 5% of the sediment; interlayer water from 20% to 11%. Because the sediment water density is high and resistance to flow is high, contorted pore-fluid channels probably develop during initial thermal dehydration. This movement of fluids is the last

major mobilization of interstitial fluids.

Burst's third stage dehydration is the progressive increase in temperature until the final structural water is driven from the clay lattice. This last stage involves "tens or possibly hundreds of millions of years for completion".

Perhaps the last major removal of fluids by initial thermal dehydration results not only in contorted pore-fluid channels, but also in the collapse of such channels and a reduction in permeability. This collapse might follow the removal of the pressure-supporting pore fluids. The fabric of such fine-grained sediments would probably show a transition from open interparticle channels to open contorted pore-fluid channels, to closed channels. This transition might be coincident with a transition from compaction dehydration to the latter stages of initial thermal dehydration. The collapse regime likely migrates from higher temperature to low temperature regimes. A mobilization front might occur updip from the collapse regime. Further studies may reveal a relationship between the abundance of contorted pore-fluid channels and the direction of hydrocarbon migration. Hydrodynamic models of pore spaces should reveal the approximate fluid pressures that occurred within a basin during initial thermal dehydration. Detailed examination of the fabric of fine-grained sediments will lead to a better understanding of the dynamic evolution of sedimentary basins.

Authigenic Processes and Hydrocarbon Migration

As evidenced by the abundance of authigenic components in grain-supported fabrics, permeability appears to be the basic control of the degree of authigenic mineral growth during diagenesis. If earlier observations as to the collapse of shale fabrics and the reduction of permeability (refer to discussion of fluid migration) are correct, the fluids (i.e. water, hydrocarbons) in the clay fabrics must migrate into grain-supported fabrics before authigenic processes begin. Bucke and Mankin (1970) recognized organic material and water-filled pores as contributing to the growth of kaolinite. The migration of water and organic type fluids from clay fabrics to grain-supported fabrics may initiate authigenic mineral growth. In contrast, Webb (1974) observed that authigenic clay minerals occurred in some sandstones lacking hydrocarbons and some sandstones containing hydrocarbons lacked such minerals. He concluded that hydrocarbon migration displaced formation waters before or shortly after kaolinite precipitation began and precipitation of clay minerals continued where hydrocarbons had not penetrated. If the migration of hydrocarbons from clay fabrics to grain-supported fabrics initiates clay mineral precipitation, Webb's latter observation is incorrect. As to his former observation, it is likely that hydrocarbon migration displaces formation waters before kaolinite precipitation begins.

A question still remains. Why did Webb find no hydrocarbons in sandstones containing authigenic clays? Perhaps

precipitation of pore-filling clays forces the hydrocarbons into open interstitial areas. Since authigenic clays gradually diminish pore volume, hydrocarbons are forced to move into other areas. In basins where grain percentages in clay fabrics vary considerably, migration of fluids from clay fabrics to grain supported fabrics probably occurs differentially in response to fabric variations. Clay mineral precipitation could be differentially initiated in such a basin. Thus Webb's final conclusion that areas of clay mineral precipitation could serve as seals preventing further hydrocarbon migration and with subsequent tectonic activity could preserve hydrocarbon traps in unlikely structural settings, is still reasonable. If such a trap were enclosed by clay mineral precipitation fronts, sediments of seemingly nominal permeability might be excellent producers due to very high reservoir or pore-fluid pressures. Such a system might show a sharp decline in production with moderate decreases in reservoir pressures because of nominal permeabilities. Secondary recovery methods would likely restore production rates, particularly methods that would restore original reservoir pressures or reservoir communication.

Summary

Authigenic clays occur as primary void fillings (pores), secondary void fillings (pits on grain surfaces and basal clevage partings), pore-linings or grain-coatings and fracture

fillings. Authigenic clays are readily recognized by their delicacy of morphology and occur dominantly in grain-supported fabrics. The dominant authigenic clays are kaolinite, which occurs as void fillings, and illite-montmorillonite(?), which occurs as pore-linings. The occurrences of authigenic clays are essentially the same as those recognized by Wilson and Pittman (1977). Tulip-bud, cabbage-head type structures, and other authigenic clays vary from morphologies described in previous works. Authigenic pyrite is present in most samples, but is more abundant in samples composed dominantly of clays. Pyrite probably forms early in diagenesis, while kaolinite and illite-montmorillonite probably form during initial thermal dehydration. Kaolinite formation may be related to hydrocarbon migration.

Allogenic components (clays and grains) are recognized by their fragmental or abraded textures and foliation. Clay fabrics reveal possible contorted pore-fluid channels that may be related to initial thermal dehydration. Grains tend to disrupt clay fabrics, increasing grain content generally resulting in decreasing degree of parallel orientation.

Radiography

Introduction

Radiography is the imaging of samples with penetrating radiation. It is an inexpensive and nondestructive process that reveals primary sedimentary structures (cross stratification, lamination, slump structures) and mineral

distribution that petrography and SEM often fail to reveal. Differential absorption and selected diffraction cause the image recorded on x-ray film.

Techniques

A Philips x-ray unit (Cu/Ni) was used as a radiation source. The samples were cut into slabs 0.3mm thick and placed between the x-ray port and a film packet. Samples were irradiated for 2 seconds.

Results

The radiographs reveal laminae, cross stratification and pyrite distribution. Pyrite occurs as black patches (Plate 22A) and is more abundant in darker areas that contain abundant matrix and disseminated organic material. The lighter areas contain relatively higher percentages of grains. The contrast between the light and dark areas reveals bedding trends. The most common bedding form is lenses of sand and silt that interfinger with areas of high matrix content (Plate 22B). Thin sections show that the lenses contain more cement than the surrounding matrix and are separated from the matrix by small fractures that are filled with authigenic pyrite. The lenses are irregular, discontinuous and resemble cut and fill structures. A few specimens contain distinct, straight laminae (Plate 23A). These laminae are caused by alternating fine and coarse material and are accentuated by lenticular, framboidal clusters of pyrite. Other laminae are irregular and discontinuous (Plate 23B), but generally

A. Black patches are pyrite; lighter areas contain higher grain population.

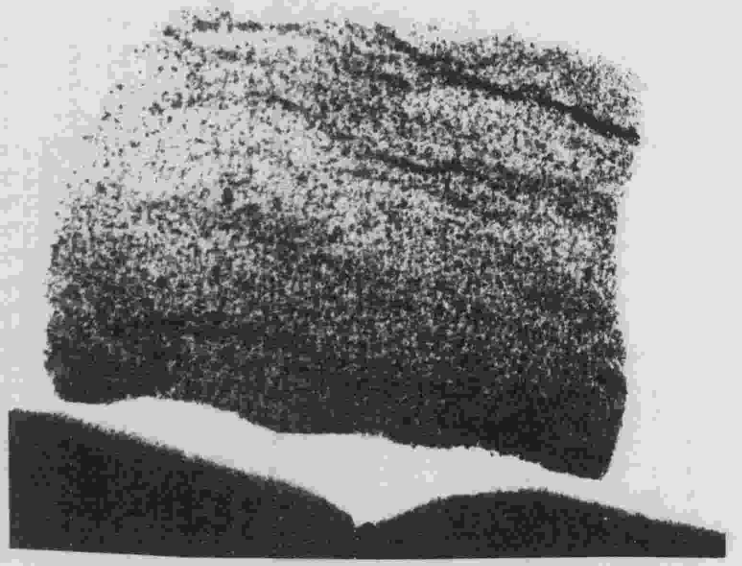

B. Irregular and lenticular bedding forms.

PLATE 22

A. Straight laminae.

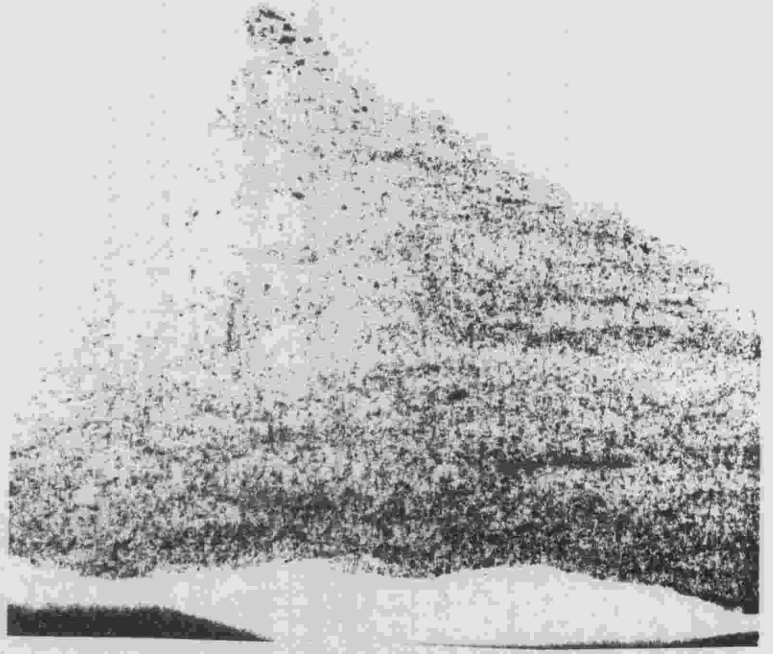

B. Irregular, discontinuous laminae.

PLATE 23

parallel bedding planes.

The features evident in the radiographs are generally more distinct in thin sections. The samples are poorly sorted; consequently, variations in material size and composition serve to reveal details of sedimentary structures. Radiography is more useful for moderately to well sorted sediments in which petrographic analysis fails to reveal sedimentary structures (Hamblin, 1962). Radiography will probably prove useful in fine-grained sediments that are well sorted.

Porosity and Permeability

Introduction

Standard porosity and permeability measurements were obtained from well files. Average porosities and permeabilities are calculated for several sample intervals (Table 4). Two whole core specimens were evaluated at SCAL (Special Core Analysis Laboratory) of Core Laboratories, Inc. SCAL mounted each core plug in the form of a right cylinder using epoxy plastic. Air permeabilities and Boyle's law porosities were determined on each core plug (Table 5).

Discussion

SCAL calculations show variations in permeability measured at different angles to bedding. Both samples measured have low grain content and exhibit a moderate (3) to high (4.5) degree of parallel orientation. A high degree of parallel orientation should result in maximum permeability

WELL	SAMPLE INTERVAL DATA	SPECIFIC INTERVAL	AVERAGE POROSITY(%)	AVERAGE HORIZ. PERMEABILITY (md)
1A	7321-7330	----------	6.0	0.01
		7329-7330	6.0	0.01
3	8262-8273	----------	2.9	0.01
		8262-8263	2.7	0.02
		8268-8269	2.8	0.01
		8272-8273	2.9	0.01
4	7410-7421	----------	3.5	0.01
		7410-7411	3.0	0.01
		7415-7416	3.1	0.01
		7420-7421	3.9	0.01
5	7450-7451	----------	4.5	0.01
		7450-7451	4.5	0.09
		7457-7458	5.0	0.01
6	7365-7380	----------	5.6	0.09
		7366-7367	7.3	0.05
		7370-7371	6.0	0.37
		7373-7374	6.5	0.03
7	7315-7329	----------	5.0	0.01
		7318-7319	5.8	0.01
		7324-7325	5.4	0.01
9	8467-8473	----------	2.7	0.09
		8467-8468	2.9	0.06
10	7608-7616	----------	10.7	0.12
		7610-7611	12.5	0.08
		7615-7616	9.2	0.02
12A	8656-8662	----------	3.9	0.01
		8658-8659	3.0	0.01
		8659-8660	2.7	0.01
		8660-8661	5.5	0.01
		8661-8662	5.5	0.01

TABLE 4 : Average porosity and permeability of sample intervals for which standard core analysis data is available. Specific data is shown for intervals from which thin sections were made.

SAMPLE NUMBER	AIR PERMEABILITY MILLIDARCYS	POROSITY, PER CENT	ANGLE TO BEDDING, DEGREES
11A	0.032	0.5	30
	0.002	1.2	60
	0.002	0.5	90
	0.003	0.5	0
2	0.002	1.0	30
	0.016	1.2	60
	0.002	1.0	90
	0.017	0.7	0

TABLE 5 : Porosity and permeability data acquired from Special Core Analysis Laboratory, Core Laboratories. Permeability is shown at various angles to bedding.

horizontal to bedding. Maximum permeability occurs at angles of 30 and 60 degrees to bedding. These angles indicate possible conjugate shears but no fractures are present. Porosity variations are the result of slight variations in the core plugs extracted from a 1 ft. interval of the core samples. As evidenced in thin section analysis, grain content varies significantly over short vertical distances. The porosities and permeabilities are very low, but similar trends may exist in sediments of greater porosity and permeability. The effective reservoir drainage of wells may be significantly better than is indicated by conventional horizontal and vertical permeability measurements. Directional permeability trends should also be evaluated in potential nuclear waste disposal sites. More extensive studies are warranted to further evaluate directional permeability in fine-grained sediments.

Clay Mineralogy

Techniques

The samples were mechanically disaggregated and the clay-sized fraction was isolated by standard pipette procedures. Wadell's (1936) modification of Stoke's law (1851) was used in calculating the settling velocities. This modification essentially compensates for the deviation of platy minerals from perfect spheres.

Concentrated clay slurries were placed on slides and dried in a desiccating jar. The slides were examined using

a Phillips x-ray diffractometer (Cu/Ni). Patterns were run from 2 to 37 degrees. X-ray patterns were made of untreated, glycolated (24 hrs., 24°C), and heat treated (550°C, 1 hr.) samples.

Thorez' (1975) techniques for describing mixed-layer clays are used in the following discussion to analyze the x-ray diffraction patterns.

Results

The only changes that occur in the clay mineralogy in the sample suite are slight changes in the mixed-layer structures. This consistency permits the construction of a type pattern (Fig. 10) that illustrates the behavior of the mixed layers when subjected to glycolation and heat treatment.

The lack of rational indices and the presence of a broad diffraction maxima between 9 and 14 Å indicate that the mixed-layer clays are randomly interstratified. After glycolation, the 10 to 12 Å portion of the pattern diminished significantly and the 12 to 14 Å area diminished slightly in intensity. The loss of portions of the diffractogram indicated the presence of an expandable component in the mixed-layer structure. The sharp peak at 7 Å was unaffected. After heat treatment, the 7 Å peak was destroyed. The peaks at 10 Å and 14 Å became noticeably intensified. The peak at 12 Å was more clearly defined, although lower in intensity than the peaks at 10 and 14 Å. The intensification

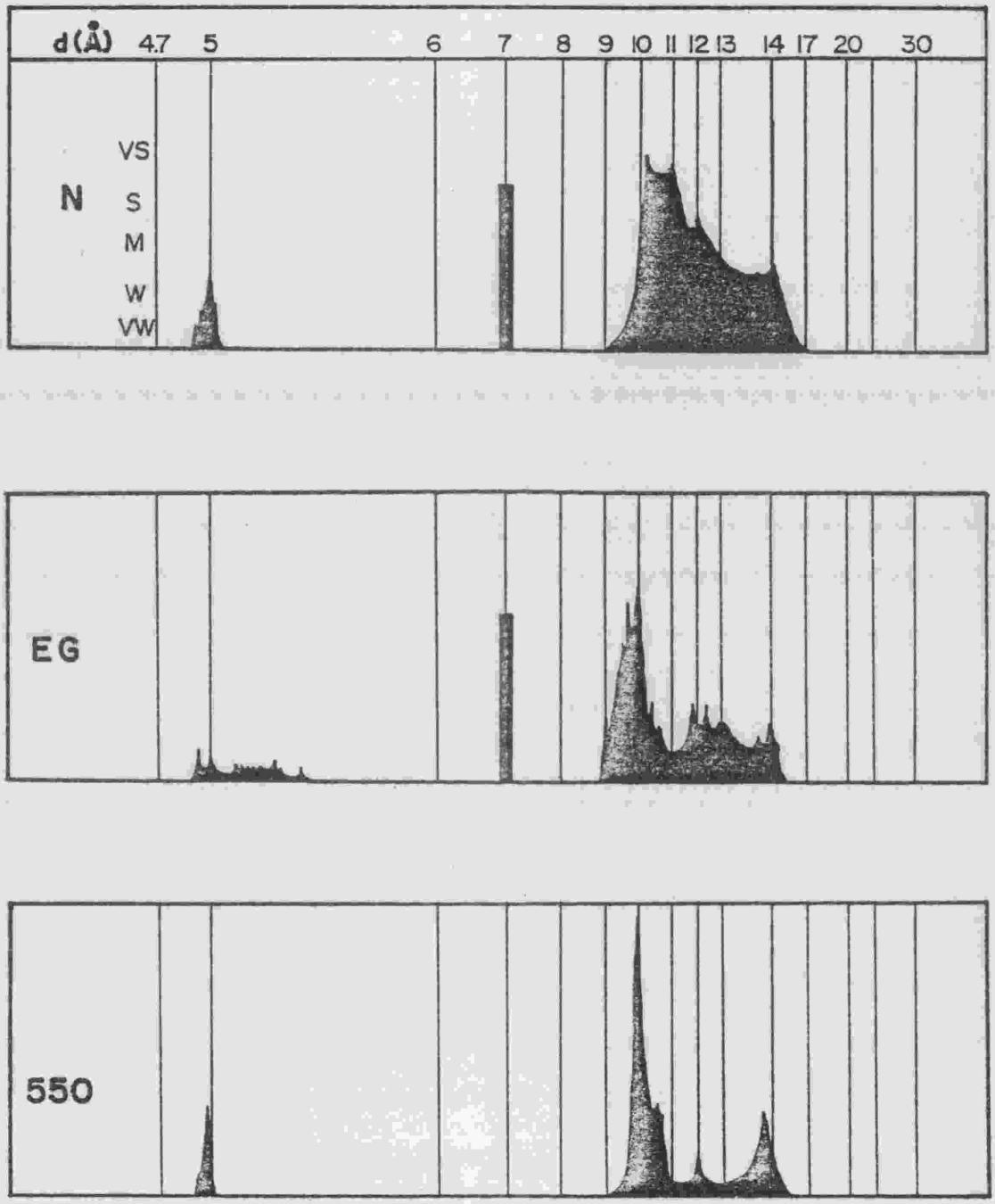

FIGURE 10: Type x-ray pattern of clay minerals in the sample suite obtained for untreated (N), glycolated(EG) and heat treated (550°C) samples.

of the peaks at 10 and 14 Å indicate the presence of illite and Mg-form chlorite (Carroll, 1970). The expandable component between 11 and 14 Å is a member of the montmorillonite group. The 7 Å peak which was destroyed by heat treatment indicated the presence of kaolinite. The peak at 5 Å verified the presence of the montmorillonite-chlorite components, first by the change in pattern upon glycolation, then by an intensity increase upon heat treatment.

The clay minerals present are kaolinite and a mixed-layer structure containing illite, montmorillonite and Mg-form chlorite. The nature of the mixed-layer structure can be defined by applying Thorez' (1975) system of codifying mixed-layer clay minerals, inspired by the work of Lucas (1963) and Thorez and others (1967, 1973). Thorez uses a system of hemicyclograms and monograms which essentially depict the behavior of numerous examples of mixed-layer clays in response to various treatments (glycolation and heat treatment).

Thorez designates the nature of the crystallites by the codes 10, 12 and 14 which are related to the interlayer spacing in angstroms. Subscripts of c, v, and m refer respectively to chlorite, vermiculite and montmorillonite. The subscripts are used to further describe the behavior of a particular component when subjected to various treatments. For example, vermiculite and chlorite both have interlayer spacings of 14 Å and this spacing is maintained upon glycolation. With heat treatment, the chlorite remains

stable, but the vermiculite collapses. By Thorez' codification, a structure that has an interlayer spacing of 14 Å and remains stable through all treatments, like chlorite, would be designated 14_c. If the structure collapsed upon heat treatment, like vermiculite, it is designated 14_v. To designate certain layers or interlayers which are unstable (disorder occurs on cation level) Thorez encloses the ciphers parenthetically (14_c-14_v). Stable layers (disorder exists in the stacking or repetition of layers) which are not distinctly separated from the interstratified aggregate are indicated by a letter or numerical designation separated from the unstable layers by a hyphen [i.e. 10-(10-14_m), C-(14_c-14_v)]. If a clay mineral occurs as a discrete constituent separated from interstratified unstable layers, it is connected to the code by a plus (+) sign [i.e. I+(10-14_m)]. If a clay mineral occurs as a distinct mineral in the mixture, a comma is used to separate it from the other constituents [i.e. C, C-(14_c-14_m)].

The best match with Thorez' data, both in his hemicyclograms and monograms, is with a combination of random mixed-layer types. These are I+10-(14-14_m) and C-(14_c-14_v), the former being predominant. These indicate that illite (I) is present as a discrete constituent, in stable form (disorder exists in stacking of layers), not distinctly separated from the interstratified aggregate (+10) and in unstable (disorder occurs on cation level) form, interstratified with montmorillonite (10-14_m). Chlorite is present

in stable form (C) not distinctly separated from an interstratified aggregate of unstable chlorite and vermiculite interlayers (14_c-14_v).

Thorez' system does not identify the proportion of the interlayer components present, nor does it indicate, quantitatively, the chemistry of the mixture. The system does accurately describe the nature of the structure, the components and the manner of occurrence of the components, based upon the reaction of the mixed-layered clays to various treatments. The value of the system would be greatly enhanced if chemical data were provided with the hemicyclograms and monograms.

Discussion

The changes that occur in the mixed-layer structure are primarily changes in the intensity of the 10, 12 and 14 Å peaks. Occasionally the 12 Å peak is not present in the heat-treated pattern or it is masked by the low amplitude diffraction maxima between 10 Å and 14 Å. This probably is the result of a lesser percentage of montmorillonite-like layers in the I+10-(10-14_m) complex and would imply that illite (unstable, stable and discrete) is dominant in the structure. According to Carroll (1970), a relatively high percentage (10%) of discrete montmorillonite must be present to be detectable. In mixed layers, where broad diffraction maxima might mask low amplitude peaks, the lowest percentage of a montmorillonite component detectable

may be considerably higher, perhaps 20 to 25%.

The variations in the intensity of the 10 and 14 Å peaks, in a similar fashion reflect slight changes in the proportion of those components in the mixed-layer structure. The 11 Å peak of the diffraction pattern generally is of greater intensity than the 10 Å peak. According to Thorez' hemicyclogram no. 2 (Thorez, p. 54), the (I-M) entities of mixed-layer structures vary considerably, depending on the percentage of montmorillonite. As the percentage of montmorillonite interlayers varies from less than 10% to 70%, the position of the peak on the untreated pattern varies from 10 Å to 14 Å. Similarly, the peak position on glycolated sample varies from 10 Å to 17 Å. In x-ray patterns of untreated samples, the maximum intensity portion of the broad diffraction maxima varied from 10.5 Å to 12 Å. If the mixed-layer structures were simple (I-M) aggregates, according to Thorez, this variation would reflect a variation of 20 to 35% in the proportion of montmorillonite interlayers. Since the structure of the mixed-layered clays in the samples is more complex than a simple (I-M) structure, these proportions may not be representative of actual proportions in the sample suite. Regardless of the percentage of montmorillonite-like interlayers, however, upon heat treatment the 9.8 Å to 10.5 Å peak predominates and a distinct intensity increase occurs at 14 Å. Were it not for the distinct intensity increase in the 14 Å peak, the pattern obtained from the sample suite could be described

in terms of illite and montmorillonite interlayers.

Whole Rock Analysis

Analytical Procedures

The silica content was determined gravimetrically. Total Fe, Al_2O_3, MgO, CaO, Na_2O, K_2O, TiO_2, MnO and SrO were determined by atomic absorption using calibration curves prepared from in-house (University of New Mexico Geology Department) standards, analyzed against U. S. Geological Survey rock standards. An adaptation of the Molybdenum Blue spectrophotometric method (Chen and others, 1956) was used for determination of P_2O_5. Water was determined by ignition loss, but the amount of Fe oxidation was taken into account by $K_2Cr_2O_7$ titration of ferrous iron in both the ignited and unignited sample. John Husler and Gina Glugla (UNM Geology Department - Staff) performed the analyses

Results

The results of whole rock analyses are summarized in Table 6. Si^{4+} content varies from 19.36 to 40.08%. Ca^{2+} variations of similar magnitude (range) correlate to variations in Si^{4+} content. A graph of Si^{4+} versus Ca^{2+} (Fig. 11) demonstrates an inversely proportional relationship between Si^{4+} content and Ca^{2+}. X-ray diffraction patterns of samples 2 and 15 show a strong calcite peak at 3.04 $\mathring{A}$. Calcite peaks of lesser intensity are present in samples 5 and 9. In samples 15_1, 15_2, 15_3, 15_t, 2, 11A and 11B, petrographic analysis reveals partial percentages of

ANALYSES IN WEIGHT PERCENT

WELL	Si^{4+}	Al^{3+}	Fe^{3+}	Fe^{2+}	Mg^{2+}	Ca^{2+}	Na^{+}	K^{+}	Ti^{4+}	P^{5+}	Mn^{2+}	Sr^{2+}	S	H_2O^{+}	H_2O^{-}	O_2	TOTAL
2	19.36	5.45	1.43	0.95	1.06	13.5	0.45	1.96	0.25	0.22	0.02	0.05	1.46	17.08	0.92	34.90	99.06
3	34.54	4.63	0.83	0.98	1.27	1.73	0.50	1.37	0.14	0.04	0.01	0.01	0.73	6.25	0.44	46.22	99.69
4	36.64	3.18	0.42	0.65	1.31	2.22	0.39	0.95	0.15	0.03	0.01	0.01	0.36	6.12	0.25	47.13	99.82
5	36.17	2.88	0.54	0.79	0.86	3.59	0.21	0.80	0.14	0.04	0.04	0.02	0.34	6.62	0.26	46.61	99.91
6	36.29	3.86	0.80	0.92	0.86	1.99	0.30	1.01	0.02	0.05	0.01	0.01	0.72	5.23	0.28	47.27	99.80
7	35.48	4.60	0.59	1.00	1.02	1.39	0.84	1.26	0.22	0.04	0.01	0.01	0.48	5.67	0.38	47.03	100.02
8	36.71	3.12	0.53	0.61	1.41	2.25	0.34	0.91	0.17	0.07	0.01	0.01	0.52	6.35	0.24	47.33	100.58
9	37.19	2.80	0.38	0.61	0.48	3.60	0.30	0.47	0.07	0.09	0.02	0.01	0.34	5.73	0.22	47.33	99.64
10	40.08	2.46	0.38	0.61	0.66	1.25	0.38	0.60	0.09	0.03	0.01	0.01	0.35	3.39	0.42	49.44	100.16
11A	25.73	7.46	1.26	1.61	2.16	3.85	0.87	2.10	0.37	0.03	0.02	0.02	1.00	12.10	0.66	40.92	100.16
B	27.88	9.42	1.13	1.22	1.52	1.42	0.85	2.50	0.34	0.05	0.01	0.01	0.98	8.44	0.95	46.57	100.35
12A	29.33	7.15	0.75	1.13	1.82	2.77	0.73	1.78	0.41	0.05	0.02	0.01	0.62	9.20	0.90	43.65	100.32
B	29.02	6.77	0.87	1.38	1.82	2.27	0.86	1.93	0.38	0.06	0.02	0.01	0.75	9.33	1.02	42.66	99.46
13	30.51	7.78	1.13	1.37	1.36	1.34	0.70	2.02	0.42	0.06	0.01	0.01	0.95	7.45	0.80	45.00	100.91
14	31.78	5.77	0.76	1.14	1.59	2.26	0.48	1.56	0.20	0.05	0.01	0.01	0.78	8.48	0.56	44.59	100.02
15_1	26.57	7.52	1.11	1.55	1.23	5.07	0.42	2.27	0.26	0.09	0.02	0.03	0.87	9.95	1.26	41.59	99.81
15_2	25.04	7.78	1.10	1.45	1.24	5.80	0.48	2.31	0.31	0.09	0.01	0.03	0.90	12.16	1.06	40.41	100.17
15_3	23.84	7.62	1.04	1.56	1.25	6.98	0.46	2.31	0.31	0.09	0.01	0.03	0.96	13.07	1.00	39.40	99.93
15_t	20.98	6.62	0.77	1.50	1.11	11.2	0.36	2.01	0.25	0.07	0.03	0.04	0.58	16.44	1.04	36.57	99.61

TABLE G : Whole rock wet chemical analysis. (analyses performed by John Husler, Univ. of N.M.)

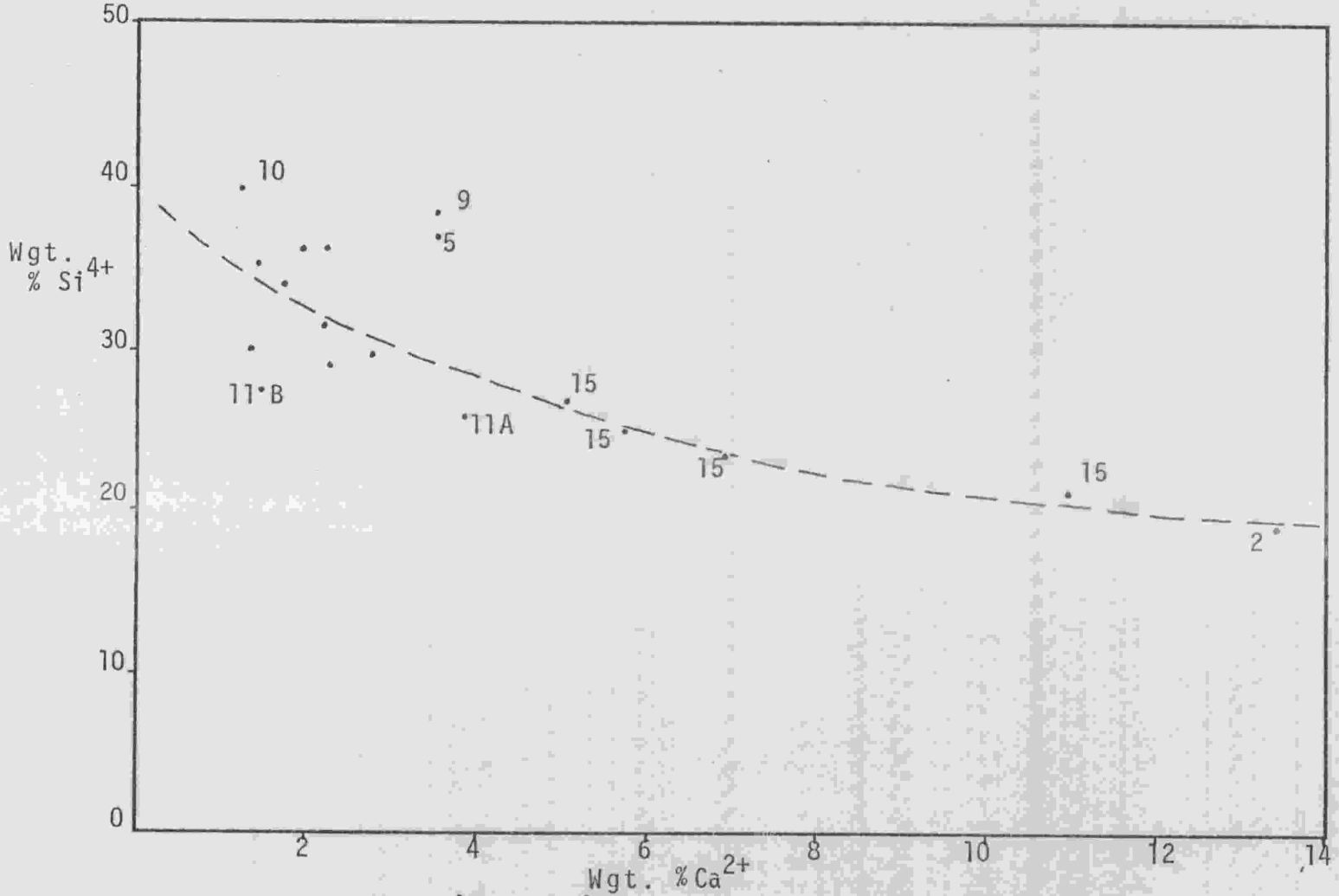

FIGURE 11 : Plot of Si^{4+} and Ca^{2+} indicating an increase in calcite with a decrease in Si^{4+}.

calcite within a few percent of the quartz content. The relatively low Si^{4+} content in those samples is due to the relatively high percentage of Ca^{2+}. This mineralogically relates to variations in quartz and calcite content.

Al^{3+} content varies from about 2.5 to 9.5%. Al^{3+} is directly proportional to K^{+} (Fig. 12). Surprisingly, some samples with relatively high Al^{3+} (9.42%) and K^{+} (2.50%) contain little potassium feldspar while samples with low Al^{3+} (2.45%) and K^{+} (0.6%) contain relatively large amounts of potassium feldspar. Since Al^{3+} and K^{+} are linearly related, potassium feldspars are not the major contributors of those elements. Grain percentages approximate the same linear relationship (Fig. 12). Samples high in Al^{3+} and K^{+} contain lower percentages of grains, and, consequently, a high percentage of matrix. Samples low in Al^{3+} and K^{+} contain high grain percentages and low percentages of matrix. Because the matrix is composed primarily of clay minerals, they are the primary contributors of Al^{3+} and K^{+}.

The abundance of Fe^{3+} and Fe^{2+} is apparently related to the abundance of clay minerals or matrix. Because the Fe^{3+} and Fe^{2+} content is low, it is sufficiently sensitive to allow an approximation of the relative importance of other elements to the clay mineralogy by plotting either Fe^{3+} or Fe^{2+} content against the content of other elements common in clay minerals. Slopes of least squares fits obtained by plotting Fe^{3+} against other elements shows little variation from slopes acquired by plotting Fe^{2+} against other elements,

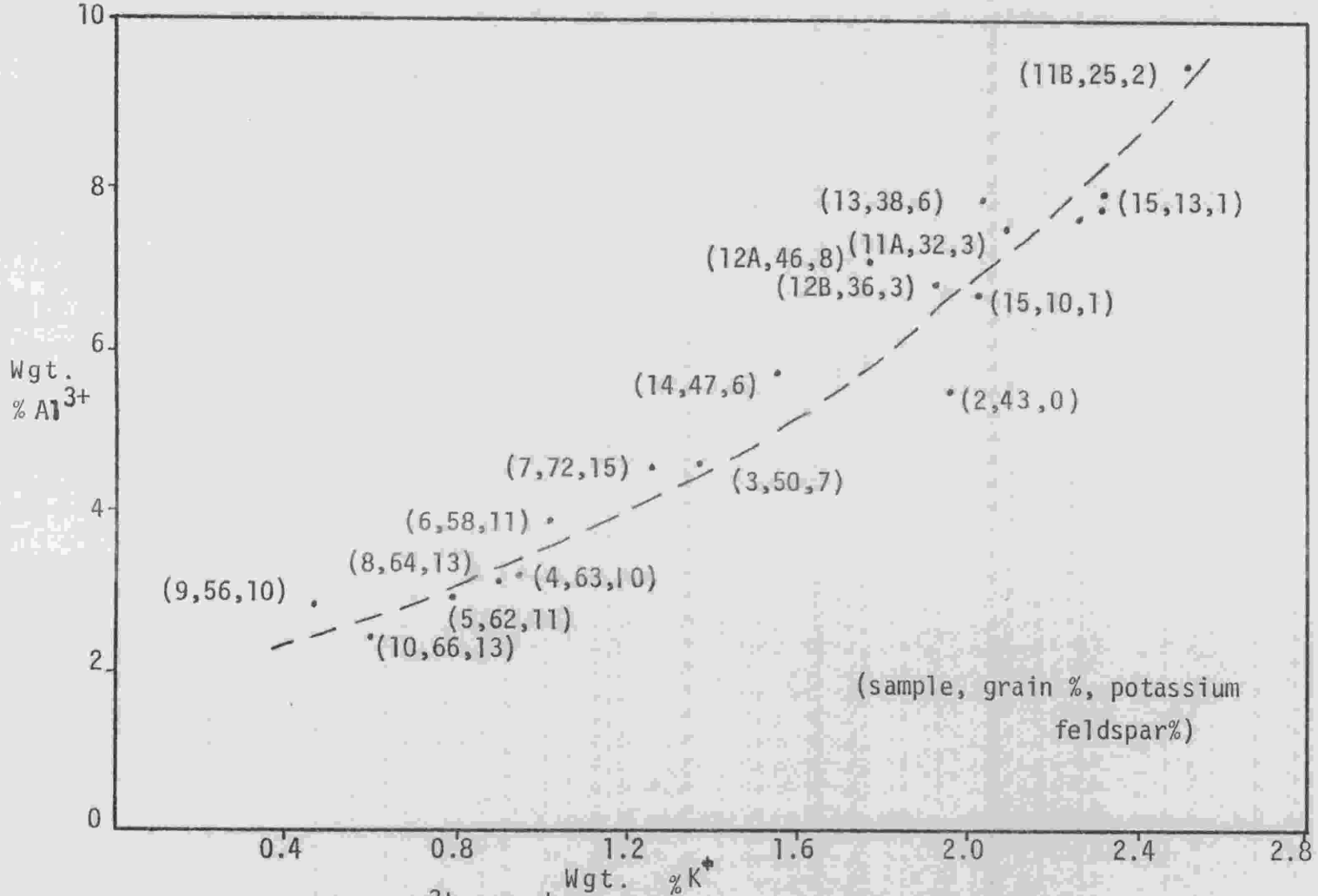

FIGURE 12 : Plot of Al^{3+} and K^{+} indicating matrix (clay minerals) as the major source of aluminum and potassium.

consequently, Fe^{3+} and Fe^{2+} are discussed as an entity (Fe^{3+}-Fe^{2+}). Although pyrite is a major contributor of Fe^{3+}-Fe^{2+}, the pyrite content, as revealed by SEM studies is related to the abundance of matrix. The pyrite content increases with a corresponding increase in matrix; therefore, the Fe^{3+}-Fe^{2+} content is proportional to the abundance of clay minerals.

Figure 13 illustrates numerous least squares fits obtained by plotting Fe^{3+}-Fe^{2+} against Mg^{2+}, Ca^{2+}, Na^{+}, K^{+}, Ti^{4+}, Al^{3+}, structural water (H_2O^{+}) and adsorbed water (H_2O^{-}). All of these elements show a distinct increase in abundance with an increase in Fe^{3+}-Fe^{2+} content. The abundance of these elements is also related to the fabric. As the percentage of matrix increases, the percentage of these elements increases. As absolute value of the slopes on Figure 13 become larger, the Fe^{3+}-Fe^{2+} content becomes less significant in respect to the element or constituent against which it is plotted. By arranging the slopes in order of decreasing absolute value, an approximation of the significance of the constituents in the clay minerals is obtained. In order of decreasing significance, the major constituents of the clay minerals are Si^{4+}, H_2O^{+}, Al^{3+}, Ca^{2+}, K^{+}, Mg^{2+}, H_2O^{-}, Fe^{3+}-Fe^{2+}, Na^{+} and Ti^{4+}.

Ca^{2+} may not be as significant as is indicated by this ordering. A plot of Mg^{2+} and Ca^{2+} (Fig. 14) reveals two distinct trends. Consideration of x-ray diffraction patterns explains the two trends. The lower trend, which <u>somewhat</u>

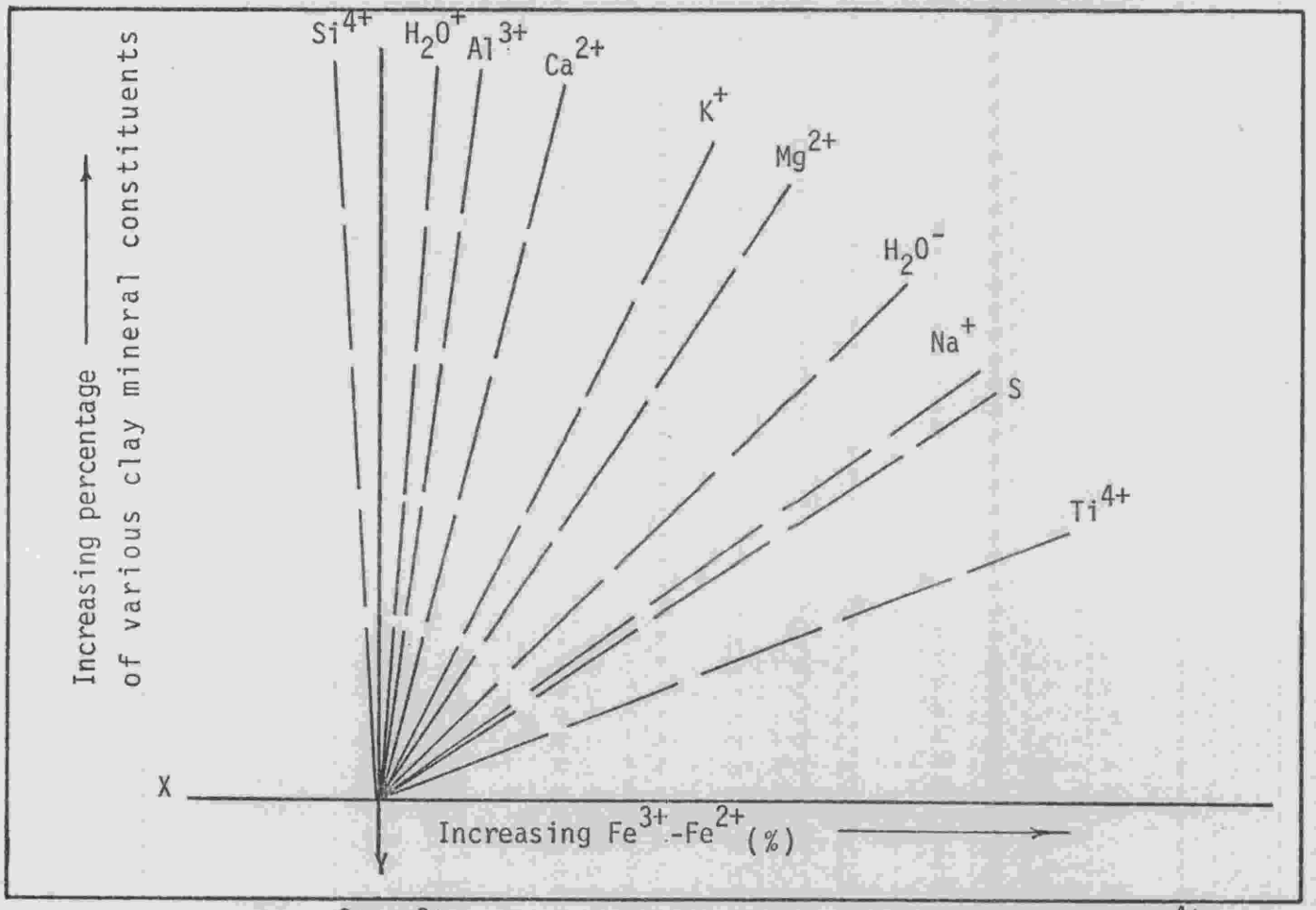

FIGURE 13: Plot of Fe^{3+}-Fe^{2+} and the probable clay mineral constituents (Si^{4+}, H_2O^+, Al^{3+}, Ca^{2+}, K^+, Mg^{2+}, H_2O^-, Na^+, Ti^{4+}) and S. Arranged in order of decreasing absolute values, the slopes provide an approximation of the relative importance of the constituents to the clay mineralogy.

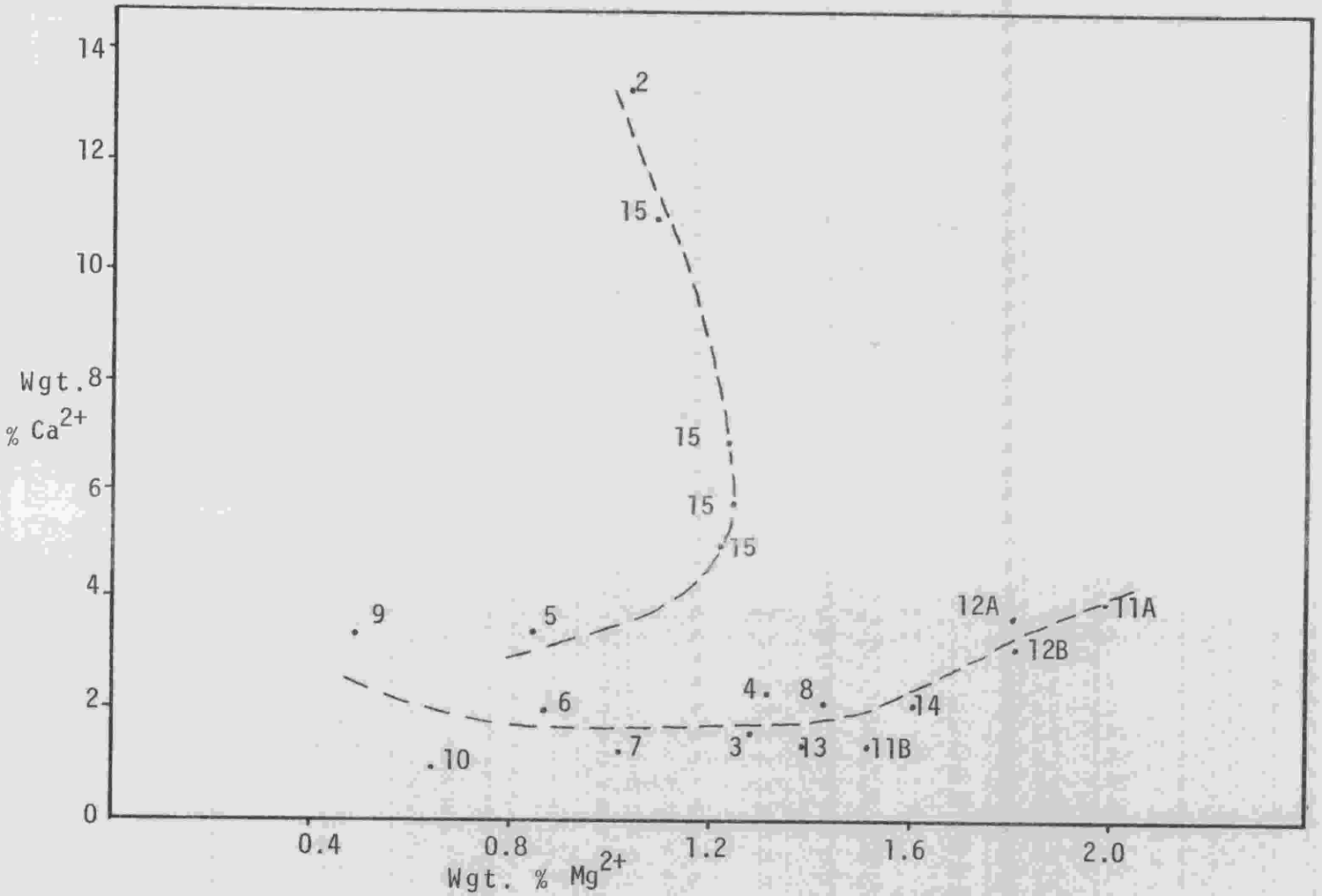

FIGURE 14: Plot of Ca^{2+} and Mg^{2+} showing dolomite trend (horizontal) and calcite trend (vertical).

parallels the Mg^{2+} axis indicates a substantial increase in Mg^{2+} content while Ca^{2+} content is relatively constant. X-ray diffraction patterns confirm a transition from dominantly calcite in sample 9, to calcite and dolomite in sample 6, and, finally, dolomite in sample 11A. Although the calcite content in these samples is fairly constant, the dolomite content increases from sample 9 to sample 11A. The second trend, somewhat parallel to the Ca^{2+} axis, indicates a marked increase in Ca^{2+} content with minor variations in Mg^{2+} content. Thin sections and x-ray diffraction patterns reveal increasing calcite content along this trend. Calcite is present throughout the sample suite, but is particularly abundant in samples 2, 15 and 5. These samples essentially define the linear relationship obtained by plotting Fe^{3+}-Fe^{2+} and Ca^{2+}. When wells with high calcite contents are removed from the plot, no distinct correlation is evident. It is apparent that the Ca^{2+} content is less significant to the clay mineralogy than K^{+}, Mg^{2+} or Fe^{3+}-Fe^{2+}. Thus, the constituents of the clay minerals in decreasing order of significance are Si^{4+}, H_2O^{+}, Al^{3+}, K^{+}, Mg^{2+}, H_2O^{-}, Fe^{3+}-Fe^{2+}, Ca^{2+}, Na^{+} and Ti^{4+}.

X-ray diffraction analysis confirmed kaolinite and two mixed-layered structures I+10-(10-14m) and C-(14c-14v) in the sample suite. Table 7 (compiled from Weaver, 1973) illustrates average chemical compositions of the dominant components of several clay minerals. The I+10-(10-14m) configuration is the dominant of the two mixed-layered types.

	Fithian Illite	Kaolinite	Montmorillonite	Dioctahedral Chlorite	Illite-Montmorillonite
SiO_2	51.74	43.54	53.73	36.82	53.54
Al_2O_3	23.98	37.05	19.33	41.70	24.79
H_2O^+	6.92	13.30	7.05	13.88(total)	6.75
K_2O	5.59	-----	0.52	0.51	5.82
Fe_2O_3	4.57	1.44	3.26	1.57	2.66
MgO	1.99	-----	2.80	3.76	2.83
H_2O^-	2.40	-----	12.42	-----	1.52
TiO_2	0.68	1.35	0.15	0.42	0.63
CaO	0.97	-----	1.65	0.25	4.13
FeO	1.09	-----	0.15	0.23	0.78
Total	99.93	96.68	101.06	99.14	103.45

TABLE 7 : Average chemical compositions of various clay minerals (compiled from Weaver,1973).

An estimate of 20-35% montmorillonite interlayers in the I+10-(10-14_m) structure was obtained using Thorez' hemicyclograms. The actual percentage is probably slightly lower due to the presence of stable and discrete illite forms in the structure. Using an approximation of 80% illite and 20% montmorillonite and calculating from the values for illite and montmorillonite in Table 7, the dominant constituents of the clay minerals in order of significance would be Si^{4+} (52.14%), Al^{3+} (23.05%), H_2O^+ (6.95%), K^+ (4.58%), H_2O^- (4.4%), Fe^{3+} (4.32%), Mg^{2+} (2.15%), Ca^{2+} (1.11%), Fe^{2+} (0.9%) and Ti^{4+} (0.57%). Assuming the C-(14_c-14_v) consists dominantly of chlorite, perhaps greater than 60%, the effect on the total composition of the clay minerals would be a slight decrease in Si^{4+}, K^+, Fe^{3+}, Fe^{2+}, Ti^{4+} and Ca^{2+} with the most pronounced decreases being K^+ and Fe^{3+}. The Mg^{2+} and total H_2O would be increased. The presence of kaolinite in the calculated mixture would result in an increase in H_2O^+ and Ti^{4+} and a reduction of K^+ in the total composition. The major difference between the graphical values and the calculated values of the importance of various constituents in the total composition of the clay minerals is the relative importance of Al^{3+}, H_2O^+ and Mg^{2+}. Considering the limited number of sample points and the assumptions of the graphical analysis, the correlation is remarkable.

The P^{5+} content is particularly high in sample 2; however, petrographic analysis reveals scattered bone fragments. The Sr^{2+} content is slightly higher in wells 2 and 15. Both of

these wells contain relatively large amounts of calcite, which is the probable source of the increased Sr^{2+}. Both of these wells also contain the highest percentage of matrix; Sr^{2+} may occupy interlayer cation sites in the clays.

Organic Analysis

Introduction

Early concepts of the origin of petroleum (oil, gas and gas condensates) centered around inorganic and organic precursors. Arguments favoring inorganic origins have gradually faded and it is now generally accepted that the precursors of petroleum are organic materials deposited in marine environments. Debate continues as to the relative importance of terrestrial and marine organic materials, but the preponderance of opinion favors marine sources (Welte, 1972). Organic material present in both modern and ancient source rocks differs considerably in chemistry from petroleum; consequently, the source material must undergo considerable changes as it is transformed to petroleum. The nature of this transformation is the least understood aspect of the origin of petroleum. Time, heat, pressure, depositional site, bacterial activity and catalytic reactions are important factors in transformation (Staplin, 1969).

Level of Organic Metamorphism (LOM)

Hydrocarbon distribution and stratigraphy are reasonably well defined by outcrop studies and subsurface mapping in the San Juan Basin. The Graneros is the deepest major

Cretaceous source bed in the San Juan Basin and should reflect the maximum level of organic metamorphism in the Cretaceous section. The basin should be an excellent test of the value of LOM studies in exploration programs. Hood and others (1975) constructed a scale of the level of metamorphism (LOM) based on Suggate's (1959) coal rank scale. The scale indicates progressively increasing levels of metamorphism from 0 (peats and lignite) to 20 (meta-anthracite). In Figure 15, the LOM scale is correlated with several other scales of metamorphism. Although spores, leaf cuticles and pollen were not directly observed in this study, the general color of the organic debris in thin sections of Graneros (yellow-brown to medium brown) indicates a LOM of about 9.5 to 11. The color of organics in the Graneros indicates a transition from an immature to a mature source bed, using the criteria of Evans and Staplin (1970) (Fig. 16). Organic geochemical analysis (organic carbon Table 8 and C_{15}^{+} soxhlet extractions plus liquid chromatographic separation Tables 9 and 10) were performed by Geochemical Laboratories, Inc. By expanding Evans and Staplin's (1970) scale of maturity based on C_{15}^{+} and color (Fig. 16) and correlating it to Hood and others' LOM scale (Figs. 15 and 17), a scale of maturity and LOM was constructed based on the hydrocarbon to non-hydrocarbon (HC/NHC) ratio (Fig. 18). The HC/NHC (Fig. 18) ranges from 0.29 to 3.24, but the average HC/NHC (0.91) is probably more representative of the overall maturity of the Graneros and indicates a LOM of

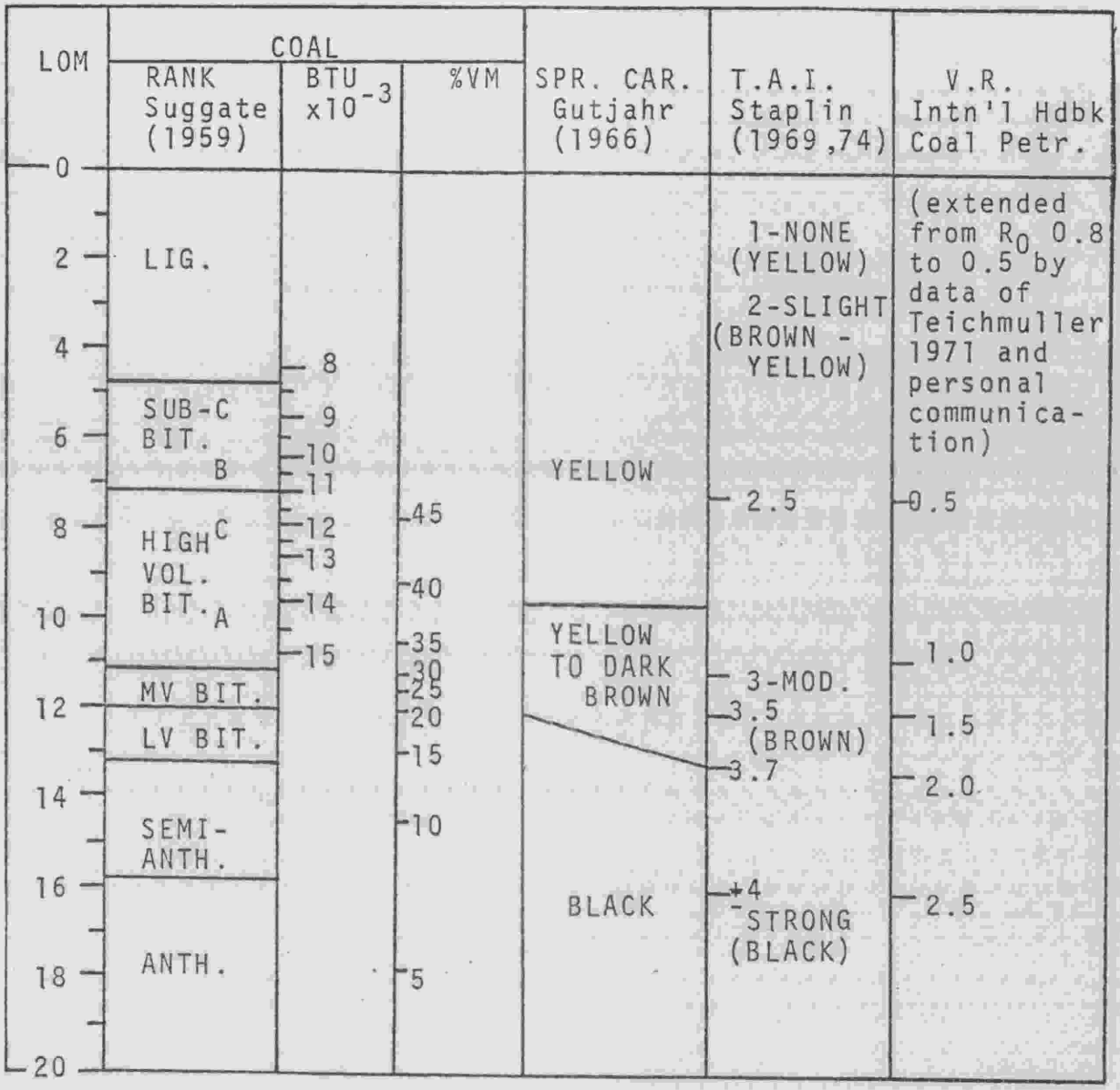

LOM - Level of metamorphism.
%VM - Volatile matter (only for humic, vitrinitic coals)
SPR. CAR. - Spore carbonization.
T.A.I. - Thermal alteration index.
V.R. - Vitrinite reflectance.
LIG. - Lignite.
BIT. - Bituminous, VOL.-Volatile, MV-Medium volatile
LV -Low volatile.
ANTH. - Anthracite.

FIGURE 15 : Scales of organic metamorphism (from Hood and others, 1975).

RANGES	C_1-C_4	C_4-C_7	C_{15}+	KEROGEN
	GAS	GASOLINE	HEAVIES	SOLIDS
IMMATURE SOURCE	MAINLY C_1	LEAN, MOST COMPONENTS ABSENT	RICH, MAINLY NONHYDROCARBONS	YELLOW
MATURE SOURCE	MAINLY C_2-C_4	RICH, ALL COMPONENTS PRESENT	RICH IN HYDROCARBONS & NSO'S	YELLOW TO BROWN
METAMORPHOSED SOURCE	MAINLY C_1	LEAN	LEAN, MAINLY HYDROCARBONS	BLACK

FIGURE 16 : Catalogue of varying composition of gaseous and liquid hydrocarbons and of insoluble organic matter in source rocks at different levels of thermal alteration (maturation), (from Evans and Staplin,1970).

Sample Number	Total Organic Carbon (%)
1 A	0.38
B	0.61
C	0.70
2	0.71
3	0.55
4	0.43; 0.44R
5	0.54
6	0.55
7	0.63
8	0.57
9	0.84
10	0.62; 0.59R
11 A	1.29
B	1.05; 1.07R
12	0.94
13	0.87
14	0.79
15	0.80

TABLE 8 : Total organic carbon; determined by Geochemical Laboratories,Inc.

Sample	-----HYDROCARBONS (%)----- Paraffin-Naphthene	Aromatic	Total	---NONHYDROCARBONS (%)---------- Eluted NSO'S	Noneluted NSO'S	Precipitd. Asphaltene	Total	HC/NonHC
1 A	56.8	19.6	76.4	10.5	4.3	8.7	23.5	3.24
B	27.8	19.5	47.3	15.9	1.5	35.4	52.8	0.90
C	29.5	22.7	52.2	14.5	0.0	33.3	47.8	1.09
2	33.6	26.8	60.4	14.6	5.0	20.0	39.6	1.52
3	20.1	9.0	29.1	48.2	12.2	10.5	70.9	0.41
4	29.0	11.7	40.7	26.4	20.8	12.1	59.3	0.69
5	31.1	8.7	39.8	41.3	11.0	7.9	60.2	0.66
6	37.2	12.5	49.7	25.5	16.3	8.4	50.2	0.99
7	24.7	15.1	39.8	27.8	10.2	22.3	60.3	0.66
8	28.7	16.1	54.8	28.0	16.2	11.0	55.2	0.81
9	14.1	8.3	22.4	33.2	9.4	35.1	77.7	0.29
10	30.6	10.2	40.8	30.3	20.1	8.8	59.2	0.69
11 A	33.9	28.4	62.3	17.2	4.1	16.4	37.7	1.66
B	23.8	19.4	43.2	16.5	0.9	39.4	56.8	0.76
12	22.5	11.7	34.2	32.1	22.9	10.8	65.8	0.52
13	18.4	10.9	29.3	43.3	13.2	14.2	70.7	0.41
14	24.3	9.2	33.5	38.2	19.5	8.7	66.4	0.50
15	31.2	9.9	41.1	18.8	9.9	30.2	58.9	0.70

TABLE 9 : C_{15+} extraction analysis; performed by Geochemical Laboratories,Inc.

Sample	Total Extract	------HYDROCARBONS (PPM)-- Paraffin-Naphthene	Aromatic	Total	-----NONHYDROCARBONS (PPM)-------- Eluted NSO'S	Noneluted NSO'S	Precipitd. Asphaltene	Total
1 A	1544	877	303	1180	162	67	135	364
B	605	168	118	286	96	9	214	319
C	724	214	164	378	105	0	241	346
2	712	239	191	429	104	36	142	282
3	925	186	83	269	446	113	97	656
4	836	242	98	340	221	174	101	496
5	1287	400	112	512	532	141	102	775
6	854	318	107	425	218	139	72	429
7	879	217	133	349	244	89	196	529
8	968	278	156	434	271	157	106	534
9	1000	141	83	224	332	94	351	776
10	802	245	82	327	241	161	71	475
11 A	837	284	238	522	144	34	137	315
B	345	82	67	149	57	3	136	196
12	694	156	81	237	223	159	75	457
13	386	71	42	113	167	51	55	273
14	675	164	62	226	258	132	59	448
15	224	70	22	92	42	22	68	132

TABLE 10: C_{15+} extraction analysis; performed by Geochemical Laboratories, Inc.

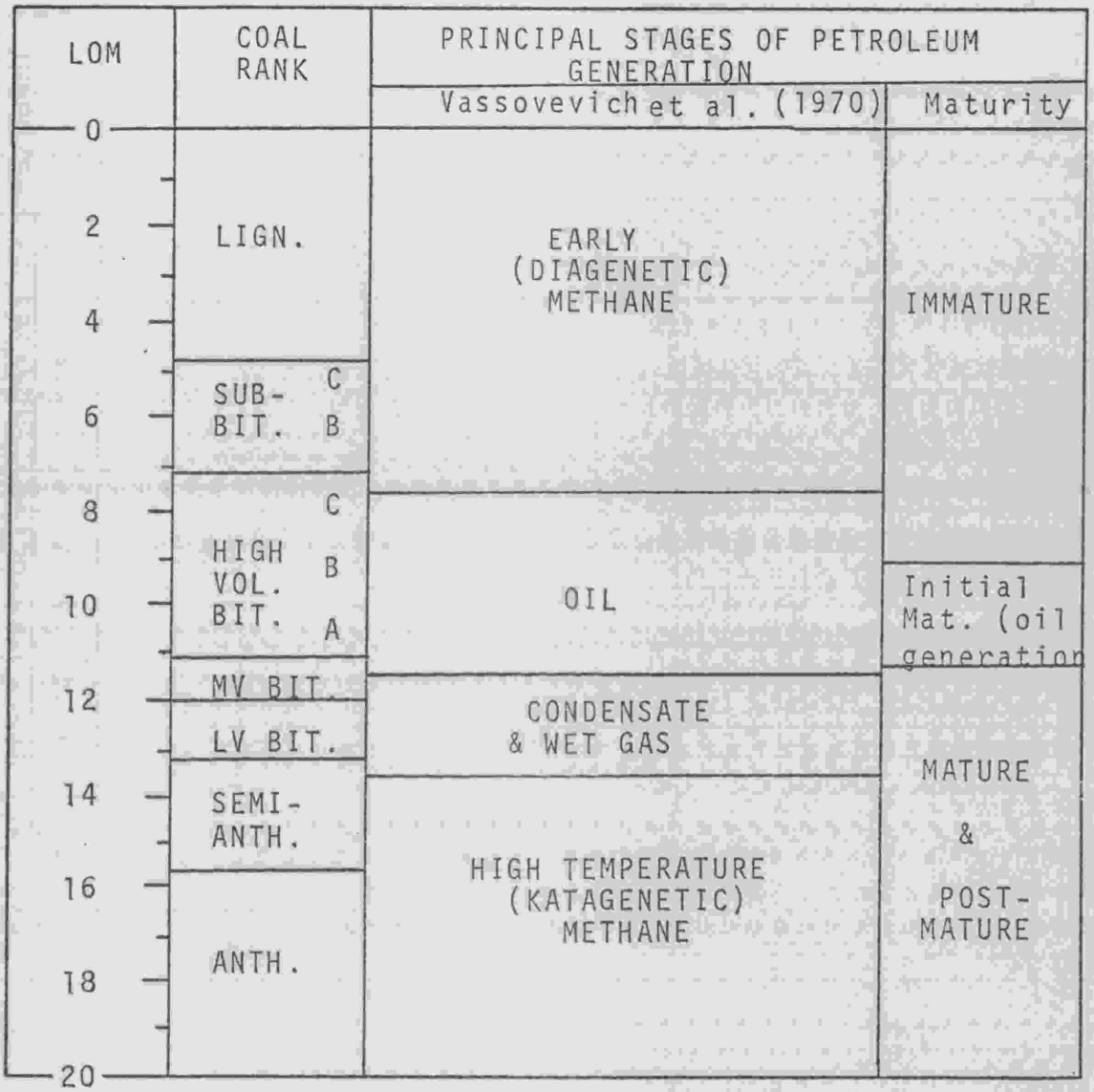

FIGURE 17 : Organic metamorphic stages of petroleum generation (adapted from Hood and others, 1975).

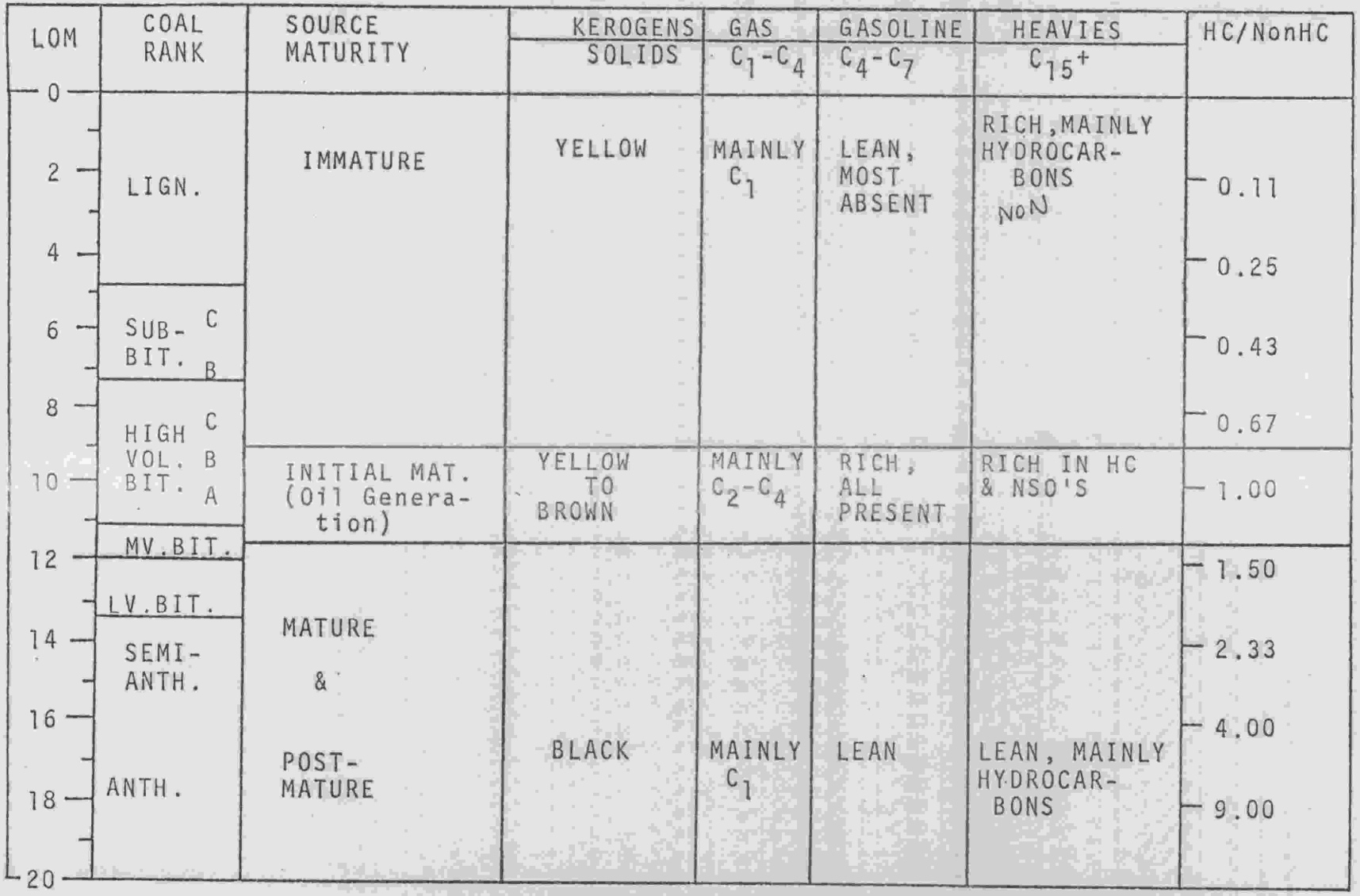

FIGURE 18 : LOM determination chart; includes hydrocarbon to nonhydrocarbon ratio.

about 9.5. The wide range of HC/NHC ratios in a source bed that appears to have generated oil in the San Juan Basin indicates that the scale may be non-linear. Further evaluation is necessary to delineate the true nature of the scale. It is probable, however, that the midpoint of the scale (HC/NHC = 1) is centered in the mature source bed range.

Hood and others (1975) also constructed a LOM determination chart (Fig. 19) based on effective heating time (t_{eff}) and maximum temperature (T_{max}). The t_{eff} is the amount of time during which a specific rock has been within 15°C of its maximum temperature (T_{max}). Bottom hole temperatures in the deepest part of the Graneros reached a maximum temperature of about 100°C a few hours after mud circulation was discontinued (Gamma-ray neutron log on well number 9, depth 8434 ft.). When correction factors calculated by Hood and others (1975) are applied, the maximum formation temperature is about 130°C. Assuming a constant rate of deposition in the San Juan Basin, the Graneros interval was within 15°C of its maximum temperature for a duration of about 20 million years (t_{eff} = 20my; T_{max} = 130°C). Using Figure 19 (Hood and others, 1975), a LOM of about 10.3 is obtained. This value agrees well with values obtained by color and HC/NHC. The LOM of the Graneros indicates that it has generated oil and immature gas. Temperature and time calculations may be in error due to a lack of detailed knowledge of paleotemperatures and rates of deposition, but even if T_{max} reached 150°C and t_{eff} was 60my,

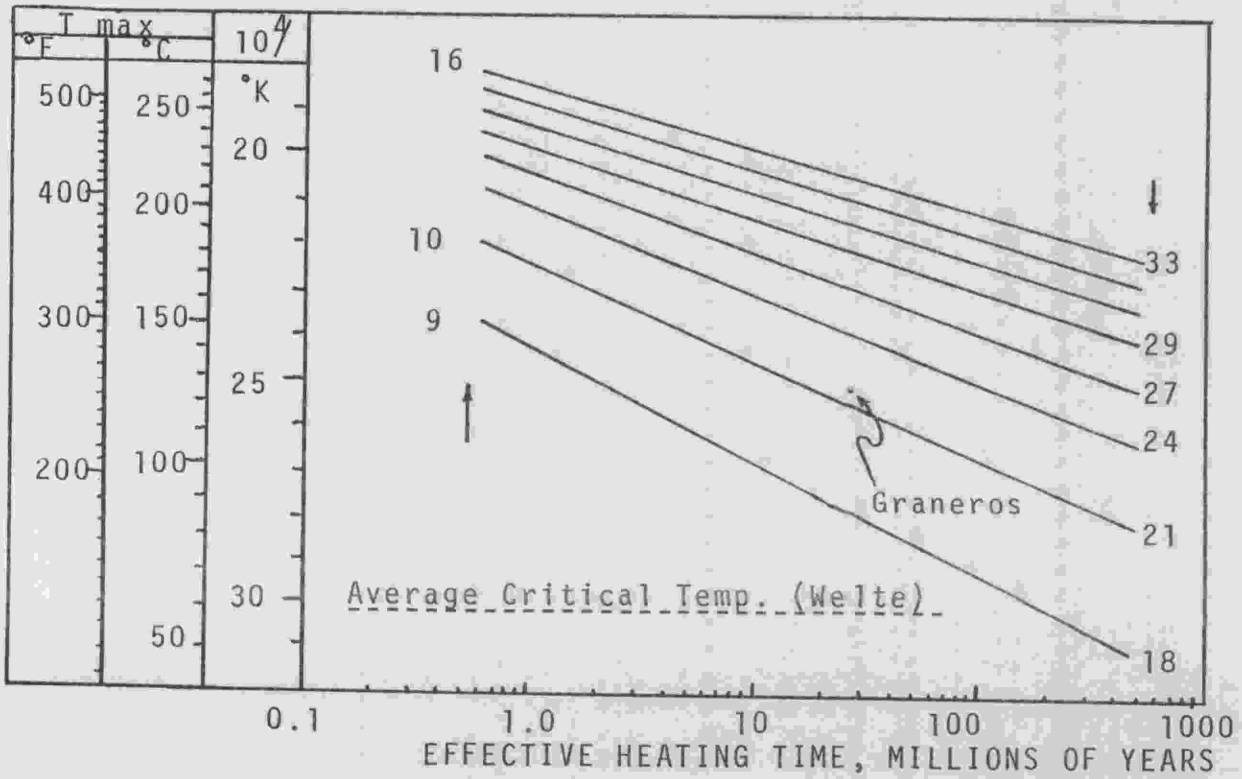

FIGURE 19 : Relation of LOM to maximum temperature and effective heating time (from Hood and others, 1975).

a LOM of about 11 would result in essentially the same petroleum yield.

The Graneros is the lowest major Cretaceous source bed; shale tongues in the Dakota Sandstone, which underlie the Graneros, may be considered as minor source beds. The Dakota Sandstone overlies a thick sequence of Jurassic and Triassic continental deposits that can be excluded as potential source beds with the exception of the Todilto Limestone, which may be the source of hydrocarbons produced from the underlying Entrada Sandstone. Welte (1972) claimed that "primary migration mechanisms (movement of dispersed petroleum compounds out of a source rock into a carrier or reservoir rock) are only active over short distances (meters or tens of meters, certainly not kilometers)". Exceptions are areas where fortuitous tectonic fracturing or very active secondary migration has occurred. The relationship between hydrocarbons produced from Cretaceous rocks and their source is complex. It is reasonably certain that the source beds for the thick Cretaceous section in the San Juan Basin are the Mancos Shale and the Lewis Shale, but these units are intercalated with numerous sandstones or potential reservoirs over a rather extensive vertical section. The generalization that the LOM decreases with decreasing depth is relatively safe. The Dakota Producing Interval reached the highest LOM of the Cretaceous section. Calculated LOM's indicate that source beds in this interval supplied oil and immature gas to nearby reservoir rocks.

A LOM of about 8 to 9 appears to be the lowest LOM at which oil is produced.

Welte (1972) observed that a minimum depth requirement is essential before kerogen degradation becomes significant. Sufficient temperature is required to overcome activation energy barriers and initiate the degradation and transformation process; an average value for this temperature is about 60°C. Using this value, the minimum t_{eff} required to reach a LOM of 8 to 9 is in the range of 15 to 20my. (Even if the Graneros were under an additional 1000 ft. of overburden in the past, the oil producing interval based on the LOM would have extended a maximum of 1000 to 1500 ft. above the Graneros and only in the structurally lowest portion of the basin.) It is probable, based on LOM calculations, that most of the oil in the San Juan Basin originated below the present position of the Carlisle-Niobrara unconformity in the structurally deepest part of the basin. Thus, oil generation is probable in the Graneros interval, with wet gas condensate and gas generated in lesser quantities (Figs. 20 and 21). Good reservoir rocks near, below, or truncated by this unconformity are likely to contain appreciable quantities of oil. Reservoir rocks stratigraphically higher are more likely to contain immature gas. The Lewis Shale probably generated immature gas and little or no oil.

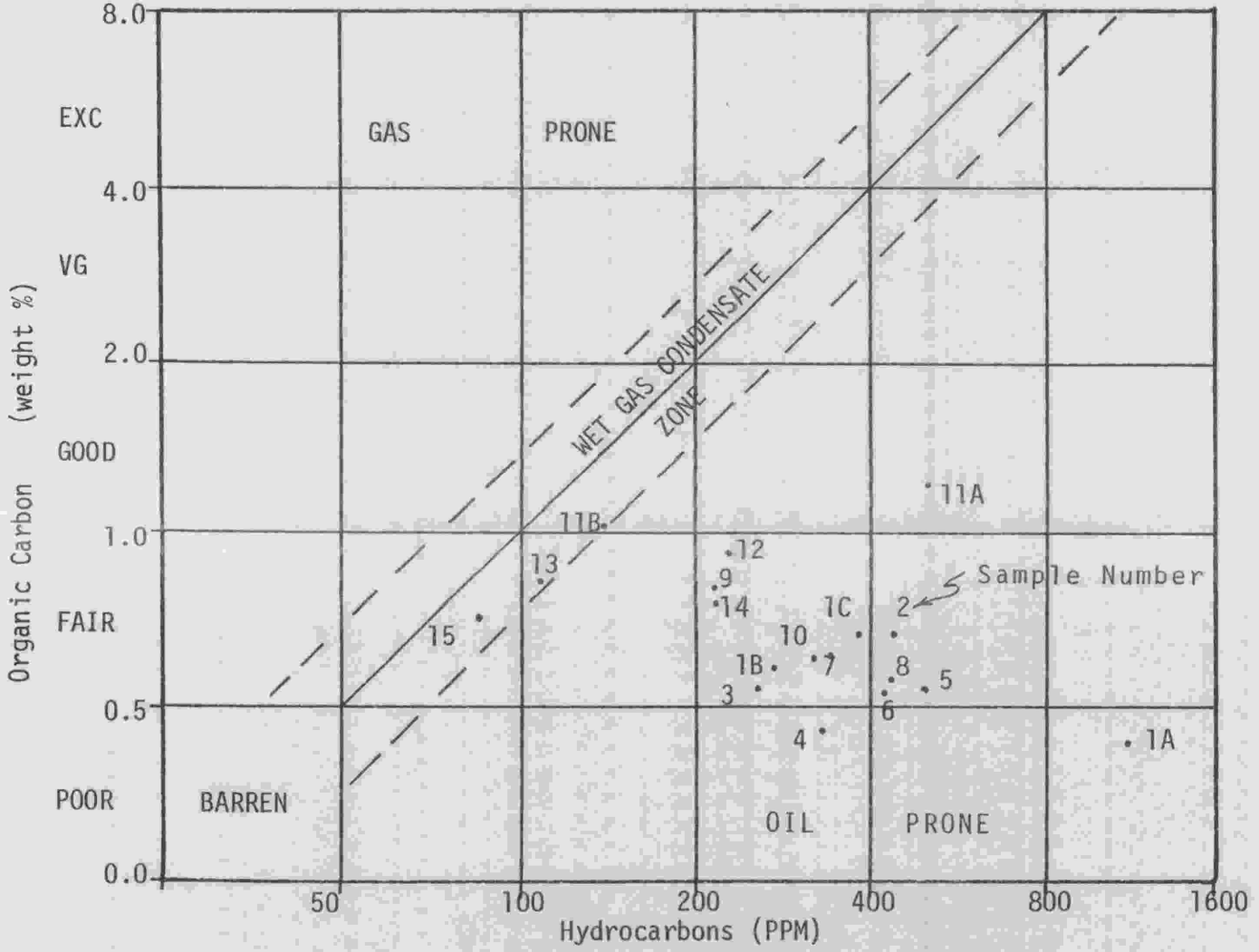

FIGURE 20 : Type of hydrocarbon production from a source bed based on total organic carbon versus hydrocarbons (courtesy Geochem.Labs,Inc., 1977).

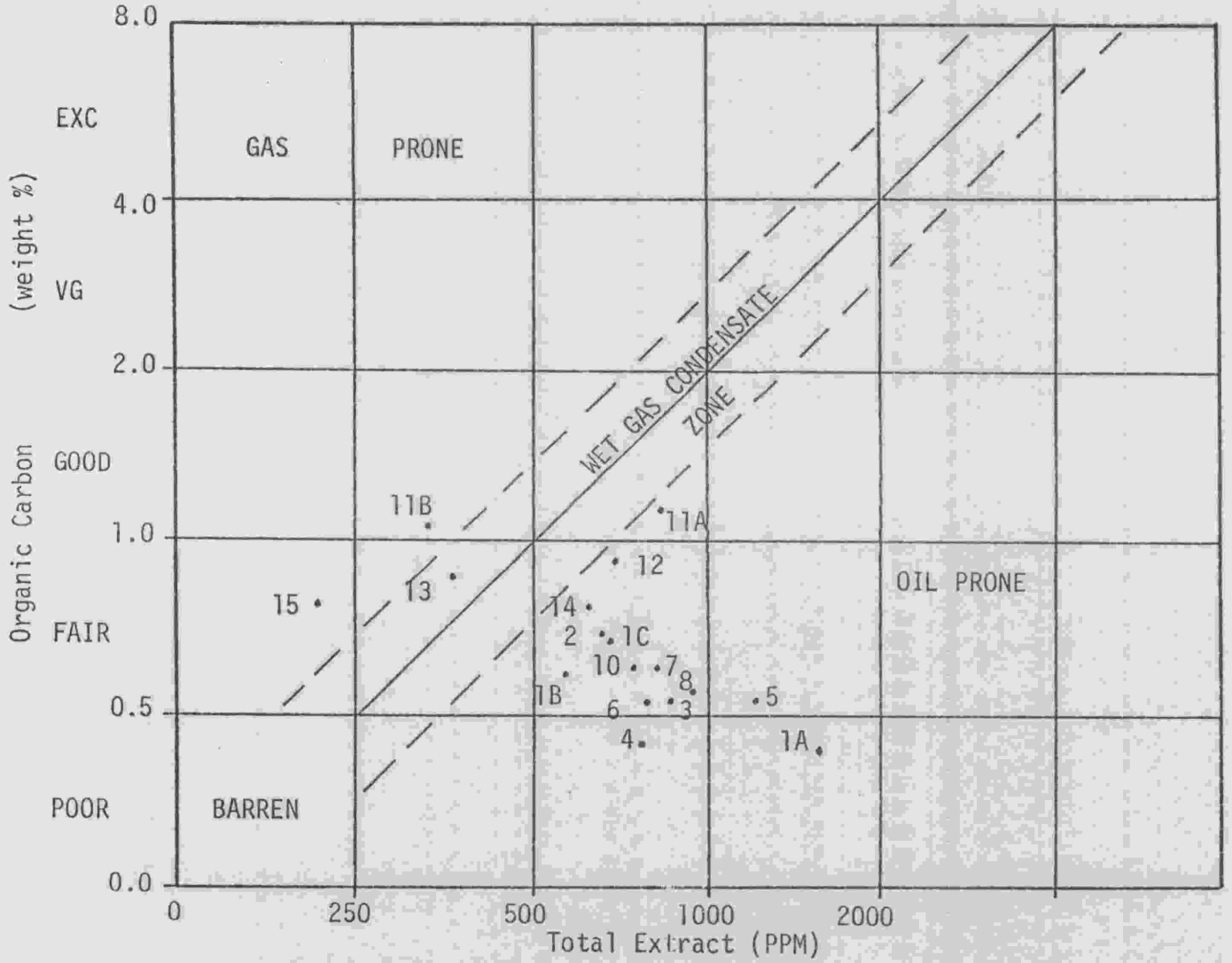

FIGURE 21 : Type of hydrocarbon production from a source bed based on total organic carbon versus total extract (courtesy Geochem.Labs, Inc.,1977).

LOM and Actual Production

Table 11 (adapted from Parker and others, 1977) shows a strong correlation between the type of hydrocarbons produced in various formations of the San Juan-Paradox Basin and the predicted hydrocarbon types based on LOM calculations. The vast majority of the oil produced in the basin has been produced from the Dakota "producing interval" and the Gallup Sandstone, of early Niobrara age. These sandstones are truncated by or are near the Carlisle-Niobrara unconformity. This unconformity was probably a concentration plane and conduit of migration for oil that originated in source beds below the unconformity. This interval is often collectively referred to as the Lower Mancos Shale and consists of the Juana Lopez or Sanostee Member, Lower Mancos Shale Member, Greenhorn Limestone Member and Graneros Shale Member. Oil and gas that originated in the lower portion of the Lower Mancos Shale migrated downward or laterally into sandstones of the Graneros and Dakota. Oil and gas that originated in the upper portion of the Lower Mancos Shale migrated into the Gallup Sandstone or basal Niobrara Sandstones. Since little gas has been produced from these sandstones, the oil might have accumulated in sufficient quantities to force the gas into stratigraphically higher reservoir rocks. (This is indicated by the high gas production from the upper units of the Mesaverde Group, although much of this gas probably originated in the Mulatto and Satan Tongues of the Mancos Shale.) Reservoirs in

PLAY	Oil	Assoc. Gas	Non-Assoc. Gas	NGL	Predicted Hydrocarbon
Nacimiento	possibly mostly charged from leaking gas wells in older rocks		0.007	-	
Farmington	0.07	?	0.95	-	
Fruitland	0.02	-	62.30	-	
Pictured Cliffs	0.13	?	2,009.00	-	
Chacra	0.01	-	75.40	-	
Mesaverde	17.40	?	4,542.00	-	
Gallup (Niobrara)	123.88	-	2.00	7.2	
Dakota-Morrison	47.00	-	2,795.00	-	
Entrada	1.00				
Pennsylvanian (includes Cutler upper Hermosa)	325.75	362	254.00	0.084	
Miss.-Devonian	40.73	298*	-	-	
Cambrian	-	-	-	-	
TOTALS	555.99	660	9,740.657	7.284	

Oil in 10^6 barrels
Gas in billions of cubic feet
NGL -----Natural Gas Liquids

* reinjected

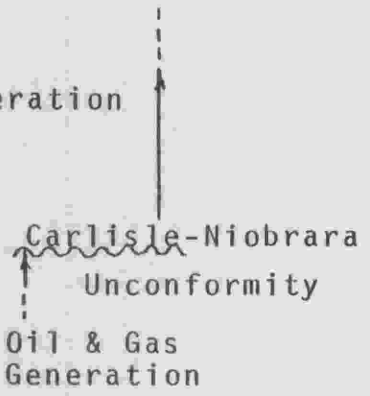

TABLE 11 : Paradox-San Juan Basin cumulative production to 12/31/75
(adapted from Parker and others, 1977)

formations stratigraphically above the Mesaverde Group have produced almost exclusively gas. Although permeable sandstone bodies are limited on the eastern and northern margins of the basin, considerable recoverable petroleum remains in fracture systems developed at points of maximum change in dip where strata are turned upward on these flanks. This type of reservoir has been located and described on the western and eastern flanks of the basin (Gorham and others, 1977).

Summary

The purpose of the study was to analyze in detail the texture, fabric and composition of fine-grained terrigenous sediments, in order to more precisely define their relationships to important reservoir properties. Rocks of Cretaceous age were chosen, as numerous producing intervals occur in Cretaceous strata of the San Juan Basin, New Mexico. The Graneros Member of the Mancos Shale was selected for detailed study because: (1) well-indurated, unweathered core samples were available, (2) it was a probable source bed for hydrocarbons, (3) the environment of deposition was well described and (4) the unit was well delineated on subsurface well logs. Petrography, scanning electron microscopy, radiography, whole rock wet chemistry, chromatography (organic analysis) and x-ray diffraction were used to analyze the samples. A brief survey of existing literature established the environment of deposition of the

Graneros. The results of the analyses were integrated with related findings of previous researchers.

The Graneros was deposited primarily in epineritic seas. The topographic relief of bordering continental areas was low and depositional rates varied. Oscillations of the shoreline are indicated by variations in silt and sand content, and the faunal assemblage in the Graneros. The very fine-grained sandy and silty zones in the Graneros were deposited during minor progradational cycles and represent either delta front sands or interdeltaic offshore sands. All of the samples contain silt and sand, and most contain greater than 25% grains, indicating that the portion of the basin from which the samples were taken was transitional between shallow, open marine and near shore waters.

Grain content varies considerably (6 to 93%) and is the dominant control of the fabric during compaction. Clays align parallel to bedding as compaction pressure increases. Grains disrupt the parallelism and the clay minerals are bent around grains. As grain percentages increase, the degree of disruption increases and clays align parallel to grain surfaces rather than bedding. In grain-supported fabrics, the pressure is transferred through grain-to-grain boundaries and the interstitial allogenic clays remain in the depositional configuration. In clay-rich sediments, the grain content controls the manner in which the stress of compaction pressure is distributed

through the sediment.

The shape of the grains affects the degree of disruption of the fabric. Elongate grains align parallel to bedding and their disruptive effect on the clays is minimized. The foliation of clays around equidimensional grains causes the clays to depart further from planes parallel to bedding. Characteristics of the Graneros samples that are conducive to a high degree of parallel orientation include a low percentage (<1 to 5%) of cement, high percentage (7 to 94%) of clay minerals, a high organic content (0.38-1.29%), and high compaction pressures. Cut and fill type structures, slump features, straight laminae and irregular discontinuous laminae are common bedforms in the Graneros.

Although texture and fabric vary considerably, the composition of the clay minerals is surprisingly consistent. X-ray diffraction and Thorez' (1975) system of codifying mixed-layer clays show kaolinite and two mixed-layer clays [I+10-(10-14_m) and C-(14_c-14_v)] throughout the sample suite. The I+10-(10-14_m) structure contains dominantly illite, which occurs in discrete, stable (disorder exists in stacking of layers) and unstable (disorder occurs on cation level) forms. The percentage of montmorillonite in the structure varies from 20 to 35. The C-(14_c-14_v) structure is primarily stable and unstable chlorite.

Despite the consistent composition of the clays, morphologies are quite variable. Maximum diversity of morphologies occurs in sediments that are grain-supported or

very nearly grain-supported. The permeability of these sediments is higher and this appears to be the dominant factor controlling formation of authigenic clays. Since grain content controls permeability, it also controls morphological variations in clay mineralogy. Authigenic clays are recognized by their delicate morphology, distinct crystalline form, occurrence as alteration products on grain surfaces and lack of compaction effects. Five modes of occurrence of authigenic clays are recognized: (1) primary void (interstitial) fillings, (2) secondary void fillings (i.e. grain pits, basal clevage partings), (3) pore-linings or grain coatings, (4) fracture fillings and (5) alteration surfaces. Dominant authigenic clays are kaolinite (pseudohexagonal "bookstacks" in void fillings) and illite-montmorillonite ("cardhouse" stacks of lobate-edged plates occurring as pore-linings). These are similar to occurrences recognized by Wilson and Pittman (1977). Tulip-bud, cabbage-head type structures and extended aggregates of face-to-face pseudohexagonal plates nonsymmetrically stacked and of variable size are newly recognized morphologies. Authigenic pyrite occurs in most samples, but increases as clay content increases. Overgrowths on anatase(?) and quartz occur in samples containing abundant authigenic clays. The size range (0.001 to 0.015mm) of authigenic clays encompasses a substantial portion of sediment sizes measured by pipette analyses. Silty or sandy shales or argillaceous siltstones and sandstones contain abundant

authigenic clays; consequently, a pipette analysis of the pan fraction of such sediments may result in considerable error. Siltstones or sandstones that appear to contain a significant quantity of fine material may have actually been well sorted at the time of deposition.

Allogenic components (clays and grains) are recognized by their fragmental or abraded textures. Allogenic fabrics show contorted pore-fluid channels that occur within clay fabrics and adjacent to grain surfaces. Because the sediment-water density is high and resistance to flow is high, contorted pore-fluid channels probably develop during initial thermal dehydration (Burst, 1969).

The effects of source, environment of deposition and diagenesis on the chemistry and structure of clay minerals, particularly in low temperature (150^{o}C) regimes, is a subject of considerable debate and remains essentially unresolved. SEM studies are quite valuable in revealing some of the genetic relationships between the various constituents, particularly clay minerals. Clay minerals in sediments strongly reflect the nature of their source material and undergo only slight modification in their depositional environments (Weaver, 1958). The composition of the clay minerals is consistent throughout the Graneros and indicates, in order of abundance, an influx of mixed-layer illite-montmorillonite, mixed-layer chlorite-vermiculite and kaolinite from the source area. Diagenetic changes in the marine environment may have caused the alteration of

some montmorillonite to illite by potassium absorption; and montmorillonite to chlorite by magnesium absorption (Johns and Grim, 1958; Milne and Earley, 1958). The original suite of clay minerals probably contained slightly higher percentages of montmorillonite and less illite and chlorite. Below the sediment-water interface, reducing conditions prevailed as indicated by the presence of authigenic pyrite. Foliation of allogenic clays around framboidal clusters of pyrite indicates pyrite formation before significant compaction. According to Berner (1970), carbonaceous material from organic matter and bacterial reduction of dissolved sulfates supplies sulfur that reacts with iron to form metastable iron monosulfides (i.e. mackinawite, greigite). These monosulfides react with native sulfur produced from the oxidation of H_2S to form pyrite a few inches below the sediment-water interface. As compaction pressure increases and pore dimensions decrease, the ionic strength of interstitial fluids and reaction rates probably increase. The paragenesis of authigenic mineral growth is revealed by the relationship between the various authigenic components in the sediment. Overgrowths on detrital grains (i.e. quartz, anatase) occur first. These overgrowths are covered by calcite cement. Abundant Ca^{2+} in the Graneros sediments probably resulted in the development of calcite cement in areas of high grain content. The loss of Ca^{2+} from solution increased the Mg^{2+}/Ca^{2+} ratio and resulted in dolomitization of calcite. Organic material may have acted as a

catalyst in the growth of authigenic clays in remaining void space. The ionic strength, temperature, pressure, catalytic agents and the activity of the interstitial solutions were conducive to the formation of authigenic illite-montmorillonite as pore-linings and grain coatings. The ratio of illite to montmorillonite in the mixed-layer (I-M) structures may have increased very slightly due to K^+ depletion in the interstitial fluids. Wijeyesekera and Freitas (1976) subjected clays to high pressure. The pore-fluids expelled from clays that had been saturated in artificial sea water showed a maximum decrease in K^+. Ca^{2+} and Mg^{2+} initially decreased, then increased to maximum pressure. K^+ showed maximum depletion and Mg^{2+} maximum increase. Initial Ca^{2+} and Mg^{2+} may allow the formation of montmorillonite interlayers and chlorite. Cabbage-head type structures occur on illite-montmorillonite coatings. Increases in interstitial Ca^{2+} and Mg^{2+} probably contributed to the growth of these structures. Organic material and water-filled pores allowed the formation of kaolinite. The interstitial fluids were probably depleted in K^+, Ca^{2+}, Mg^{2+} and Na^+ as illite-montmorillonite, cabbage-head structures and tulip-bud structures crystallized. Since occasional quartz overgrowths occur over grain-coating clay minerals, the chemical activity of interstitial fluids must have oscillated with increasing pressure and temperature.

Since permeability appears to be the dominant controlling factor in the degree of authigenic mineral growth, the

genetic sequence suggested above must have occurred prior to the last major reduction in permeability. The limited distortion and compaction of authigenic clays indicates that the last major reduction in permeability is caused primarily by authigenic mineral development. In the final stages of dehydration due to compaction, the pore volume is substantially decreased, yet mobile pore-fluids remain and thermal effects progressively increase. It is probable that the sequence of authigenic mineral growth is initiated during the initial thermal dehydration. The growth of authigenic components continues throughout initial thermal dehydration until the last mobile pore-fluids are removed. Petroleum precursors undergo thermal maturation throughout this process and act as catalysts to authigenic reactions. The last major mobilization not only results in the migration of petroleum products from source beds to reservoir rocks, but also contributes to the cessation of authigenic mineral growth. Although the morphologies of authigenic clay minerals in more permeable sediments vary markedly from clay minerals (primarily allogenic) in matrix-supported sediments, the overall composition of the clay mineral assemblages is essentially the same. This suggests that the chemistry of pore-fluids in clay-rich, grain-supported sediments in a sequence dominated by fine-grained, matrix-supported sediments is reflective of the composition of the overall clay mineral assemblage.

The Graneros is the stratigraphically lowest major

Cretaceous source bed in the San Juan Basin; consequently, it reflects the greatest thermal maturation level of organic material in Cretaceous source beds. LOM calculations indicate that oil generation occurs in the Graneros and possibly as high in the section as the Carlisle-Niobrara unconformity in the structurally deepest part of the basin. Above the Carlisle-Niobrara unconformity primarily immature gas is generated. A prediction of hydrocarbon type (based on organic analyses, LOM calculations and stratigraphic distribution) that should occur in various reservoir beds in the basin correlates well with the actual production records from these reservoir beds.

APPLICATIONS

Petroleum Exploration and Development

Exploration programs involve a thorough investigation of a province, integrating sedimentology, stratigraphy and structure. An exploration well is often drilled and potential reservoir rocks are examined. If economically producible hydrocarbons are not found, the data obtained is integrated into the exploration concept and a new location is considered. Valuable information, however, is usually left behind.
A detailed examination of fine-grained terrigenous sediments can establish several important facts: (1) whether or not a potential source bed has generated hydrocarbons; (2) the nature of the hydrocarbons generated; (3) the

migration direction of the hydrocarbons and (4) secondary (diagenetic) traps.

LOM analysis establishes whether or not a potential source bed has generated hydrocarbons and the probable hydrocarbons produced. If hydrocarbons have been generated, the area may be considered a petroleum province. It is important to establish the type of hydrocarbon generation (oil, gas or gas condensate) because each has unique physical and chemical properties (i.e. viscosity, density, cloud point, pour point) and responds differently in a reservoir rock. A reservoir with permeability and porosity that results in nominal oil production may allow excellent gas production.

More than one well is required to establish the direction of migration of the hydrocarbons. Silty or sandy trends within clay fabrics are probable migration routes. Distorted pore-fluid channels indicate that migration of high pressure fluids has occurred. Sufficient delineation of silty zones and distorted pore-fluid channels may establish directional trends within a basin. The formation of authigenic clays, particularly kaolinite, is enhanced by the presence of organic-rich fluids. Such fluids begin to migrate from source beds during initial thermal dehydration. Saline solutions in reservoir rocks that are interbedded with source rocks may inhibit the formation of kaolinite. Organic fluids migrating from source rock into reservoir rock initiate or accelerate authigenic clay crystallization.

The clays cause a major reduction in permeability behind the migration front as the fluids move up dip. If tectonic activity causes a major dip reversal, the hydrocarbons are prevented from migrating up dip by restricted permeability. The authigenic clays preserve or trap hydrocarbons in unlikely structural positions. In order to establish the probability of such traps, a complete geological study is required. Petrographic, sedimentological, stratigraphic, structural and detailed source bed studies are required. Organic and source bed studies are not tools that stand independently, but when integrated with other geologic data they provide a complete geologic reconstruction of a basin.

Studies of source beds also provide data that is useful in the exploitation of hydrocarbon accumulations. Reservoirs that are producing hydrocarbons are likely to contain authigenic clays if they are permeable sandstone or fractured silty zones in source beds. The authigenic clays are delicate; consequently, acid treatments or "frac" treatments will substantially improve production by locally improving permeability. These treatments will also extend the drainage radius of wells, thereby allowing wider well spacings and reduced development costs.

Nuclear Waste Disposal

Evaporite deposits are presently being considered as nuclear waste disposal sites. Fine-grained terrigenous sediments offer a favorable alternative. The dominant

constituents of fine-grained terrigenous sediments are clay minerals. Consequently, debate centers around the physical and chemical properties of clay minerals and whether those properties are detrimental or advantageous with respect to nuclear waste disposal.

Extensive data exists on the behavior of very small quantities of various clay minerals (i.e. structure, composition, ion exchange capacity, water adsorption). Grim (1968) discussed in detail numerous properties of clays, but the present discussion is limited to a few general observations pertinent to clay-rich sediments as hosts for nuclear waste disposal. Table 12 summarizes some of the properties considered. The high ion exchange capacity of clays acts as a fixation mechanism to numerous cations. Nishita and others (1955) used leaching procedures to determine the fixation and extractability of five fission products (Sr^{90}, Y^{91}, Ru^{106}, Cs^{137} and Ce^{144}) in soils and clays. Leached fractions were divided into two groups, <u>water-soluble</u> (leached by 50 ml. of distilled water and 50 ml. of neutral NH_4A_c immediately after water leaching) and <u>exchangeable</u> (leached by 50 ml. of NH_4A_c without pre-leaching with H_2O) fractions. The <u>nonexchangeable</u> fraction was the portion remaining in the soil or clay sample. The relative relationships of the radioisotopes in the clay minerals were:

Water-soluble fraction:

bentonite; $Ru^{106} > Sr^{90} > Cs^{137} > Y^{91}, Ce^{144}$

kaolinite; $Sr^{90} > Ru^{106}, Cs^{137} > Y^{91} > Ce^{144}$

Exchangeable fraction:

bentonite; $Sr^{90} > Cs^{137} > Y^{91}, Ce^{144} > Ru^{106}$

kaolinite; $Y^{91}, Ce^{144} > Sr^{90} > Cs^{137} > Ru^{106}$

Nonexchangeable fraction:

bentonite; $Ru^{106} > Ce^{144}, Y^{91} > Cs^{137} > Sr^{90}$

kaolinite; $Ru^{106} > Cs^{137} > Y^{91}, Ce^{144} > Sr^{90}$

The pH of leaching solutions substantially affected the extractability of certain cations. The extractability of Sr^{90} was approximately constant. Cs^{137} extractability decreased slightly as pH increased above 3.5, but below 3.5 it decreased rapidly. Y^{91} and Ce^{144} extractability decreased sharply above pH 5.5. Bentonite was more effective in fixing Ce^{144} in nonexchangeable form than kaolinite. It is apparent from the work of Nishita and others (1955) that radioisotopes are exchangeable with clay mineral cations. The effectiveness of the nonexchangeable fixation of a radioisotope in clay depends on the clay mineral composition and the pH of the ambient solutions. Since radioisotopes are adsorbed on clays, a desirable characteristic of a host clay for waste disposal is small particle size. Smaller particles have greater surface areas per unit volume; consequently, ion exchange sites are more numerous.

Most studies involving thick sequences of clay-rich sediments have resulted indirectly from petroleum exploration. Potential nuclear waste disposal sites are very thick (thousands of feet) sequences of clay-rich sediments.

It is essential to understand the physical and chemical behavior of these thick sequences as a unit. This understanding is facilitated by analyzing considerable data already gathered as a by-product of petroleum exploration. The permeability of clay-rich sediments is very low and interstitial fluids are restricted in mobility. Most clays have a high water adsorption capacity and this is a point of concern to opponents of waste disposal in shales. Apparently, opponents of waste disposal in shales fear that high temperatures generated by nuclear waste products will mobilize this water and the water will transport toxic fission by-products away from the immediate storage site. When clays are initially deposited, the water content accounts for up to 80% of the sediment by volume. This is reduced to about 30% after a few thousand feet of burial, most of which (20-25%) is interlayer water. Approximately 50% of this water is removed during initial thermal dehydration, leaving about 5% pore water and 11% interlayer water. The water removed during initial thermal dehydration is the last major mobilization of interstitial fluid. During and after this removal of fluids, permeability is substantially reduced by authigenic clay crystallization and, to a minor extent, by slight compaction due to fluid removal. Clay-rich sediments that have undergone initial thermal dehydration might be suitable sites for nuclear waste storage, particularly clay-rich sediments with pore-lining and void-filling authigenic clays. Subsequent additions of water result

in a swelling of the clays and a corresponding reduction in permeability. Although temperatures generated by decay of nuclear waste greatly exceed those required for thermal mobilization, it is likely that the effects will be very localized. Contact aureoles around igneous intrusions truncating shales are very narrow. Ion migration is probably also very restricted. A sufficient thickness of clay-rich sediment should allow adequate heat dissipation. A slight amount of water should enhance a storage site since it promotes ion exchange and fixation. Interstitial and adsorbed water impart plasticity to clay-rich sediments. Plasticity is desirable since any fractures that may occur will be annealed almost as quickly as they are formed. Some fractured shales produce oil and gas, but wells producing from these reservoirs have a limited drainage radius. It should be pointed out that such fracture systems are located at points of maximum tectonic stress, hardly a desirable feature of a potential nuclear waste disposal site. The Graneros is quite heterogenous lithologically, yet permeabilities vary only slightly. Grain contents as high as 30% have little effect on permeabilities.

Small particle size, high plasticity, low permeability, high ion exchange capacity and high water adsorption capacity are desirable qualities of clay-rich sediments selected for nuclear waste storage sites. Shales with high montmorillonite content are desirable host rocks for nuclear waste disposal (Table 12). Mixed-layer clays also possess

Item	Kaolinite Group	Illite Group	Chlorite Group	Montmoril-lonite Group
Particle size (in microns)	4.0-0.3	0.3-0.1	0.3-0.1(?)	0.2-0.02
Relative ion exchange	Slight	Moderate	Moderate	Large
Relative water adsorption	Slight	Moderate	Moderate	Very Large
Relative permeability	Large	Moderate	Moderate	Small
Relative plasticity	Slight	Moderate	Moderate	Large
Occurrence in recent sediments	Common	Abundant	Common	Common
Occurrence in ancient sediments	Common	Abundant	Common	Common

Table 12. Summary of Clay Properties and Occurrence (adapted from Krumbein and Sloss, 1963).

the same desirable physical and chemical properties, particularly those containing a high percentage of montmorillonite interlayers.

Conceptual, experimental and observational data indicate that clay-rich sediments might be excellent nuclear waste storage sites. To conclusively demonstrate this, fissionable materials should be placed in an appropriate storage site and the storage vicinity monitored for a few hundred thousand years. Unfortunately, our present energy situation requires more immediate procedures. Again, existing data may resolve the problem. In the area of the Oklo Mine in the Republic of Gabon, it appears that sufficient fissionable material was concentrated to produce several naturally occurring active reactors. Brookins (1976) has presented this area as convincing evidence of the effectiveness of shales as nuclear waste disposal sites. He points out that the location is hardly ideal because of zones of high permeability, high porosity and numerous fractures. Despite these conditions, the host rocks (impure shales with high carbonate content) were quite effective in restricting fission by-products to the proximity of the site. Brookins (1976) attributed this to adsorption of these by-products on clay minerals. Rb^{+}, Cs^{+} and Ba^{2+} probably replace K^{+} in clay minerals, ^{22}Ra as Ra^{+} is adsorbed on clay minerals and Th is restricted by its extreme insolubility.

Since breeder reactor technology represents an enormous energy source for future generations, an effective means of

disposing of nuclear waste materials must be developed. Evidence indicates that clay-rich sediments might be excellent nuclear waste disposal sites; however, since leakage from these sites could result in tragic consequences, further research on the texture, fabric and composition of large accumulations of fine-grained, terrigenous sediments is essential.

CONCLUSIONS

1) Grain content determines the configuration of fabric during compaction and affects permeability thus controlling authigenic mineralization.
2) Authigenic mineralization occurs during initial thermal dehydration and, although authigenic morphologies are quite variable, they reflect the overall composition of the clay minerals in the unit.
3) Scanning electron microscopy reveals contorted pore-fluid channels and the paragenesis of authigenic components, thus aiding in determining the chemical and physical evolution of a sequence of fine-grained terrigenous sediments.
4) Permeability is sometimes greater at angles of 30 and 60 degrees to bedding than when measured parallel to bedding.
5) Level of Organic Metamorphism (LOM) calculations are valuable tools in oil and gas exploration and reveal that the portion of the Mancos Shale below the Carlisle-Niobrara unconformity, in the structurally deepest part of the San Juan Basin, generated the oil that occurs in the basin.
6) Fine-grained terrigenous sediments that contain montmorillonite-rich clays that have undergone initial thermal dehydration might be excellent nuclear waste disposal sites.

REFERENCES

Bates, T.F., 1971, The kaolin minerals, in the electron-optical investigation of clays; Mineralogical Society Monograph 3; Mineralogical Society (Clay Minerals Group) London; pp. 109-157.

Bauer, L.D. and Winterkorn, H.W., 1936, Sorption of liquids by soil colloids, II, surface behavior in the hydration of clays, Soil Sci., v. 40, pp. 403-418.

Berner, R.A., 1970, Sedimentary pyrite formation, Am. Jour. Sci., v. 268, pp. 1-23.

Blatt, H.; Middleton, G. and Murray, R., 1972, Origin of sedimentary rocks; Prentice-Hall, Inc.; Englewood Cliffs, N. Jer.

Bowles, F.A.; Bryant, W.R. and Wallin, C., 1969, Micro-structure of unconsolidated and consolidated marine sediments; Jour. Sed. Petrol.; v. 39, pp. 1546-1551.

Brookins, D.G., 1976, Shale as a repository for radioactive waste: the evidence from Oklo; Environmental Geology; v. 1, pp. 255-259.

Bucke, D.P., Jr. and Mankin, C.J., 1970l Clay-mineral diagenesis within interlaminated shales and sandstones; Jour. Sed. Petrol.; v. 41, pp. 971-981.

Burst, J.F., 1969, Diagenesis of Gulf Coast clayey sediments and its possible relation to petroleum migration; A.A.P.G. Bull.; v. 53, no. 1, pp. 73-93.

Carroll, D., 1970, Clay minerals: a guide to their x-ray identification; U.S.G.S. Special Paper 126.

Casagrande, A., 1940, The structure of clay and its importance in foundation engineering, in contributions to soil mechanics, 1924 to 1940; Boston Soc. Civil Engrs., pp. 72-125.

Chayes, F., 1949, A simple point counter for thin-section analysis; Am. Mineralogist; v. 34, pp. 1-11.

Chen, P.S., Jr.; Toribara, T.Y. and Warner, H.; 1956, Microdetermination of Phosphorus; Anal. Chem.; v. 28, pp. 1756-1758.

Dickey, P.A., 1975, Possible primary migration of oil from source rock in oil phase; A.A.P.G. Bull.; v. 59, no. 2, pp. 337-345.

Englehardt, Wolf V. and Gaida, K.H., 1963, Concentration changes of pore solutions during the compaction of clay sediments; Jour. Sed. Petrol.; v. 33, no. 4, pp. 919-930.

Evans, C.R. and Staplin, F.L., 1970, Regional facies of organic metamorphism; Geochem. Explor.: Can. Inst. Min. and Metal.; Spec. Vol. 11, pp. 517-520.

Fassett, J.E., 1974, Cretaceous and Tertiary rocks of the eastern San Juan Basin, New Mexico and Colorado; New Mexico Geol. Soc. Guidebook, 25th Field Conf., Ghost Ranch (Central-Northern N.M.); pp. 225-238.

Flesch, G.A. and Wilson, M.D., 1974, Petrology of Morrison Formation (Jurassic) sandstones of the Ojito Spring quadrangle, Sandoval County, New Mexico; New Mexico Geol. Soc. Guidebook, 25th Field Conf., Ghost Ranch (Central-Northern N.M.); pp. 197-210.

Galehouse, J.S., 1969, Counting grain mounts: number percentage vs. number frequency; Jour. Sed. Petrol.; v. 39, pp. 812-815.

Gard, J.A., 1971, The electron-optical investigation of clays; Mineralogical Society Monograph 3; Mineralogical Society (Clay Minerals Group); London.

Gillott, J.E., 1969, Study of the fabric of fine-grained sediments with the scanning electron microscope; Jour. Sed. Petrol.; v. 39, no. 1, pp. 90-105.

Gipson, J., Jr., 1965, Application of the electron microscope to the study of particle orientation and fissility in shale; Jour. Sed. Petrol.; v. 35, no. 2, pp. 408-414.

_____, 1966, A study of the relations of depth, porosity and clay mineral orientation in Pennsylvanian shales; Jour. Sed. Petrol.; v. 36, pp. 888-903.

Glagolev, A.A., 1933, On the geometrical methods of quantitative mineralogical analysis of rocks; Trans. Inst. Econ. Min., Moscow; v. 59, pp. 1-47.

Gorham, F.D., Jr.; Woodward, L.A.; Callendar, J.F. and Greer, A.R., 1977, Fracture permeability in Cretaceous rocks of the San Juan Basin; New Mexico Geol. Soc. Guidebook, 28th Field Conf., San Juan Basin III, pp. 235-241.

Grim, R.E., 1968, Clay Mineralogy, McGraw-Hill Book Company, N.Y.

_____ and Cuthbert, F.L., 1945, Some clay-water properties of certain clay minerals; Jour. Am. Ceram. Soc., v. 28, pp. 90-95.

Grose, Trowbridge L., 1972, Tectonics, in Rocky Mtn. Assoc. Geol. Atlas, Ed.-in-Chief, William W. Mallory, p. 37.

Hamblin, W.K., 1962, X-ray radiography in the study of structures in homogeneous sediments; Jour. Sed. Petrol.; v. 32, pp. 201-210.

Hardy, W.B., 1926, Friction, surface energy and lubrication, in Colloid Chemistry, J. Alexander (ed.); v. 1, pp. 301-330.

Heling, D., 1970, Micro-fabrics of shales and their rearrangement by compaction; Sedimentology; v. 15, pp. 247-260.

Hood, A.; Gutjahr, C.C.M. and Heacock, R.L., 1975, Organic metamorphism and the generation of petroleum; A.A.P.G. Bull.; v. 59, no. 6, pp. 986-996.

Hower J.; Eslinger, E.V.; Hower, M.E. and Perry, E.A., 1976, Mechanism of burial metamorphism of argillaceous sediment: 1. Mineralogical and chemical evidence; Geol. Soc. of Am. Bull.; v. 87, pp. 725-737.

Ingram, R.L., 1953, Fissility of mudrocks; Geol. Soc. of Am. Bull.; v. 64, pp. 869-878.

Johns, W.D., Jr. and Grim, R.E., 1958, Clay mineral composition of recent sediments from the Mississippi River delta; Jour. Sed. Petrol.; v. 28, pp. 186-199.

Kahn, J.S., 1956, The analysis and distribution of packing in sand-size sediments; Jour. Geol.; v. 64, pp. 385-395.

Krumbein, W.C. and Sloss, L.L., 1963, Stratigraphy and sedimentation, W.H. Freeman and Company, San Francisco.

Lamb, G.M., 1968, Stratigraphy of the lower Mancos Shale in the San Juan Basin; Geol. Soc. of Am. Bull.; v. 79, no. 7, pp. 817-834.

Lambe, T.W., 1953, The structure of inorganic soils; Jour. Soil Mech. Found. Div.; v. 79, pp. 1-49.

Langmuir, I., 1917, The constitution and fundamental properties of solids and liquids; Jour. Am. Chem. Soc.; v. 39, pp. 1848-1906.

Low, P.F., 1961, Physical chemistry of clay-water interaction; Advan. Agron.; v. 13, pp. 269-327.

Lucas, J., 1963, La transformation des mineraux argileux dans la sedimentation; Etudes sur les argiles due Trias.; Bull. Mem. Carte Geol. Als Lorr.; v. 23, p. 202.

Meade, R.H., 1966, Factors influencing the early stages of the compaction of clays and sands - review; Jour. Sed. Petrol.; v. 36, pp. 1085-1101.

Milne, I.H. and Earley, J.W., 1958, Effect of source and environment on clay minerals; A.A.P.G. Bull.; v. 42, pp. 328-338.

Nishita, H.; Kowalewsky, B.W.; Steen, A.J. and Larson, K.H., 1955, Fixation and extractability of fission products contaminating various soils and clays, I, Sr^{90}, Y^{61}, Ru^{106}, Cs^{137} and Ce^{144}; Soil Sci., v. 81, pp. 317-326.

O'Brien, N.R., 1968, Electron microscope study of black shale fabric; Naturwissenschaften; v. 55, pp. 490-491.

_____, 1970a, The fabric of shale - an electron-microscope study; Sedimentology; v. 15, pp. 229-246.

_____, 1970b, Comparison of the fabric of a sensitive Pleistocene clay with laboratory flocculated clay using the scanning electron microscope; Maritime Sediments; v. 5, pp. 58-61.

Odom, I.E., 1967, Clay fabric and its relation to structural properties in mid-continent Pennsylvanian sediments; Jour. Sed. Petrol.; v. 37, no. 2, pp. 610-623.

Parker, J.M.; Riggs, E.A. and Fisher, W.L., 1977, Oil and gas potential of the San Juan Basin; New Mexico Geol. Soc. Guidebook; 28th Field Conf., San Juan Basin III; pp. 227-234.

Peterson, J.A.; Loleit, A.J.; Spencer, C.W. and Ullrich, R.A., 1915, Sedimentary history and economic geology of San Juan Basin; A.A.P.G. Bull.; v. 49, no. 11, pp. 2076-2119.

Picard, M. Dane, 1971, Classification of fine-grained sedimentary rocks; Jour. Sed. Petrol.; v. 41, no. 1, pp. 179-195.

Powers, M.C., 1953, A new roundness scale for sedimentary particles; Jour. Sed. Petrol.; v. 23, pp. 117-119.

Quigley, R.M. and Thompson, C.D., 1966, The fabric of anistropically consolidated sensitive marine clay; Can. Geotech. Jour.; v. III, pp. 61-73.

Rosenqvist, I. Th., 1959, Physico-chemical properties of soils; soil-water systems; Am. Soc. Civil Engrs. Proc.; Jour. Soil Mech. Found. Div.; v. 85, pp. 31-53.

_____, 1963, The influence of physico-chemical factors upon the mechanical properties of clays; Norwegian Geotech. Inst.; v. 54, pp. 1-19.

Ross, C.S. and Kerr, P.F., 1930, The kaolin minerals: U.S.G.S. Prof. Paper 165-E; pp. 151-180.

Rubey, W.W., 1930, Geologic studies of fine-grained Upper Cretaceous sedimentary rocks of the Black Hills region; U.S.G.S. Prof. Paper 165-A, pp. 1-54.

Sarkisyan, S.G., 1971, Application of the scanning electron microscope in the investigation of oil and gas reservoir rocks; Jour. Sed. Petrol.; v. 41, pp. 289-292.

Sears, J.D.; Hunt, C.B. and Hendricks, T.A., 1941, Transgressive and regressive Cretaceous deposits in southern San Juan Basin, New Mexico; U.S.G.S. Prof. Paper 193-F.

Staplin, F.L., 1969, Sedimentary organic matter, organic metamorphism and oil and gas occurrence; Bull. of Can. Petrol. Geol.; v. 17, no. 1, pp. 47-66.

Stokes, G.G., 1851, On the effect of the internal friction of fluids on the motion of pendulums; Cambridge Philos. Soc. Trans.; v. 9, pt. 2, pp. 8-106.

Suggate, R.P., 1959, New Zealand coals, their geological setting and its influence on their properties; New Zealand Dept. Sci. Industry Research; Bull. 134; p. 113.

Tan, T.K., 1958, Discussion of soil properties and their measurement; 4th Inter. Conf. on Soil Mech. Found. Eng. Proc.; v. 3, pp. 87-89.

Taylor, J.M., 1950, Pore-space reduction in sandstones; A.A.P.G. Bull.; v. 34, pp. 701-716.

Terzaghi, K., 1925, The physical properties of clays; M.I.T. Tech. Eng. News; v. 9, pp. 10, 11, 36.

Thorez, J. and Van Leckwijk, W., 1967, Les maneraux argileux et leurs alterations dans le Namurien inferieur de la Belgique (synclinal de Namur); Ann. Soc. Geol., Belgique; v. 90, pp. 329-380.

_____ and Bourguignon, P., 1973, Mineralogie des argiles de dissolution des calcaires dinantiens en Condroz (Belgique); Ann. Soc. Geol., Belgique; v. 96, pp. 59-85.

_____, 1975, Phyllosilicates and clay minerals, a laboratory handbook for their x-ray diffraction analysis; Editions G. Lelotte, B4820, Dison (Belgique).

Udden, J.A., 1898, Mechanical composition of wind deposits; Augustana Library Publication; no. 1.

Vivaldi, J.L. Martin and Robertson, R.H.S., 1971, Palygorskite and sepiolite (the hormites), in the electron-optical investigation of clays; Mineralogical Society Monograph 3; Mineralogical Society (Clay Minerals Group) London; pp. 255-275.

Wadell, H., 1936, Some practical sedimentation formulas; Geol. Foren Forhandl.; v. 58, pp. 397-407.

Weaver, C.E., 1958, Geologic interpretation of argillaceous sediments: Part I. origin and significance of clay minerals in sedimentary rocks; A.A.P.G. Bull.; v. 42, no. 2, pp. 254-271.

_____ and Pollard, Lin D., 1973, The chemistry of clay minerals; Elsevier Sci. Pub. Co., N.Y.

Webb, J.E., 1974, Relation of oil migration to secondary clay cementation, Cretaceous sandstones, Wyoming; A.A.P.G. Bull.; v. 58, no. 11, pp. 2245-2249.

Welte, D.H., 1972, Petroleum exploration and organic geochemistry; Jour. Geochem. Explor.; v. 1, pp. 117-136.

Wentworth, C.K., 1922, A scale of grade and class terms for clastic sediments; Jour. Geol.; v. 30, pp. 377-392.

Wijeyesekera, D.C. and De Freitas, M.H., 1976, High-pressure consolidation of kaolinitic clay; Geol. notes, A.A.P.G. Bull.; pp. 293-298.

Wilson, M.D. and Pittman, E.D., 1977, Authigenic clays in sandstones: recognition and influence on reservoir properties and paleoenvironmental analysis; Jour. Sed. Petrol.; v. 47, no. 1, pp. 3-31.

Winterkorn, H.W., 1943, The condition of water in porous systems; Soil Sci.; v. 55, pp. 109-115.